Politecnico di Torino

MSc Energy and Nuclear Engineering
A.a. 2023/2024
November 2024

Energy Design for a Nearly Self-Sustaining Residential Building: Technical and Economic Feasibility of Advanced Heating and Cooling Systems

Supervisors:
Prof. Ferraris Monica
Prof. Simavilla Nieto David

Candidate:
Franzini Andrea
S316774

Table of Contents

Energy Design for a Nearly Self-Sustaining Residential Building: Technical and Economic Feasibility of Advanced Heating and Cooling Systems 1

List of Figures. 3

List of Tables. 5

1. Introduction 7

1.1 Importance of energy efficiency in the residential building sector 7

1.2 Goals of the resource 7

1.3 Structure of the Thesis 8

2. Data collection and building modeling 9

2.1 Data sources and collection methodology 11

2.2 Building modeling using HULC 17

2.3 Modeling of the swimming pool 19

3. Solar Control strategies 29

4. Selection of the appropriate Energy System Equipment 33

4.1 Selection Criteria 33

4.2 Selected system description: Adsorption Chiller 35

4.2.1 Principles of operation 35

4.2.2 Mathematical models [1] 40

4.2.3 Common pairs of adsorbent and refrigerant liquid 43

4.2.4 Typical adsorption chillers efficiencies. 44

4.2.5 Comparison between an adsorption chiller and an adsorption chiller: is it truly advantageous? 45

4.3 Air-Water Heat Pump 49

4.4 PCM: Phase Change Materials 50

4.5 Hybrid Thermal – Photovoltaic Solar Panels 55

4.5.1 Product selection and technical specifics. 55

4.5.2 Thermal efficiency calculation. 62

4.5.3 Calculation for determining the maximum number of panels that can be installed on the building's rooftop. 63

5. Definition of Energy System Configuration. 67

5.1 Proposed system combinations. 67
5.2 Preliminary comparative analysis and expected results. 69
6. Energy Simulations and Sizing. 72
6.1 Energy Demands of the Building. 72
6.2 Technical sizing, configuration 1 79
6.3 Economic Analysis, Configuration 1. 96
6.4 Economic analysis of the solar power plant. 99
6.5 Economic analysis of the heat pump and the electrical boiler. 102
6.6 Economic analysis of the adsorption chiller. 104
6.7 Global system's Economic Analysis. 107
6.8 Technical sizing, configuration 2. 111
6.9 Economic Analysis, Configuration 2. 118
6.10 Economic Analysis of the hybrid solar panels' field. 119
6.11 Economic analysis of the Heat Pump and the Electrical Boiler. 121
6.12 Economic Analysis of the global system. 124
6.13 Comparison between configurations and selection of the most viable option. 126
6.14 Configuration 3, technical and economic analysis. 130
6.15 PCMs Economic Analysis. 139
6.16 Economic Analysis, global investment. 140
6.17 Comparison between the two best configurations. 144
7. Conclusions 146
Bibliography 148
Appendix A 150

List of Figures.

Figure 1: Selected location 7
Figure 2: model of the building implemented in HULC 18
Figure 3: Swimming pool heat flows. 23
Figure 4: HULC input data. 29
Figure 5: Thermal behavior of the building. 30
Figure 6: Solar control improvements. 31
Figure 7: Results of the solar control improvements strategies. 31
Figure 8: general scheme of a chiller. 36
Figure 9: adsorption chiller scheme. 37
Figure 10: adsorption chiller connected to a solar pannel. 38
Figure 11: driving switching unit. 39
Figure 12: P-T diagram for the ideal basic cycle. 39
Figure 13: Useful nomenclature for the equations. 40
Figure 14: Sorbent-Sorbate couples. 43
Figure 15: Efficiencies of the system. 44
Figure 16: Absorption cooling system. 45
Figure 17: Comparison of the two systems COPs typical values. 47
Figure 18: PCM general functioning scheme. 50
Figure 19: PCM functioning diagram. 50
Figure 20: day and night thermal fluxes from and to PCMs. 51
Figure 21: micro-encapsulated PCMs properties. 52
Figure 22: PCMs properties. 53
Figure 23; PCMs properties. 54
Figure 24: composition of the Abora Solar panel. 56
Figure 25: Efficiencies of the Panel. 58
Figure 26: Dimensions of the Panel. [] 58
Figure 27: Building's rooftop dimensions. 63
Figure 28: Minimum inter distance between panels. 64
Figure 29: Final layout of the solar panels' installation. 65
Figure 30: Optimal orientation of the panels, on AutoCAD. 65
Figure 31: First simulation's results. 72
Figure 32: Daily winter day % thermal charge variation. 75
Figure 33: Summer Day daily % thermal charge. 76
Figure 34: Daily DHW % charge. 77
Figure 35: Shift between thermal energy production and demand, without a storage system. 82
Figure 36: Match between Thermal energy production and demand with a storage tank. 83
Figure 37: frequency curve for dimensioning the heating supply system. 87

Figure 38: technical specifics of the heat pump. 88
Figure 39: Scheduled time program for the functioning of the heat pump. 90
Figure 40: roVa shield price. 93
Figure 41: NPV and PBT of the solar panels field. 100
Figure 42: NPV for the heating supply system. 103
Figure 43: NPV and PBT of global investment. 108
Figure 44: NPV and PBT for the hybrid solar panels' field. 120
Figure 45: NPV and PBT, configuration 2. 122
Figure 46: NPV and PBT for global investment. 125
Figure 47: Recap of the most valuable figures of the chapter. 129
Figure 48: NPV and PBT for the global system's WACC analysis. 141
Figure 49: comparison between configuration 3 and 3.1 143
Figure 50: comparison between configuration 1 and configuration 3.1 144
Figure 51: Psychrometric chart. 150

List of Tables.

Table 1: Technical specifics of the building 12
Table 2: Minimum air flows for buildings 13
Table 3: Average Global Irradiance for a typical day of each month 16
Table 4: Adults' swimming pool dimensions. 19
Table 5; Children's swimming pool dimensions. 19
Table 6: Adults' swimming pool calculations. 19
Table 7: Children's swimming pool calculations. 20
Table 8: Monthly net water temperature, from “DBHE 2019- ANEJO G”. 22
Table 9: Average net water temperature for the thermal period considered, from “DBHE 2019- ANEJO G”. 22
Table 10: Monthly ambient temperature values, from the NASA database, year 2022... 22
Table 11: Average ambient temperature values for each thermal period, considered for the calculations. 22
Table 12: Monthly wind speed values. 23
Table 13: Average wind speed values for each thermal period. 23
Table 14: Total thermal energy demand of the swimming pool. 28
Table 15: General specifics of the hybrid panel 56
Table 16: electrical specifics of the hybrid panel. 57
Table 17: thermal specifics of the panel. 57
Table 18: General specifics of the BASIC kit’s solar panel 60
Table 19: General specific of the BASIC+ kit’s solar panel. 61
Table 20: Average Ambient Temperature. 62
Table 21: Calculated thermal efficiencies. 63
Table 22: Specifics of the maximum number of panels configuration. 66
Table 23: Total energy demands of the building. 72
Table 24: Hourly winter day thermal energy charges. 74
Table 25: Hourly summer day thermal energy charges. 75
Table 26: Hourly DHW charges. 76
Table 27: Winter Day % thermal energy needed from the swimming pool. 77
Table 28: Summer Day % thermal energy needed from the swimming pool. 78
Table 29: Specifics of the Adsorption Chiller. 80
Table 30: Technical features of the roVa shield. 92
Table 31: Tank's surfaces values. 93
Table 32: total monetary investment of the configuration 1. 96
Table 33: Solar Panels field's parameters for the WACC theory analysis. 99
Table 34: WACC theory for the Solar Panels field. 100
Table 35: Heat Pump and electrical Boiler economic parameters for the WACC theory. 102
Table 36: NPV and PBT of the heat pump and boiler investment. 102

Table 37: Economic analysis of the adsorption chiller. 105
Table 38: Economical analysis of an hypothetical 50% reduction of the adsorption chiller price. 106
Table 39: Global Economic Analysis of the system. 108
Table 40:technical specifics of the solar panels' field and of the storage tank. 112
Table 41: Geometrical dimensions of the solar field thermal storage tank. 113
Table 42:aerogel coating's technical dimensioning. 117
Table 43: total monetary investment, configuration 2. 118
Table 44; Input data for the WACC analysis of the second configuration. 119
Table 45: Solar field's WACC analysis. 119
Table 46: Input data for the WACC analysis of configuration 2. 121
Table 47: output of the WACC analysis, configuration 2. 122
Table 48: Input for the global WACC analysis. 124
Table 49: output from the WACC analysis for the global system. 125
Table 50: technical results of PCM's sizing process. 132
Table 51: technical sizing of the solar panles field results. 134
Table 52: scheduled time program for the heat pump's functioning. 137
Table 53; Total investment, configuration 3. 138
Table 54: Input for the WACC theory analysis, configuration 3. 139
Table 55: output of the WACC theory for PCMs investment. 139
Table 56: input data for the global system's WACC analysis. 140
Table 57: output results for the global system's WACC theory analysis. 141
Table 58: outcomes of configuration "3.1" 142
Table 59: NPV and PBT of configuration 3.1 142

1. Introduction

1.1 Importance of energy efficiency in the residential building sector

The residential building sector accounts for a significant portion of global energy consumption, approximately 40% of total energy use worldwide, and it is a major contributor to greenhouse gas emissions due to its reliance on fossil fuels for heating, cooling, and lighting. As urbanization accelerates and energy demand increases, enhancing energy efficiency in buildings has become imperative to reduce environmental impacts and meet international targets. Improving energy efficiency not only lowers energy consumption and operational costs but also plays a crucial role in mitigating climate change and promoting sustainable development.

The implementation of innovative technologies and advanced energy systems in buildings can lead to substantial improvements in energy efficiency without compromising occupant's comfort. Integrating renewable energy sources, energy storage systems, and advanced thermal insulation materials is essential for transitioning towards sustainable energy practices in the built environment. Such advancements contribute to reducing dependency on fossil fuels, lowering greenhouse gas emissions, and promoting energy self-sufficiency.

1.2 Goals of the resource

This study aims to design and evaluate advanced energy systems for a residential complex consisting of 63 apartments and two swimming pools, located at **C. Ana María Matute, 28805 Alcalá de Henares, Madrid, Spain**.

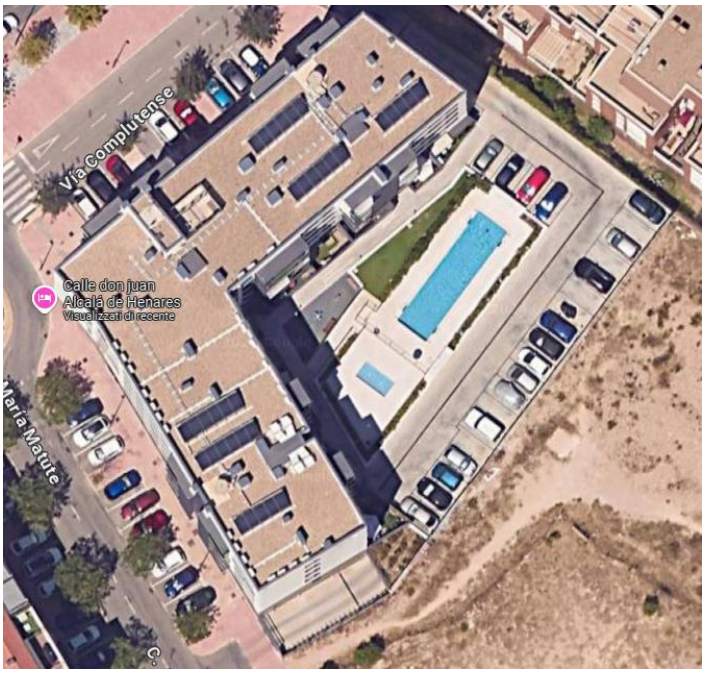

Figure 1: Selected location

The primary aim is to meet the building's thermal demands for both heating and cooling using innovative energy solutions that ensure economic feasibility and environmental sustainability. The research seeks to close the gap between the theoretical potential of advanced energy technologies and the practical implementation challenges in real-world applications.

The specific goals of the research are:

- **Evaluation of different energy system configurations**: Developing and analyzing three configurations based on various combinations of advanced technologies to identify the optimal solution in terms of energy efficiency, operational costs, and initial investment.
- **Analysis of environmental impact**: Assessing each configuration for its potential in reducing CO_2 emissions, contributing to climate change mitigation and compliance with environmental regulations.
- **Economic feasibility study**: Conducting a detailed analysis to evaluate the financial sustainability of the proposed solutions, considering both initial capital expenditure and long-term operational benefits.

The technologies investigated in this study include:

- **Hybrid solar panels**: These kinds of systems simultaneously generate electrical and thermal energy, maximizing the utilization of available solar radiation and enhancing overall system efficiency.
- **Thermal energy storage systems**: Devices that store excess thermal energy during periods of low demand or high production for use during peak demand periods, improving energy management and reducing waste.
- **Air-water heat pumps**: Technologies that extract thermal energy from ambient air to provide efficient heating and cooling, offering a renewable alternative to conventional heating systems.
- **Adsorption chillers**: Cooling systems that utilize physical adsorption processes to generate cooling with minimal electrical energy consumption, powered by low-grade thermal energy.
- **Phase Change Materials (PCMs)**: Innovative materials applied to building envelopes to enhance thermal inertia, absorbing and releasing heat during phase transitions to stabilize indoor temperatures and reduce the energy demand of the building itself.

1.3 Structure of the Thesis

The thesis is organized into the following chapters:

- **Chapter 2 – Data Collection and Building Modeling**: This chapter details the methodologies used for data collection, including climatic data, building characteristics, and energy demands. It also describes the process of modeling the

building using specialized software tools such as HULC, highlighting the importance of accurate representation for reliable simulation results.

- **Chapter 3 – Solar Control Strategies**: Analysis of the solutions implemented to enhance solar control, including the installation of shading devices like blinds and screens. The impact of these strategies on reducing cooling loads, improving indoor comfort, and contributing to overall energy efficiency is discussed.
- **Chapter 4 – Selection of Energy System Components**: A comprehensive evaluation of the selected equipment is presented, focusing on technical specifications, performance efficiencies, operational complexities, and compatibility with the building's energy requirements.
- **Chapter 5 – Definition of Energy System Configurations**: Illustration of the three developed configurations, providing a detailed rationale for the selection of each technology. A preliminary comparative analysis is conducted to assess the potential advantages and limitations of each configuration.
- **Chapter 6 – Energy Simulation and Sizing**: Description of the methodologies used for simulating the energy systems and sizing the components. Models created using Excel are detailed, including assumptions made, parameters considered, and the approach for ensuring that the systems effectively meet the building's energy demands.
- **Chapter 7 – Economic Analysis and Option Evaluation**: Presentation of the economic assessment of the different configurations, encompassing capital investment costs, operational expenses, maintenance considerations, and an evaluation of long-term economic benefits such as payback periods and return on investment.
- **Chapter 8 – Conclusions**: Summarization of the main findings, highlighting the potential environmental benefits and economic challenges associated with implementing advanced energy systems in residential buildings. Practical implications are discussed, and recommendations for future research and implementation strategies are provided.

Through this structure, the thesis aims to contribute to the field of energy efficiency in residential buildings, offering insights into the practical application of advanced energy technologies. It addresses the challenges of integrating such systems into existing building practices to achieve sustainable energy solutions, emphasizing the importance of coordinated efforts among stakeholders to overcome economic and technical barriers.

2. Data collection and building modeling

In this chapter, the methodologies adopted for collecting all the necessary data for the study are thoroughly detailed. A systematic approach was taken to ensure that the data gathered are both accurate and reliable, which is essential for the credibility of the research outcomes.

Data acquisition encompassed a variety of sources and techniques. Some information was sourced from existing documents, technical manuals and regulatory guidelines. These documents provided essential insights into the building's design specifications, material properties, and compliance with local construction codes.

Other data was obtained by developing specific computational models tailored to aspects of the project. For instance, custom models were created for the swimming pool to accurately simulate its thermal behavior and energy requirements. These models considered variables such as water volume, surface area, usage patterns, and environmental conditions to estimate heating needs and operational parameters.

Additionally, certain elements of the building's energy performance were analyzed using specialized simulation software. The **HULC** (Herramienta Unificada LIDER Calener) software was employed for this purpose. HULC is the standard tool in Spain for energy modeling of buildings and is recognized for its alignment with national standards and regulations. Utilizing HULC ensured that the energy simulations conformed to the methodologies prescribed by Spanish authorities, thereby enhancing the validity of the results.

The application of HULC facilitated detailed simulations of the building located at **C. Ana María Matute, 28805 Alcalá de Henares, Madrid, Spain**. The software enabled a comprehensive assessment of the building's thermal dynamics, energy consumption patterns, and identification of potential areas for efficiency improvements. Parameters such as insulation quality, glazing types, building orientation, and shading devices were integrated into the model to accurately reflect the actual conditions of the structure.

In addition to HULC, other computational tools and software platforms were utilized for data processing and analysis. These tools assisted in handling extensive datasets, performing complex calculations, and effectively visualizing the results. The integration of multiple software solutions allowed for a multifaceted evaluation of the building's energy performance from different analytical perspectives.

The combination of data derived from documentation, custom-developed models, and advanced simulation tools resulted in a robust and comprehensive dataset underpinning the study. This multi-pronged approach ensured that all relevant variables influencing the building's energy efficiency were accounted for. The methodologies employed also enabled cross-validation of results, thereby reinforcing the reliability and accuracy of the findings.

Subsequent sections of this chapter delve into the specifics of each data collection method and modeling technique. Detailed explanations of the assumptions made, parameters selected, and procedures for calibrating and validating the models are provided. The processes of aligning the simulation outputs with real-world data are also discussed. This thorough documentation underscores the meticulous nature of the research approach and establishes a solid foundation for the analyses presented in later chapters.

2.1 Data sources and collection methodology

- **Technical documents**

A comprehensive set of data was obtained from the project's documentation, including technical reports, construction specifications, design memoranda, and detailed construction drawings, which were kindly provided by the owners of the establishment. These documents offered valuable insights into the architectural design, material specifications, and construction methodologies of the building, serving as a foundational resource for the modeling process.

The data extracted encompasses critical information necessary for accurate energy modeling and simulation. This includes details on building geometry, envelope characteristics, thermal properties of construction materials, HVAC system configurations, and compliance with local building codes and regulations. By integrating this information, a more precise and reliable model of the building's energy performance could be developed.

In summary, the most significant data required for the modeling is compiled and presented in table 1. This table provides a structured overview of the key parameters and variables considered in the study, facilitating a clear understanding of the inputs used in the simulations. The thoroughness of the data collection process ensures that the subsequent analysis and results are grounded in accurate and comprehensive information. In addition, the sources for each data are added to the table.

All these information provided are also necessary as the input for HULC.

Table 1: Technical specifics of the building

Data	Value	Source
Altitude	593 m	https://es-es.topographic-map.com/map-w5h5k/Alcal%C3%A1-de-Henares/?center=40.48409%2C-3.36408&zoom=13
Climate Zone	D3	Código Técnico de Edificación. Anejo B Zonas Climáticas. Tabla a-Anejo B. Zonas climáticas. Datos de lectura de tabla: • Provincia: Madrid • Altitud: 551 – 600 m
Type of housing	New edification	Memoria descriptiva del proyecto
Total Ventilation	1488 l/s	Código Técnico de Edificación. HS 3 (Salubridad). Tabla 2.1. Caudales mínimos para ventilación de caudal constante en locales habitables.
City	Madrid	Memoria descriptiva del proyecto
Location	Alcalà de Henares	Memoria descriptiva del proyecto
Normative to consider for the thermal installations	RITE (2021)	
Normative to consider for the edification	CTE HE 2019	
Use of the building	Residencial in open blocks	Memoria descriptiva del Proyecto- Grupo I, Vivienda Multifamiliar
Maximum Height	15,58 m	Memoria descriptiva del Proyecto
Built Surface	5103,68 m2	Memoria descriptiva del Proyecto- Area de Edificabilidad Computable

- **Calculation of the Building's Ventilation Rate**

The ventilation rate of the building is required by the software to perform all the energy calculations. Table 2 presents all the assumptions to determine this value, in accordance with

the "Código Técnico de Edificación (CTE), HS 3 (Salubridad), Table 2.1: Minimum flow rates for constant flow ventilation in habitable rooms."

Table 2: Minimum air flows for buildings

TIPO DE VIVIENDA	CAUDAL MINIMO qv EN l/s				
	LOCALES SECOS (1) (2)			LOCALES HUMEDOS (2)	
	DORMITORIO PRINCIPAL	RESTO DE DORMITORIOS	SALAS DE ESTAR Y COMEDORES (3)	MINIMO EN TOTAL	MINIMO POR LOCAL
0 o 1 DORMITORIO	8	0	6	12	6
2 DORMITORIOS	8	4	8	24	7
3 O MÁS DORMITORIOS	8	4	10	33	8

According to HS3 of the CTE, the ventilation flow rate is calculated per dwelling unit, depending on the number of dry rooms (bedrooms, living room, dining room, etc.) and wet rooms (bathrooms and kitchen). In residential ventilation systems, fresh air is supplied to dry rooms and extracted from wet rooms. Essentially, the required ventilation flow rate per dwelling is the greatest of the following:

1. The minimum flow rate that must enter through the dry rooms, determined by the number of bedrooms and other dry rooms, using the data from Table 2.
2. The minimum flow rate that must exit through the wet rooms, calculated as:

$$Q_{wet} = N_{wet\ rooms} \times Q_{minper\ wet\ room}$$

   where:

   - $N_{wet\ rooms}$= Number of wet rooms (bathrooms plus kitchen)
   - $Q_{minper\ wet\ room}$ = Minimum flow rate per wet room from Table 2
3. The minimum total flow rate per dwelling, as specified for wet rooms.

For Type 1 Dwellings:

1. Minimum flow rate for dry rooms:
   - Number of bedrooms: 1
   - From Table 2: $Q_{dry,type1} = 8\frac{L}{s}$
2. Minimum flow rate for wet rooms:
   - The unheated room counts as a wet room.

- Number of wet rooms: 1
- Minimum ventilation per wet room:

$$Q_{\text{min,per wet room}} = 12\frac{L}{s}$$

Therefore: $Q_{\text{wettype1}} = 1 \times 12\frac{L}{s} = 12\frac{L}{s}$

3. Minimum total flow rate per dwelling (wet rooms):
    - For dwellings with 0 to 1 bedroom:

$$Q_{\text{total,Type1}} = 12\frac{L}{s}$$

4. Selected ventilation rate:
    - The greatest value among the above:

$$Q_{\text{Type1}} = 12\frac{L}{s}$$

5. Total ventilation for Type 1 dwellings:

$$Q_{\text{Total,type1}} = Q_{\text{Type1}} \times N_{\text{Type1}} = 12\frac{L}{s} \times 2 = 24\ L/s$$

For Type 2 Dwellings:

1. Minimum flow rate for dry rooms:
    - Number of bedrooms: 2
    - From Table 12: $Q_{\text{dry,type2}} = 12\frac{L}{s}$
2. Minimum flow rate for wet rooms:
    - The unheated room counts as a wet room.
    - Number of wet rooms: 1
    - Minimum ventilation per wet room: $Q_{\text{min,per wet room}} = 14\frac{L}{s}$
    - Therefore: $Q_{\text{wet,type2}} = 14\frac{L}{s}$
3. Minimum total flow rate per dwelling (wet rooms):
    - For dwellings with 1 to 2 bedrooms:

$$Q_{\text{total,type2}} = 24\ L/s$$

4. Selected ventilation rate:

- The greatest value among the above:

$$Q_{type2} = 24 \frac{L}{s}$$

5. Total ventilation for Type 2 dwellings:
    - $N_{type\ 2\ dwellings} = 61$
    - $Q_{totaltype2} = Q_{type2} \times N_{type2} = 1462 \frac{L}{s}$

Total Minimum Ventilation Flow Rate Required:

Adding the flow rates for both dwelling types:

$$Q_{Total} = 1488 \frac{L}{s}$$

Therefore, the minimum ventilation flow rate required for the entire building is 1,488 L/s.

Note: All calculations are based on the requirements specified in the CTE HS 3 and the data provided in Table 2. The unheated room is considered a wet room for the purposes of these calculations. The selected ventilation flow rate for each dwelling type is the highest value obtained from the three criteria, ensuring compliance with the minimum ventilation standards.

- **Climatic and solar data**

The data collection process using PVGIS was essential for acquiring detailed solar irradiance information specific to the selected site. Values for the hourly global solar radiation were downloaded to accurately represent the solar energy potential for the specific location. This high-resolution temporal data is crucial for precise modeling and simulation of the building's solar energy systems.

Due to the dual nature of the selected solar panels, which are hybrid systems capable of simultaneously converting solar energy into both electrical and thermal energy, the standard photovoltaic and thermal power outputs are not directly provided by PVGIS. The software typically generates data for conventional photovoltaic systems only. However, in this case, the hybrid functionality of the panels necessitates a customized approach to analyze their performance effectively.

Furthermore, PVGIS was instrumental in determining the optimal installation parameters for the solar panels. The software calculated the ideal tilt angle (Slope) and orientation (Azimuth) to maximize solar energy capture at the specified location. The **optimal Slope and Azimuth** were found to be **36°** and **-2°**, respectively. These values are particularly significant as they correspond closely to the geographic latitude and the optimal orientation toward the sun for the given site. By aligning the panels according to these calculated angles, the system can achieve maximum efficiency in converting available solar irradiance into usable energy.

These optimal positioning parameters are fundamental for the accurate sizing and design of the solar panel system. Proper alignment ensures that the panels receive the highest possible amount of solar radiation throughout the year, thereby enhancing the overall energy yield. This is especially important for hybrid panels, as maximizing both electrical and thermal outputs directly contributes to meeting the building's energy demands and sustainability objectives.

For simplicity, monthly average values of global solar irradiance are represented in Table 3.

Table 3: Average Global Irradiance for a typical day of each month

Hourly Irradiance [W/m2]																							
Hour of the day	00:45	01:45	02:45	03:45	04:45	05:45	06:45	07:45	08:45	09:45	10:45	11:45	12:45	13:45	14:45	15:45	16:45	17:45	18:45	19:45	20:45	21:45	22:45	23:45
Global Irradiance gennaio [W/m2]	0	0	0	0	0	0	0	0	0	91	341	491	598	647	608	531	408	244	2	0	0	0	0	0
Global Irradiance febbraio [W/m2]	0	0	0	0	0	0	0	0	1	209	407	560	687	700	709	615	493	328	116	0	0	0	0	0
Global Irradiance marzo [W/m2]	0	0	0	0	0	0	0	0	93	302	500	641	748	743	759	670	536	365	177	6	0	0	0	0
Global Irradiance aprile [W/m2]	0	0	0	0	0	0	0	24	179	370	541	672	754	790	768	664	544	376	194	37	0	0	0	0
Global Irradiance maggio [W/m2]	0	0	0	0	0	0	3	58	224	426	604	732	817	832	778	682	563	391	215	59	4	0	0	0
Global Irradiance giugno [W/m2]	0	0	0	0	0	0	15	62	234	437	623	769	848	875	844	748	623	436	247	80	22	0	0	0
Global Irradiance luglio [W/m2]	0	0	0	0	0	0	3	55	221	439	642	808	923	968	929	836	690	489	279	87	21	0	0	0
Global Irradiance agosto [W/m2]	0	0	0	0	0	0	0	35	202	427	639	808	921	970	938	838	675	471	254	62	1	0	0	0
Global Irradiance settembre[W/m2]	0	0	0	0	0	0	0	8	179	408	618	777	884	903	869	737	586	379	171	9	0	0	0	0
Global Irradiance ottobre [W/m2]	0	0	0	0	0	0	0	0	110	335	511	662	755	755	735	619	461	272	49	0	0	0	0	0
Global Irradiance novembre[W/m2]	0	0	0	0	0	0	0	0	4	236	408	563	639	646	595	489	360	172	0	0	0	0	0	0
Global Irradiance dicembre [W/m2]	0	0	0	0	0	0	0	0	0	157	371	523	634	645	612	517	380	178	0	0	0	0	0	0

2.2 Building modeling using HULC

- **Description of the software**

HULC (Herramienta Unificada LIDER Calener) is an advanced tool developed for energy certification and simulation of buildings, in compliance with the Spanish Technical Building Code (Código Técnico de la Edificación, CTE). It integrates the functionalities of previous tools LIDER and CALENER, offering a unified platform for comprehensive energy performance assessment of buildings.

A key feature of HULC is its ability to create highly detailed three-dimensional geometrical models. Users can precisely reconstruct the building's physical structure, defining exact dimensions, shapes, and orientations of architectural elements such as walls, floors, roofs, windows, and doors. This detailed geometric modeling is essential for accurately simulating how the building interacts with environmental factors like solar radiation, wind, and temperature variations.

Moreover, HULC allows for the specification of material properties for every component of the building. Users can assign specific materials to each element, including thermal conductivity, density, specific heat capacity, and thickness. The software includes a comprehensive database of construction materials compliant with Spanish regulations, but it also permits the input of custom materials to reflect innovative or non-standard construction practices.

By incorporating detailed material characteristics, HULC can simulate the thermal behavior of the building envelope with high accuracy. It calculates thermal transmittance (U-values) for all building elements, considering factors such as insulation levels, thermal bridges, and material layering. This precision enables the assessment of heat transfer through the building fabric, which is crucial for evaluating heating and cooling demands.

For the building under analysis, HULC's advanced modeling capabilities facilitate a meticulous representation of its unique architectural features and construction techniques. The software's ability to model complex geometries and assign specific materials to each component allows for an accurate simulation of the building's energy performance under real-world conditions.

In addition, HULC integrates climatic data specific to the building's location, including solar irradiance, temperature profiles, humidity levels, and wind patterns. This data is crucial for assessing how the building interacts with its environment over time. The software performs dynamic simulations that consider hourly variations in weather conditions, enabling a comprehensive analysis of energy consumption throughout the year.

HULC also supports the input of building usage patterns, occupancy schedules, and internal heat gains from occupants, equipment, and lighting. Users can define HVAC systems, ventilation strategies, and renewable energy technologies integrated into the building. This holistic approach allows for the evaluation of different design options and operational strategies to optimize energy efficiency.

The software generates detailed reports on the building's energy demand for heating, cooling, domestic hot water, and lighting. It provides insights into potential areas for improvement and verifies compliance with regulatory requirements. HULC's outputs are essential for architects, engineers, and energy consultants aiming to enhance building performance and achieve sustainability goals.

In summary, HULC is a powerful tool that enables the creation of highly detailed three-dimensional building models, incorporating precise geometries and material properties of every component. Its advanced simulation capabilities allow for accurate assessment of the building's thermal behavior and energy performance. By utilizing HULC, professionals can optimize building designs to maximize energy efficiency, reduce operational costs, and contribute to environmental sustainability.

- **Reconstruction of the building model**

Using HULC, the building was meticulously modeled by adhering closely to the technical specifications provided in the documentation of the project.

The geometrical features were accurately reconstructed to ensure a reliable representation of the physical structure within the simulation environment. For illustrative purposes, an image of the finalized model is included, showcasing the outcome of the modeling process. Detailing the entire procedure would be excessively lengthy for the purposes of this thesis, so image 2 serves to effectively convey the essential aspects of the modeling work.

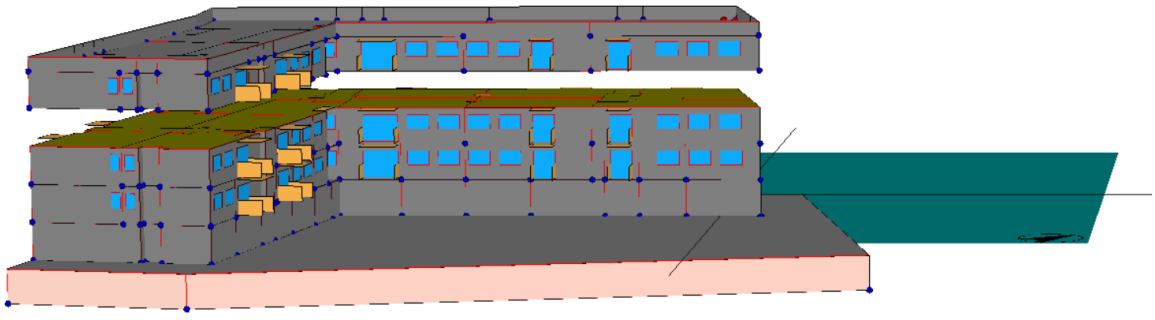

Figure 2: model of the building implemented in HULC

2.3 Modeling of the swimming pool

- **Calculations to obtain the dimensions of the swimming pool**

The dimensions necessary for the analysis of the two swimming pools were obtained directly from the project documentation. The building is equipped with two swimming pools: one designed for adults, and one intended for children. These pools have different sizes and specifications to accommodate their respective users.

Detailed measurements are presented in Tables 4 through 7, which include comprehensive data on both pools. The tables provide dimensions such as length, width, depth, and total volume. Additionally, they include calculations of the free surface area and the lateral surface area for each pool.

Accurately determining these dimensions is essential for performing precise thermal and energy calculations. The data provided serves as the foundation for modeling the energy demands of the pools, enabling the design of efficient heating and maintenance systems that meet the operational requirements.

Table 4: Adults' swimming pool dimensions.

Adults' swimming pool		
Variable	Name	Value
V_{a}	Volume Adult pool	$65{,}7\ m^3$
d_{a}	Deepness of the Adult pool	$2\ m$
L_{a}	Length Adult pool	$5{,}73\ m$

Table 5; Children's swimming pool dimensions.

Children's swimming pool		
Variable	Name	Value
V_{c}	Volume Children's pool	$2{,}4\ m^3$
d_{c}	Deepness Children's pool	$0{,}4\ m$
L_c	Length Children's pool	$2{,}45\ m$

Table 6: Adults' swimming pool calculations.

Adults' swimming pool calculations			
Variable	Name	Equation	Value
A_{fa}	Free surface Adults' Swimming pool	$\frac{V_{\mathrm{a}}}{d_{\mathrm{a}}}$	$32{,}85\ m^2$
A_{la}	Lateral surface Adults' swimming pool	$\sqrt{A_{\mathrm{fa}}} * 4 * d_{\mathrm{a}}$	$45{,}85\ m^2$

Table 7: Children's swimming pool calculations.

Children's swimming pool calculations			
Variable	Name	Equation	Value
A_{fc}	Free surface Children's Swimming pool	$\frac{V_{\mathrm{c}}}{d_{\mathrm{c}}}$	$6\ m^2$
A_{lc}	Lateral surface Children's swimming pool	$\sqrt{A_{\mathrm{fc}}} * 4 * d_c$	$3{,}92\ m^2$

- **Swimming pool energy balance: assumptions and calculations.**

Assumptions: To perform the energy balance analysis of the swimming pools, several assumptions were established to simplify the calculations and ensure consistency. These assumptions are detailed as follows:

1. Division of Calculation Periods: The analysis was segmented into two distinct periods based on seasonal thermal characteristics:
    - May to September: Designated as the summer thermal period, characterized by higher ambient temperatures and increased solar irradiance.
    - October to April: Designated as the winter thermal period, associated with lower ambient temperatures and reduced solar exposure.
2. Use of Seasonal Average Values: To calculations, seasonal average values were utilized for key environmental parameters:
    - Representative average ambient air temperatures for each period.
    - Average temperatures of the incoming water supply.
    - Average wind speeds affecting convective heat transfer at the pool surface.

These average values provide a realistic approximation of environmental conditions over the respective periods.

3. Operational Hours and Pool Cover Usage:
    - May to September:
        - The swimming pool operates for 12 hours daily, during which it is exposed to ambient conditions and subject to thermal losses.
        - For the remaining 12 hours, the pool is covered with a high thermal resistance tarp, significantly reducing thermal losses due to evaporation, convection, and radiation.

- Thermal losses during the covered hours are considered negligible and are therefore excluded from the calculations.
- Total number of days: 153 days.
- Total operational hours: 1.836 hours.
- Total period hours: 3.672 hours.

- October to April:
  - The swimming pool operates for 8 hours daily.
  - For the remaining 16 hours, the pool remains covered, reducing thermal losses as described above.
  - Thermal losses during covered hours are likewise neglected.
  - Total number of days: 211 days.
  - Total operational hours: 1.688 hours.
  - Total period hours: 5.064 hours.

4. Constant Pool Water Temperature: The set-point temperature of the swimming pool water is maintained at 25°C throughout the entire year, regardless of seasonal variations. This assumption simplifies thermal calculations by providing a consistent reference temperature for assessing heat losses.
5. Negligible Heat Gains from Solar Radiation: It is assumed that any heat gains from direct solar radiation on the pool surface are negligible or effectively offset by concurrent losses. Therefore, solar gains are not explicitly included in the energy balance calculations.
6. Steady-State Conditions: The calculations presume steady-state thermal conditions during each operational period. Transient effects and the thermal inertia of the pool structure and water are not considered, which simplifies the mathematical modeling.
7. Uniform Ground Temperature: The ground temperature adjacent to the pool walls and bottom is assumed to be constant for each period to facilitate the calculation of conduction losses:
   - May to September: T_{ground}=18°C, representing the average ground temperature during the warmer months.
   - October to April: T_{ground} =12°C, representing the average ground temperature during the cooler months.
8. Water Renewal Rate: The pool water is assumed to be renewed at a continuous rate of 2.5% of the total water volume per day to maintain water quality standards. This renewal process is considered to occur uniformly over each 24-hour period.

9. Wind Speed at Pool Surface: The wind speed impacting the pool surface is assumed to be equal to the measured ground-level wind speed for the location. This simplification aids in calculating convective and evaporative heat losses without accounting for potential variations in microclimate conditions.

The values assumed are presented in Tables 8 through 13.

Note: The assumptions outlined above are critical for standardizing the calculation process and ensuring that the energy balance accurately reflects the operational conditions of the swimming pools. By establishing clear parameters and conditions, the analysis can effectively inform the design and optimization of the heating systems required to maintain the desired water temperature.

Table 8: Monthly net water temperature, from "DBHE 2019- ANEJO G".

	January	February	March	April	May	June	July	August	September	October	November	December
Net water Temperature [°C]	8	8	10	12	14	17	20	19	17	13	10	8

Table 9: Average net water temperature for the thermal period considered, from "DBHE 2019- ANEJO G".

Period	Average Temperature Values [°C]
May-September	17,4
October-April	9,5

Table 10: Monthly ambient temperature values, from the NASA database, year 2022.

	January	February	March	April	May	June	July	August	September	October	November	December
Ambient Temperature [°C]	5	7	10	12	18	24	28	27	21	16	9	6

Table 11: Average ambient temperature values for each thermal period, considered for the calculations.

Period	Average Temperature Values [°C]
May-September	23,6
October-April	8,5

Table 12: Monthly wind speed values.

	January	February	March	April	May	June	July	August	September	October	November	December
Wind speed [km/h]	8,8	7,9	11	11,6	10,5	10,6	11	10,5	9,2	9,4	11,7	7,7
Wind speed [m/s]	2,44	2,19	3,06	3,22	2,92	2,94	3,06	2,92	2,56	2,61	3,25	2,14

Table 13: Average wind speed values for each thermal period.

Period	Average Temperature Values [m/s]
May-September	2,88
October-April	2,70

Energy Balance calculation display: Image 3 shows the energy balance for the swimming pool, with all the inlet and outlet heat fluxes.

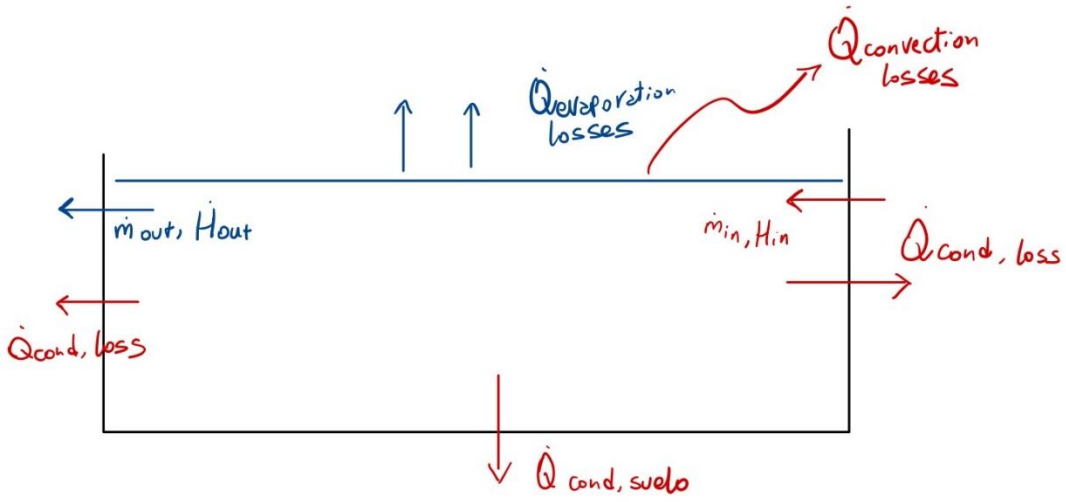

Figure 3: Swimming pool heat flows.

Equations to obtain the losses values:

1. Evaporation Losses

Here, the ASHRAE 2007 method has been utilized. It uses an empirical correlation to calculate the emission tax, the evaporation mass flow. It is given in kg/h; The formula is the following:

$$(1) \qquad E = \frac{(0{,}089 + 0{,}0782 v_{\mathrm{air}}) A_{\mathrm{p}} \Delta P}{L}$$

Where:

- L is the latent evaporation heat, equal to 2272 $\frac{kJ}{kg}$
- v_{air} is the average value of the wind speed on the swimming pool surface, considered equal to the wind ground speed, in $\frac{m}{s}$
- A_p is the free surface of the swimming pool, in m^2
- $\Delta P = P_w - P_a$, where P_w is the saturation air pressure at the temperature of the water and P_a is the vapor air pressure at ambient temperature.

Using this E, the power losses due to evaporation are obtain as follows:

$$(2) \qquad \dot{Q}_{\mathrm{evap}} = E[L + C_{\mathrm{s}}(T_{\mathrm{wp}} - T_{\mathrm{wn}})]$$

Where:

- E is expressed in kg/s.
- $C_{\mathrm{s}} = 4{,}186\ \frac{kJ}{kgK}$
- Twp is the set point temperature for the swimming pool, 25°C.
- Twn is the net water temperature.

2. Renovation Losses

The water in the pools must be renewed. Typically, a 2.5% renewal of the total water volume during the day is considered. Additionally, the water renewal is a process that is carried out continuously throughout the day. So, in the equation, this is the reason why an 86400 coefficient appears. It is the total amount of seconds in the day.

$$(3) \qquad \dot{Q}_{\mathrm{renov}} = \frac{m_{\mathrm{wp}} R}{86400} C_{\mathrm{p}} (T_{\mathrm{wp}} - T_{\mathrm{wn}})$$

Where:

- m_{wp} is the total mass of the swimming pool, 86100 kg.
- R is the renovation tax, 2,5%
- The others are already explained above.

3. Convection Losses

These losses involve the free surface of the pool. The formula is as follows:

$$(4) \qquad \dot{Q}_{\mathrm{conv}} = hA\Delta T$$

Where:

- h=convective heat transfer coefficient; For calm water surfaces it is equal to $0{,}6246\ \frac{W}{m^2K}$
- A is the free surface of the swimming pool.
- $\Delta T = T_{\text{pool}} - T_{\text{ambient}}$

4. Irradiation losses

The irradiation losses are given by the following formula:

(5) $\dot{Q}_{\text{irrad}} = \varepsilon\sigma A(T_{\text{pool}}^4 - T_{\text{ambient}}^4)$

Where:

-ε is the emissivity of the water. Its average value is set to be equal to 0,87.

-σ is the Boltzman constant, equal to $5{,}67x10^{-8}\ \frac{W}{m^2K^4}$

5. Conduction losses

These losses involve the side surface and the bottom of the pool. The pool walls are considered to have thicknesses of 300 mm for the side surface and 800 mm for the bottom surface, both made of concrete. The formula for calculating conduction losses is as follows:

(6) $\dot{Q}_{\text{conduction}} = U_{\text{lat}}A_{\text{lat}}(T_{\text{water}} - T_{\text{ground}}) + U_{\text{ground}}A_{\text{ground}}(T_{\text{water}} - T_{\text{ground}})$

Where:

- U_{lat} is equal to $2{,}94\ \frac{W}{m^2K}$ for vertical surfaces made of concrete, with a thickness of 300mm.
- $U_{ground} = 0{,}5\ \frac{W}{m^2K}$ for horizontal surfaces made of concrete, with a thickness of 800mm.
- T_{ground} is the temperature of the ground. Later assumptions on its value will be made.
- $\text{A}_{\text{ground}} = A_{freesurface}$

Results: The results will be divided into two groups: the first will show the figures related to the period May-September, and the second will show what was obtained for the period October-April.

1. May-September

Evaporation Losses

By using the equation (1), and setting these values:

- $\Delta P = P_{\mathrm{w}}(25°C) - P_{\mathrm{a}}(23{,}6°C)$=262,2 Pa
- $P_{\mathrm{w}}(25°C)$=3169,2 Pa [23]
- $P_{\mathrm{a}}(23{,}6°C)$=2907 Pa [22]
- $v_{\mathrm{air}} = 2{,}88\ m/s$

$E = 1{,}41\frac{kg}{h} = 0{,}000391\frac{kg}{s}$ is obtained.

Now, using equation (2) and setting

- $T_{\mathrm{wn}} = 17{,}4°C$

$\dot{Q}_{\mathrm{evap}} = 0{,}90155kW$

Now, considering a total hour of 1836, which is the number of hours in which the swimming pool remains open to the ambient, the energy losses are:

$Q_{\mathrm{evap}} = \dot{Q}_{\mathrm{evap}} * \ t = 1655{,}24\ kWh$

Renovation Losses

Using equation (3) and setting $T_{\mathrm{wn}} = 17{,}4\ °C$, the following figure is obtained:

$\dot{Q}_{\mathrm{rennov}} = 0{,}6269\ kW$

And, considering an operation time equal to the total amount of hour in this period, so 3672 h, the energy is obtained:

$Q_{\mathrm{renov}} = \dot{Q}_{\mathrm{renov}} * \ t = 2301{,}9\ kWh$

Convection Losses

Using equation (4), with

- $\Delta T = T_{\mathrm{pool}} - T_{\mathrm{ambient}}$ *=1,4°C*

$\dot{Q}_{\mathrm{convection}} = 0{,}034kW$

Considering t=1836h, exactly the time in which the swimming pool remains open,

$Q_{\mathrm{conv}} = \dot{Q}_{\mathrm{conv}} * \ t = 62{,}37\ kWh$

Irradiation Losses

Setting $T_{\mathrm{ambient}} = 23{,}6°C$, and using (5)

$\dot{Q}_{\mathrm{irradiation}} = 0{,}2824kW$

Also in this case, the operation time is 1836h, so that

$Q_{\mathrm{irradiation}} = \dot{Q}_{\mathrm{irradiation}} * t = 518{,}56kWh$

Conduction Losses

Using (6) and setting $T_{\text{ground}} = 18°C$, an average value for the period May-September, this result is obtained:

$\dot{Q}_{\text{conduction}} = 0{,}392\ kW$

And considering an operation time equal to the total amount of hour in the period, so 3672 h,

$Q_{\text{conduc}} = \dot{Q}_{\text{cond}} * \ t = 1439{,}6\ kWh$

2. October-April

Evaporation Losses

By using the equation (1), and setting these values:

- $\Delta P = P_{\text{w}}(25°C) - P_{\text{a}}(8{,}5°C)$=2061,2 Pa
- $P_{\text{w}}(25°C)$=3169,2 Pa [23]
- $P_{\text{a}}(8{,}5°C)$=1108 Pa [22]
- $v_{\text{air}} = 2{,}7\ m/s$

$E = 10{,}58 \frac{kg}{h} = 0{,}002939 \frac{kg}{s}$ is obtained.

Now, using equation (2) and setting

- $T_{\text{wn}} = 9{,}5°C$

$\dot{Q}_{\text{evap}} = 6{,}87 kW$

Now, considering a total hour of 1688, which is the total number of hours in which the swimming pool remains open to the ambient, the energy losses are:

$Q_{\text{evap}} = \dot{Q}_{\text{evap}} * \ t = 11591{,}34\ kWh$

Renovation Losses

Using equation (3) and setting $T_{wn} = 9{,}5\ °C$, the following figure is obtained:

$\dot{Q}_{\text{rennov}} = 1{,}28\ kW$

And, considering an operation time equal to the total amount of hour in this period, so 5064 h, the energy is obtained:

$Q_{\text{renov}} = \dot{Q}_{\text{renov}} * \ t = 6474{,}4\ kWh$

Convection Losses

Using equation (4), with

- $\Delta T = T_{\text{pool}} - T_{\text{ambient}}$=16,5 °C

$\dot{Q}_{\text{conv}} = 0{,}4kW$

Considering t=1688h, exactly the time in which the swimming pool remains open,

$Q_{\text{conv}} = \dot{Q}_{\text{conv}} * \ t = 675{,}85\ kWh$

Irradiation Losses

Setting $T_{ambient} = 8{,}5°C$, and using (5)

$\dot{Q}_{\text{irradiation}} = 3{,}08kW$

Also in this case, the operation time is 1688h, so that:

$Q_{\text{irradiation}} = \dot{Q}_{\text{irradiation}} * t = 5206{,}02kWh$

Conduction Losses

Using (6) and setting $T_{\text{ground}} = 12°C$, an average value for the period April-October, this result is obtained:

$\dot{Q}_{\text{conduction}} = 0{,}728\ kW$

And considering an operation time equal to the total amount of hour in the period, so 5064 h,

$Q_{\text{cond}} = \dot{Q}_{\text{cond}} * \ t = 3687{,}04\ kWh$

Now, by summing all the data obtained, each related to its own period, the values in table 14 are obtained, related to the total energy demand of the pool.

Table 14: Total thermal energy demand of the swimming pool.

Period	May-September	October-April
Total Demand [kWh]	8.800	34.900

3. Solar Control strategies

After establishing the building model in HULC and configuring the essential input parameters - including climatic zone, location, and building type, as detailed in the attached figure 4 for brevity - a preliminary simulation was conducted.

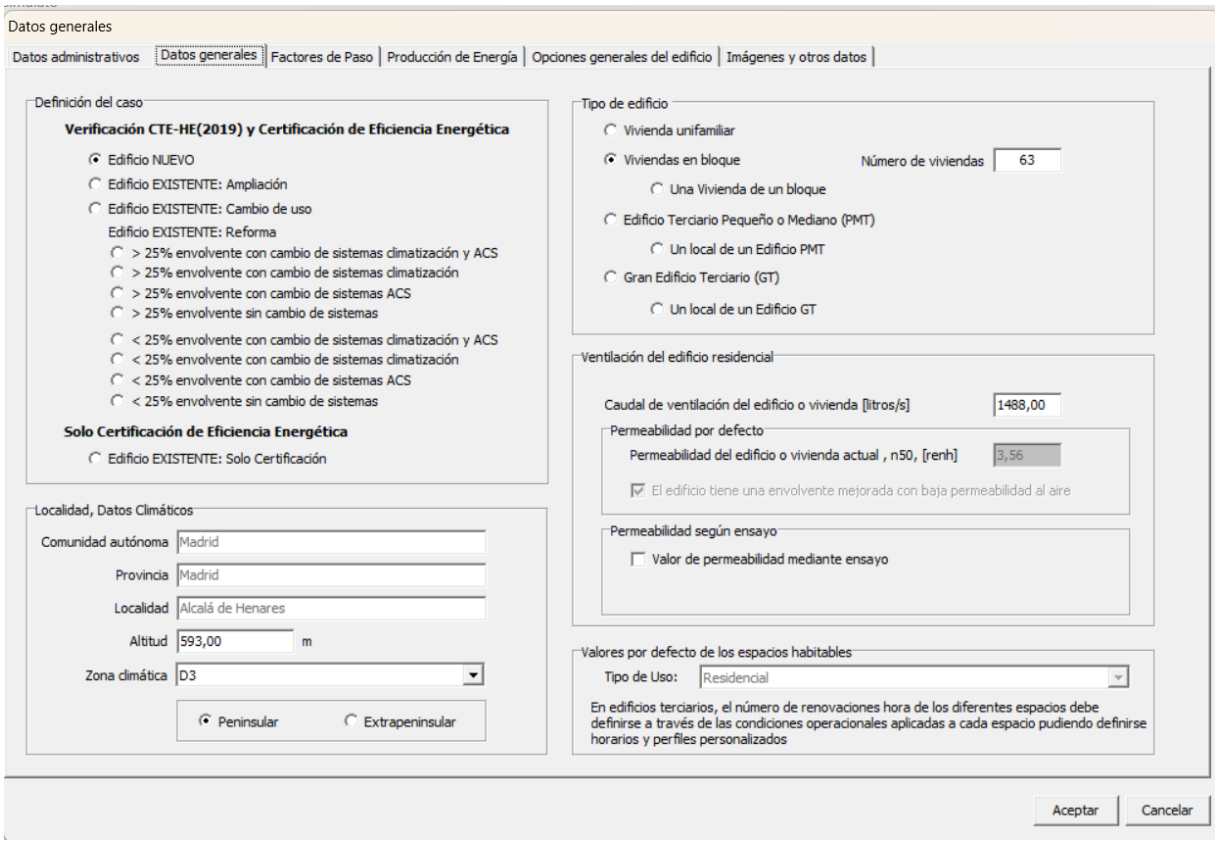

Figure 4: HULC input data.

This initial simulation revealed that the building's **solar control** was inadequate, exceeding the maximum limits imposed by regulations for new constructions (2 kWh/mq). Specifically, the simulation indicated that the building was subject to excessive solar gains, which could lead to overheating during peak sun exposure periods and increased energy consumption for cooling systems.

Calidad de la envolvente térmica

		Valores límite	
Transmitancia térmica global, K [W/m²K]	0.52	0.58	CUMPLE
Demandas del edificio Objeto:			
- Calefacción [kWh/m²año]	25.17		
- Refrigeración [kWh/m²año]	15.14		
Control solar, q_sol;jul [kWh/m².mes]	5.50	2.00	NO CUMPLE
Relación de cambio de aire a 50 Pa, n50 [1/h]	3.56	5.08	CUMPLE
Compacidad [m³/m²]	2.61		
Superficie útil de cálculo, Aútil [m²]	5144.95		
Superficie de cerramientos opacos, Aopacos [m²]	8161.16		
Superficie de huecos, Ahuecos [m²]	494.39		
Longitud de puentes térmicos, Lpt [m]	2697.75		

Detalle por componentes:

Huecos | Opacos | Puentes Térmicos | Espacios

Núm.	Nombre	Construcción	Área [m²]	U [W/m²K]	Orientación	% Marco	g_gl;wi	g_gl;sh,wi	F_sh;obst	Ganancia_jul [kWh/m²]
1	P03_E01_PE001_V	ventanas	2.01	2.02	NO	10.00	0.70	0.63	0.99	51.31
2	P03_E01_PE002_V	puertas	5.50	2.52	NO	10.00	0.70	0.63	0.99	51.31
3	P03_E01_PE003_V	ventanas	0.80	2.02	NE	10.00	0.70	0.63	1.00	46.55
4	P03_E02_PE002_V	ventanas	3.85	2.02	SE	10.00	0.70	0.63	1.00	61.69
5	P03_E02_PE003_V	ventanas	2.01	2.02	SE	10.00	0.70	0.63	1.00	61.71
6	P03_E02_PE004_V	ventanas	2.01	2.02	SE	10.00	0.70	0.63	1.00	61.71
7	P03_E02_PE004_V_1	ventanas	2.01	2.02	SE	10.00	0.70	0.63	1.00	61.71
8	P03_E02_PE005_V	ventanas	1.86	2.02	NE	10.00	0.70	0.63	1.00	46.55
9	P03_E04_PE001_V	puertas	5.50	2.52	NO	10.00	0.70	0.63	0.99	51.31
10	P03_E04_PE002_V	ventanas	2.01	2.02	NO	10.00	0.70	0.63	0.99	51.31
11	P03_E04_PE002_V_1	ventanas	2.01	2.02	NO	10.00	0.70	0.63	0.99	51.31
12	P03_E05_PE004_V	ventanas	2.01	2.02	SE	10.00	0.70	0.63	0.98	60.98
13	P03_E05_PE004_V_1	ventanas	2.01	2.02	SE	10.00	0.70	0.63	0.99	61.30
14	P03_E05_PE005_V	puertas	3.85	2.52	SE	10.00	0.70	0.63	0.99	61.65
15	P03_E06_PE001_V	ventanas	2.01	2.02	NO	10.00	0.70	0.63	0.99	51.31
16	P03_E06_PE001_V_1	ventanas	2.01	2.02	NO	10.00	0.70	0.63	0.99	51.31

Figure 5: Thermal behavior of the building.

Conversely, the value obtained for the global thermal transmittance was encouraging, suggesting that the building's insulation levels were satisfactory and met the required standards. The favorable U-value indicates that the building envelope effectively reduces heat transfer through conduction, thereby minimizing heating and cooling loads associated with thermal transmission.

To address the identified issue with solar control, a decision was made to implement additional measures aimed at enhancing the building's ability to manage solar radiation. Devices dedicated to improving solar control were incorporated, specifically through the installation of internal blinds and external shading devices on windows and doors. These solutions are designed to reduce the amount of direct solar radiation entering the building, thereby preventing excessive heat gain and improving indoor thermal comfort. By combining both internal and external shading solutions, the building can effectively mitigate solar heat gain while still allowing for natural daylighting and maintaining views to the outside.

In figure 6 are attached all the devices decided to be suitable for the goal. In figure 6 the monetary investment for the specific number of each device can be detected. For the price of each device, the mean value of each device is taken into account in order to simplify the study.

Name		N° units	Price per unit, €	Total price, €
PASTEL COLOR OUTDOOR SHUTTERS (V 1750X1150 mm)	UD	104	216,84	22551,36
PASTEL COLOR OUTDOOR SHUTTERS (V 700X1150 mm)	UD	20	128,4	2568
WHITE COLOR INDOOR CURTAINS (P 2500X2200 mm)	UD	40	180,89	7235,6
WHITE COLOR INDOOR CURTAINS (P 1750X2200 mm)	UD	8	126,63	1013,04

Figure 6: Solar control improvements.

These modifications were then integrated into the existing building model in HULC. The simulation was rerun with the updated parameters to evaluate the effectiveness of the implemented solar control measures. The results demonstrated a significant improvement in the building's solar control performance. The solar gain values were reduced to levels within the limits prescribed by the regulations, ensuring compliance with legal requirements for new constructions. In figure 7 these improvements can be detected.

Figure 7: Results of the solar control improvements strategies.

Furthermore, the solar control contributed to a reduction in the building's cooling loads, leading to potential energy savings and improved operational efficiency. By minimizing unwanted solar heat gain, the building's reliance on mechanical cooling systems can be decreased, resulting in lower energy consumption and reduced greenhouse gas emissions associated with electricity use. This not only benefits the building's operational costs but also aligns with broader sustainability goals and environmental considerations. It can be noticed on HULC that the energy demand for cooling decreases from a value of 15,14 $\mathrm{kWh/m^2_{year}}$ to a value equal to 9,71 $\mathrm{kWh/m^2_{year}}$, resulting in a 35% reduction of this energy demand.

This iterative process underscores the importance of integrating effective solar control strategies during the design phase of a building project. Incorporating shading devices is a cost-effective strategy that can significantly enhance a building's performance without the

need for extensive modifications to the original design. It demonstrates how relatively simple additions can have a substantial impact on energy consumption and regulatory compliance.

In conclusion, the initial simulation identified a critical issue with solar control that could have negatively affected the building's energy performance and compliance with legal standards. Through the strategic implementation of internal and external shading devices, the building's solar gains were successfully reduced to acceptable levels.

4. Selection of the appropriate Energy System Equipment

In this section, the systems selected for the building's energy sizing will be presented, along with the selection criteria adopted. A detailed description of the systems currently less known in the market will also be provided, with particular emphasis on their technical characteristics and potential applications.

4.1 Selection Criteria

The selection of equipment for the energy systems in this project was guided by a comprehensive set of criteria aimed at achieving maximum energy efficiency, minimizing environmental impact, and optimizing the exploitation of renewable energy sources, particularly solar energy. A primary objective of the study was to harness, to the fullest extent possible, the most abundant and freely available energy resource on Earth—solar energy—especially given the favorable climatic conditions of Madrid, where the building is situated. This focus on solar energy utilization played a pivotal role in determining the technologies and equipment integrated into the building's energy system.

In striving for energy efficiency, the selection process prioritized equipment and technologies that demonstrated superior operational efficiency and low energy consumption. Machines capable of delivering the required thermal and electrical outputs with minimal energy input were considered essential to reduce operational costs and decrease the building's overall energy demand. This approach aligns with broader sustainability goals, as reducing energy consumption directly contributes to lowering greenhouse gas emissions associated with energy production. High-efficiency equipment not only reduces operational expenses but also enhances the building's performance in terms of energy utilization, thereby contributing to a more sustainable built environment.

Environmental impact was a critical consideration throughout the selection process. Technologies that minimized emissions, utilized environmentally friendly refrigerants, and had a lower ecological footprint were favored. The integration of equipment capable of exploiting abundant or "free" energy sources, such as solar radiation, was deemed essential to reduce reliance on fossil fuels and mitigate the environmental impact of the building's energy consumption. By selecting technologies that leverage renewable energy and minimize harmful emissions, the project aims to contribute positively to environmental sustainability and align with global efforts to combat climate change.

The capacity to harness renewable energy sources, particularly solar energy, was central to the equipment selection. Given Madrid's advantageous climatic conditions, characterized by high levels of solar irradiance, the potential for solar energy exploitation is significant. Therefore, technologies that could efficiently capture and convert solar energy into usable thermal and electrical energy were prioritized. The selection of hybrid solar panels, capable of simultaneously generating electrical and thermal energy, exemplifies this criterion. These panels maximize the utilization of the available solar resource, enhancing the overall energy efficiency of the building's systems and reducing dependence on external energy supplies.

Moreover, the integration of adsorption chillers was a strategic decision aimed at leveraging the thermal energy produced by the solar panels. Adsorption chillers can produce cooling using thermal energy with minimal electrical consumption, making them highly efficient and environmentally friendly. By utilizing the thermal energy generated by the hybrid solar panels, the adsorption chillers form a synergistic relationship with the solar energy system, enhancing the overall efficiency of the energy system and reducing electrical consumption. This integration is particularly advantageous during periods of high solar irradiance, which coincides with peak cooling demand, thus aligning energy supply with demand and optimizing system performance.

The selection of air-to-water heat pumps also aligns with the criteria of energy efficiency and environmental sustainability. These heat pumps are highly efficient in transferring heat from the ambient air to water for heating purposes and can also provide cooling. They exploit an abundant and renewable energy source - the ambient air - which contributes to reducing the building's dependence on non-renewable energy sources. Their high coefficients of performance mean that they can deliver more heating or cooling energy than the electrical energy they consume, further enhancing energy efficiency and contributing to operational cost savings.

In addition, the incorporation of thermal energy storage systems was considered essential to improve the management of energy supply and demand. By storing excess thermal energy produced during periods of high solar irradiance, these systems enable the energy system to balance energy availability with consumption needs, reducing waste and enhancing efficiency. This approach contributes to lowering operational costs and maximizing the utilization of renewable energy sources. Thermal energy storage provides flexibility in energy management, allowing for the decoupling of energy production and consumption, which is particularly valuable in systems reliant on variable renewable energy sources like solar power.

Phase Change Materials (PCMs) were also considered for integration into the building's envelope to enhance thermal inertia and improve energy efficiency. PCMs can absorb and release thermal energy during phase transitions, helping to stabilize indoor temperatures and reduce heating and cooling loads. This passive energy-saving technology contributes to reducing energy consumption without requiring additional energy input, aligning with the criteria of energy efficiency and environmental sustainability. The use of PCMs enhances the building's ability to maintain comfortable indoor conditions with less reliance on active heating and cooling systems, thus contributing to energy savings and improved occupant comfort.

The adaptability of equipment to the specific climatic conditions of Madrid was another significant consideration in the selection process. Equipment needed to perform optimally under the local temperature ranges, solar irradiance levels, and other weather-related factors to ensure efficiency and reliability. Technologies well-suited to the climatic conditions can operate more efficiently and have longer lifespans, reducing maintenance requirements and enhancing the overall performance of the energy system.

Operational reliability and maintenance considerations were important factors as well. Equipment with proven reliability, lower maintenance requirements, and longer lifespans were preferred to ensure uninterrupted operation and reduce long-term costs. Reliable equipment reduces the risk of system failures and associated downtime, which can negatively impact building operations and occupant comfort. By selecting robust and dependable technologies, the project aims to ensure consistent performance and minimize maintenance-related disruptions and expenses.

Economic feasibility was also a critical criterion in the selection process. While advanced technologies often involve higher initial investments, the selection process aimed to balance performance with cost-effectiveness. The potential for operational cost savings through reduced energy consumption and the utilization of free energy sources like solar radiation was considered to enhance the economic viability of the selected technologies. Life-cycle cost analyses were performed to assess the long-term financial benefits of the equipment, considering factors such as energy savings, maintenance costs, and potential incentives or subsidies for renewable energy systems.

Furthermore, the compatibility and integration of the selected technologies were important to ensure that the various components of the energy system would work together effectively. The seamless integration of hybrid solar panels, adsorption chillers, heat pumps, thermal energy storage systems, and PCMs enhances the overall efficiency of the system. By designing the energy system with components that complement each other, the project maximizes the benefits of each technology and creates a synergistic effect that improves performance and sustainability.

In conclusion, the selection criteria for the energy system equipment were centered around maximizing the use of abundant and free solar energy, enhancing energy efficiency, minimizing environmental impact, ensuring reliability, and achieving economic feasibility. By selecting technologies that meet these criteria, such as hybrid solar panels, adsorption chillers, air-to-water heat pumps, thermal energy storage systems, and phase change materials, the project aims to create a highly efficient and sustainable energy system. This system leverages the abundant solar resource available in Madrid to meet the building's energy demands effectively, reduces operational costs, and contributes to environmental sustainability. The integration of these technologies demonstrates how advanced energy systems can be designed to exploit renewable energy sources, optimize performance, and align sustainability objectives in modern building design.

4.2 Selected system description: Adsorption Chiller

4.2.1 Principles of operation

In this system, a pair consisting of a solid adsorbent material and a refrigerant liquid is utilized. The adsorbent material adsorbs and releases the refrigerant liquid through physical interactions, such as Van der Waals forces. Due to the nature of these attractive forces, the adsorbent and refrigerant can be decoupled by applying thermal energy.

As the solid sorbent cannot circulate due to its chemical properties, adsorption chillers are designed with two separate chambers, each containing the adsorbent material. These chambers are enclosed in a vacuum-sealed unit, along with the evaporator and condenser, to ensure optimal operation.

General definition of the COP, Coefficient of Performance

In general, the coefficient of performance is defined as follows:

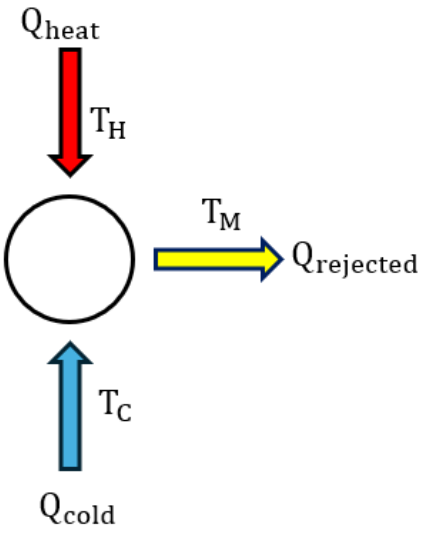

Figure 8: general scheme of a chiller.

$$COP = \frac{Q_{cold}}{Q_{hot} + W_{pump}}$$

In an adsorption chiller, $W_{pump} = 0$.

The II Law of Thermodynamics applied to the basic process of a thermally driven chiller (according to the scheme shown in Figure), leads to an expression for the maximum possible coefficient of performance, COP_{ideal}:

$$COP_{ideal} = \frac{T_C}{T_H} \times \frac{T_H - T_M}{T_M - T_C}$$

Detailed description of the process

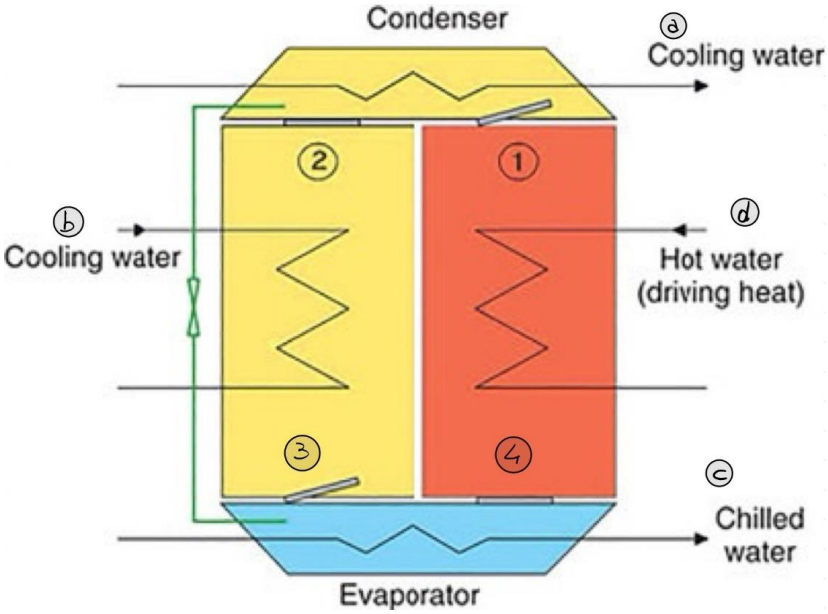

Figure 9: adsorption chiller scheme.

- Phase 1: Desorption process

The initial state is characterized by the refrigerant liquid being adsorbed into the solid sorbent material within the right chamber (depicted in orange). The solid adsorbent material, which contains water, is heated by the hot water flowing through the right pipeline (stream ‘d’). As a result of this heating, the water previously adsorbed in the solid sorbent is desorbed. In systems of this type, the water temperature within the pipeline typically ranges between 60 and 80°C when sourced from thermal-solar collectors, temperatures that are readily achievable using solar thermal panels.

When valve number one (labeled 1 in Fig. 9) is opened, water vapor flows into the condenser. Condensation occurs when the pressure in the orange chamber exceeds the saturation pressure corresponding to the condenser temperature, and only when the condenser temperature is lower than that of the vapor. The valve is closed once all the generated vapor has entered the condenser. At this stage, it is necessary to remove heat from the vapor originating from the adsorbent material. A common approach, as illustrated in the accompanying figure, involves circulating cooling water through the condenser (stream ‘a’ in Fig. 9), ensuring it is at a lower temperature than the vapor being cooled. This cooling water is typically sourced from the outlet of stream 'b', as shown in Fig. 10.

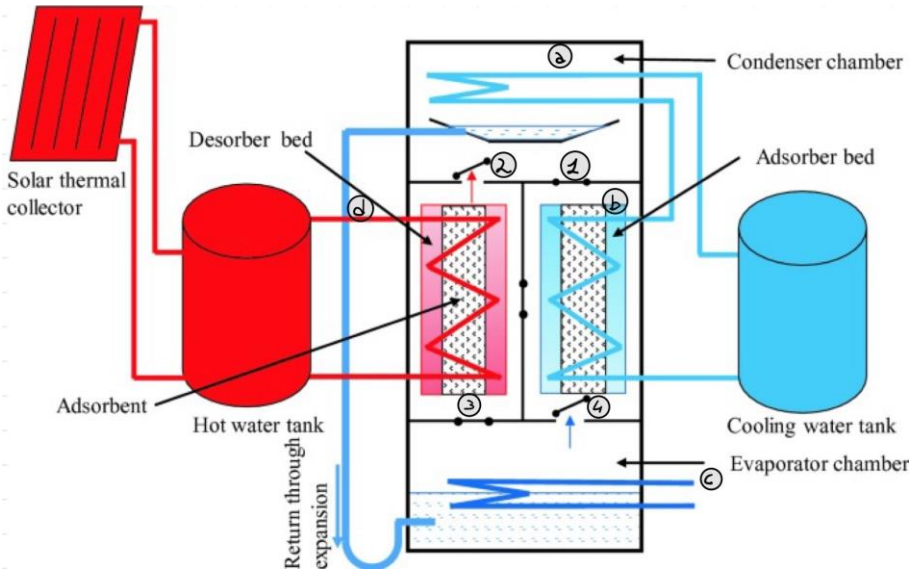

Figure 10: adsorption chiller connected to a solar pannel.

In extreme cases, cooling towers may be required to dissipate excess heat. For residential cooling systems, fan coils are commonly employed to reject this heat.

Simultaneously, the adsorbent material in the left, yellow chamber (Fig. 10) is cooled by the circulation of cooling water (stream ‘b’) to prepare the material for the subsequent adsorption process by lowering its temperature. Typically, the inlet temperature of the cooling water ranges between 25 and 30°C, allowing the use of standard tap water.

The condensed water is directed through a throttling valve (depicted as the green valve in Fig. 10) to the evaporator, where it evaporates under reduced pressure, absorbing heat from the chilled water circuit (stream ‘c’). This refrigeration process cools the water within the cooling circuit, as the evaporation of the condensed water from the throttling valve absorbs heat. Chilled water typically reaches outlet temperatures between 5 and 15°C, depending on the desired cooling intensity.

- Phase 2: Mass Recovery process

When all the refrigerant water from the throttling valve has evaporated, and all the vapor from the left, yellow chamber has condensed and passed through the throttling valve, the lower valve in the left chamber, labeled as valve ‘3’ (Fig. 9), is opened, while valve ‘1’ is closed. The vapor generated in the evaporator then rises and encounters the adsorbent material in the left, yellow chamber. Since the adsorption process is exothermic, the adsorbent material continues to be cooled by the ongoing circulation of cooling water (stream ‘b’). During this phase, the temperature of the adsorbent material in the right chamber decreases, while the temperature in the left chamber rises, as shown in Fig. 10. The process concludes when the pressure in both chambers equalizes. At the end of this process, the water is fully adsorbed by the sorbent material in the left chamber.

- Phase 3: Heat recovery process

Valve ‘3’ (Fig. 9) is closed once the pressure equilibrium between the two chambers is reached. In this stage, the flows of streams ‘b’ and ‘d’ are reversed to bring the system back to its initial configuration, with the roles of the two chambers swapped. Specifically, the system transitions from a configuration where the right chamber is for desorption and the left chamber is for adsorption (as depicted in Fig. 9) to one where the left chamber handles desorption and the right chamber handles adsorption (as shown in Fig. 9).

The reversal of the hot and cooling water flows circulating through the pipelines is managed by a flow-switching unit, illustrated in Fig. 11.

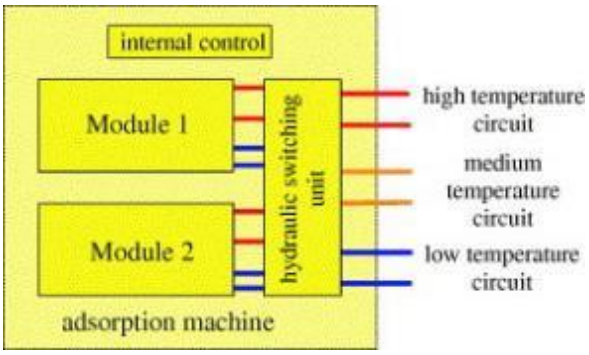

Figure 11: driving switching unit.

- Phase 4: Desorption process, now realized by the left chamber.
- Phase 5: Mass recovery process, equal to point 2, but witch chambers reversed, both on the streaming flows and in the valves’ action.
- Phase 6: Heat recovery process, same as 3, but with chambers, flows of streams and action of the valves reversed.

The cycle process will go round and round along phase 1 → phase 2 → phase 3 → phase 4 → phase 5 → phase 6. The cycle time includes the heating/cooling time, the heat recovery time and the valves switching time. Typically, the cycle time averages around 5 minutes. By repeating the adsorption/desorption cycle, the system continuously generates the refrigeration effect.

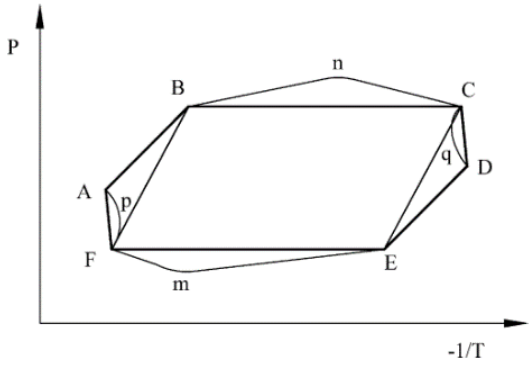

Figure 12: P-T diagram for the ideal basic cycle.

In Figure 12 the ideal cycle is shown. A-B and D-E are the heat recovery processes. B-C and E-F are the adsorption/desorption processes. C-D and F-A are the mass recoveries. The letters 'n' and 'm' represent the fact that the heat exchangers capacity of all heat exchangers is limited, so the practical cycles must take these limitations into account.

4.2.2 Mathematical models [1]

In these models, commonly these assumptions are made:

1. Temperature and pressure are uniform throughout the whole adsorber.
2. The refrigerant is adsorbed uniformly by the adsorber, and it is in the liquid phase.
3. The pressure difference between the adsorber and the condenser/evaporator is neglected.
4. The heat conduction of the shell connecting the adsorbers to the condenser or the evaporator is neglected, and the heat exchange between the two chambers containing the sorbent material is completely isolated.
5. The system has no heat losses to the environment.
6. The heat and mass transfer process that take place inside the evaporator is not considered.

Nomenclature:

a	constant in Van der Waals equation, Pa m^6 kg^{-2}
A	area, m^2
b	constant in Van der Waals equation, m^3
c	specific heat, kJ kg^{-1} $°C^{-1}$
COP	coefficient of performance
KA	performance coefficient of heat exchanger, kW $°C^{-1}$
L	latent heat of vaporization, kJ kg^{-1}
M	mass, kg
$M_{e,0}$	mass of residual refrigerant in evaporator, kg
$\dot{m}$	mass flow rate, kg s^{-1}
n	times of data acquisition in one cycle
P	pressure, Pa
Q	heat power, kW
R	gas constant, J kg^{-1} K^{-1}
T	temperature, K
v	specific volume, m^3 kg^{-1}
x	adsorption capacity, kg kg^{-1}
ΔH	isosteric heat of adsorption, kJ kg^{-1}
τ	time, s
δ, θ, ϑ	flag functions
Ψ	mass, kg

Subscript

a	adsorbent
ad	adsorber
ads	adsorption
al	aluminium
c	condenser
chill	chilled water
cool	cooling water
cond	condensing
cu	cuprum
des	desorption
e	evaporator
evap	evaporating
h	heat, hot
in	inlet
mr	mass recovery
out	outlet
ref	refrigeration
s	silica gel, saturation
w	water
wv	water vapor

Superscript

i	the order number of the data acquisition interval

Figure 13: Useful nomenclature for the equations.

The equations are:

1. Adsorption equilibrium equation:

Boelman equation:

$$x = 0{,}346\left(\frac{P_s(T_w)}{P_s(T_s)}\right)^{1/1{,}6} \quad (1)$$

Where $P_s(T_w)$ and $P_s(T_s)$ are respectively the corresponding saturation vapor pressure of the refrigerants at the temperature T_w (water vapor) and T_s (silica gel).

The saturation vapor pressure and temperature are correlated as follows:

$$P_s = 0{,}0000888(T - 273{,}15)^3 - 0{,}0013802(T - 273{,}15)^2 + 0{,}0857427(T - 273{,}15) + 0{,}4709375 \quad (2)$$

2. Energy equations:

2.1 Energy balance for the adsorber/desorber

$$\frac{d}{dt}\left\{\left[M_a\left(c_a + c_{p,w}x\right) + c_{cu}M_{tube,ad} + c_{al}M_{fin,ad}\right]T_a\right\} = M_a\Delta H\frac{dx}{dt} + (1-\delta)c_{wv}M_a\frac{dx_{ads}}{dt}(T_e - T_a) + \dot{m}_w c_{p,w}(T_{ad,in} - T_{ad,out}) \quad (3)$$

Where: $\delta = \begin{cases} 0, & \text{adsorption proces} \\ 1, & \text{desorption proces} \end{cases}$ (4)

$$\frac{T_{ad,out} - T_a}{T_{ad,in} - T_a} = \exp\left(\frac{-KA_{ad}}{\dot{m}_w c_{p,w}}\right) \quad (5)$$

2.2 Energy balance for the condenser

$$c_{cu}M_c\frac{dT_c}{dt} = \delta\left[-LM_a\frac{dx_{des}}{dt} + c_{wv}M_a\frac{dx_{des}}{dt}(T_c - T_a) + \dot{m}_{cool}c_{p,w}\left(T_{cool,in} - T_{cool,out}\right)\right] \quad (6)$$

$$\frac{T_{cool,out} - T_c}{T_{cool,in} - T_c} = \exp\left(\frac{-KA_c}{\dot{m}_{cool}c_{p,w}}\right) \quad (7)$$

2.3 Energy balance for the evaporator

$$\frac{d}{dt}\left[\left(c_{p,w}M_{c,w} + c_{cu}M_e\right)T_e\right] = (1-\delta)\left[-LM_a\frac{dx_{ads}}{dt} + \dot{m}_{chill}c_{p,w}\left(T_{chill,in} - T_{chill,out}\right)\right] + \delta\left[\theta c_{p,w}(T_e - T_c)M_a\frac{dx_{des}}{dt} - (1-\theta)LM_a\frac{dx_{des}}{dt}\right] \quad (8)$$

$$\frac{T_{chill,out} - T_e}{T_{chill,in} - T_e} = \exp\left(\frac{-KA_e}{\dot{m}_{chill}c_{p,w}}\right) \quad (9)$$

Where: $\theta = \begin{cases} 1, & T_c \leq T_e \\ 0, & T_c > T_e \end{cases}$ (10)

As can be noticed, energy equations for the condenser and the evaporator are more complex. The condensation process occurs firstly in the evaporator during the desorption process because the evaporator temperature is lower than the condenser temperature and it is also lower than the saturation temperature of the refrigerant vapor. The condensation process will occur only in the condenser after the evaporator temperature rises higher than the saturation temperature.

3. Liquid refrigerant equilibrium in the evaporator

$$\frac{dM_{e,w}}{dt} = M_{e,0} - M_a \frac{dx}{dt} \quad (11)$$

4. Equilibrium equations in the mass recovery process

During the mass recovery process, the condensers will remain inactive, while the evaporator in the desorbing chamber will initiate evaporation, and the evaporator in the adsorbing chamber will condense the water vapor, acting as a condenser. The desorption process of the desorber and the adsorption process of the adsorber will both accelerate due to the pressure difference between the desorbing and adsorbing chambers. The distinct equations applicable in this phase of the desorption/adsorption process are detailed below.

Mass equilibrium:

$$-M_a \frac{dx_{des}}{dt} + \dot{m}_{e,evap} = \dot{m}_{e,cond} + M_a \frac{dx_{ads}}{dt} = \dot{m}_{mr} \quad (12)$$

Energy equation in the evaporator:

$$\frac{d}{dt}\left[\left(c_{p,w}M_{e,w} + c_{cu}M_e\right)T_e\right] = -L\Psi + \vartheta \dot{m}_{chill} c_{p,w}\left(T_{chill,in} - T_{chill,out}\right) \quad (13)$$

Where: $\Psi = \begin{cases} \dot{m}_{e,evap}, & \text{for desorbing chamber} \\ \dot{m}_{e,cond}, & \text{for adsorbing chamber} \end{cases}$ (14)

And: $\vartheta = \begin{cases} 1, & T_e \leq T_{chill,in} \\ 0, & T_e > T_{chill,in} \end{cases}$ (15)

In these equations, $\dot{m}_{e,evap}$ and $\dot{m}_{e,cond}$ are, in order, the mass flow rates of refrigerant evaporated in the desorbing chamber's evaporator and condensed in the adsorption chamber's evaporator. The vapor is assumed to be incompressible, and the flow resistance of the water vapor is neglected. The pressures in the chambers can be calculated as follows:

$$P_{wv,des} - P_{wv,abs} = \frac{v_{wv}\dot{m}^2_{mr}}{2A^2} \quad (16)$$

In which A is the sectional area of the mass recovery channel.

Here below is the Van der Waals equation, which is used to calculate the state parameters for the water vapor:

$$\left(P_{wv} + \frac{a}{v^2}\right)(v - b) = RT_{wv} \quad (17)$$

5. Performance parameters

Refrigerant capacity:

$$Q_{ref} = \frac{\int_0^{t_{cycle}} c_{pw}\dot{m}_{chill}(T_{chill,in} - T_{chill,out})dt}{t_{cycle}} \quad (18)$$

Heating power:

$$Q_h = \frac{\int_0^{t_{cycle}} c_{p,w}\dot{m}_h(T_{h,in} - T_{h,out})dt}{t_{cycle}} \quad (19)$$

Coefficient of Performance:

$$COP = \frac{Q_{ref}}{Q_h} \quad (20)$$

4.2.3 Common pairs of adsorbent and refrigerant liquid

In the table represented in Figure 14, common pairs commonly found in the market are listed, along with their operating temperatures and the heat absorbed from the environment.

Table 1.2 Comparison of adsorption chiller's working pair ([48–52]).

Adsorption working pair	Driving temperature (°C)	Evaporating temperature (°C)	Adsorption heat (kJ kg^{-1})
Activated carbon–methanol	80–100	−3	1800–2000
Silica gel–water	60–85	6.7	1000–500
Zeolite–water	70–250	5	3300–4200
Activated carbon–ammonia	Up to 150	−5	2000–2700
Activated carbon–ethanol	60–95	7	940–1200

Figure 14: Sorbent-Sorbate couples.

Market available systems use water as refrigerant and silica gel as sorbent, but R&D on systems using zeolites as sorption material is ongoing. In this system a silica gel-water adsorption chiller is considered.

Physical Adsorption of Silica Gel

Silica gel is a partially dehydrated form of polymeric colloidal silicic acid. Its chemical composition can be expressed as follows:

$$SiO_2 \times nH_2O$$

The adsorption/desorption equation for silica is basically:

$$SiO_2 \times nH_2O(l) = SiO_2 \times (n-1)H_2O(l) + H_2O(v)$$

Where states for liquid phase and v states for vapor phase. The adsorptive action of silica gel for vapors is purely physical. When the particles become saturated, they do not undergo any change in size or shape, and even when completely saturated, the particles are perfectly dry. The adsorptive property of silica gel arises from its very high value of porosity; it has been estimated that 1 m^3 of gel contains pores with a surface area of about 2.8×107 m^2. The dimensions of the pores are sub-microscopic (20–200 A˚). Silica gel adsorbs vapor from a gas mixture until its pores are filled. The amount of condensable vapor adsorbed in silica gel at any temperature increases as the partial pressure of the vapor in the surrounding gas reaches its own value for partial pressure of vapor.

Just to make an example and report some figures, a kilogram of silica gel at 27°C in contact with air saturated at this temperature is proven to adsorb up to 0.4 kg of water. When vapor is adsorbed in silica gel, the heat liberated is equivalent to the latent heat of evaporation of the adsorbed liquid plus the additional heat of wetting. The sum of the latent heat and the heat of wetting is equal to the heat of adsorption. During the adsorption process, the vapor latent heat becomes sensible heat, which is dissipated into the adsorbent, the metal of the adsorbent container, and the surrounding atmosphere. The action of silica gel is instantaneous under dynamic adsorption conditions.

4.2.4 Typical adsorption chillers efficiencies.

- Typical COP (Coefficient of Performance) values for adsorption chillers revolve around 0.5-0.6. This value can be enhanced by incorporating two or more adsorption chillers, thereby rendering the cooling process continuous and uninterrupted.

- For an adsorption chiller using a couple composed of silica gel and water, these values of efficiencies related to the driving temperature can be detected:

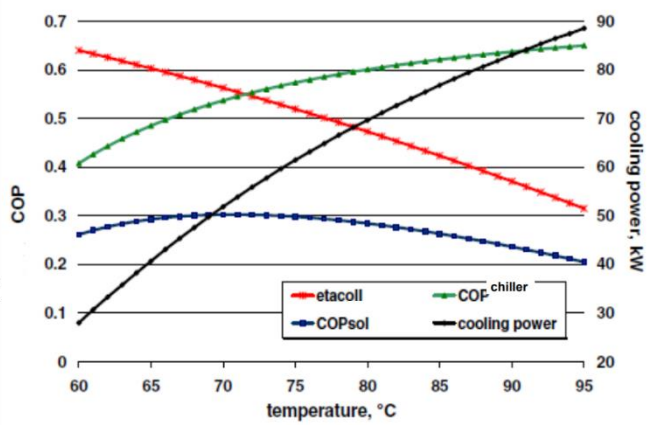

Figure 15: Efficiencies of the system.

In Fig. 15, the trends of the different efficiencies of a system consisting of an adsorption chiller and a solar thermal panel are illustrated. It is evident that while the COP of the chiller and its cooling effect increase significantly with rising temperatures, the efficiency of the solar collector exhibits the opposite trend, decreasing as temperature increases. It can be reasonably inferred that the total efficiency of the system must account for all the efficiencies of the individual components. Notably, on Fig. 15, the total efficiency initially rises, reaching a peak, before decreasing sharply.

What must be done is to establish a driving temperature that maximizes the total COP of the system, seen as a unique unit. In the range of temperature in which it is planned to work in this project (60-80 °C given by solar panels) the COP_{sol}), which is the total efficiency of the system, reaches its maximum values.

4.2.5 Comparison between an adsorption chiller and an adsorption chiller: is it truly advantageous?

Primarily, it is advantageous to elucidate the nature of an absorption chiller and explicate its operational principles.

An absorption chiller is a refrigeration system that employs the principle of absorption to extract heat from an environment or a fluid. The key difference with adsorption chillers lies here: absorption chillers rely on absorption of a gas into a liquid, which involves much stronger and more durable chemical bonds compared to the weaker physical forces driving the adsorption process. This will certainly lead to the use of more energy to break the bonds that have formed between the refrigerant liquid and the absorbent element.

The typical operation of the absorption system is as follows:

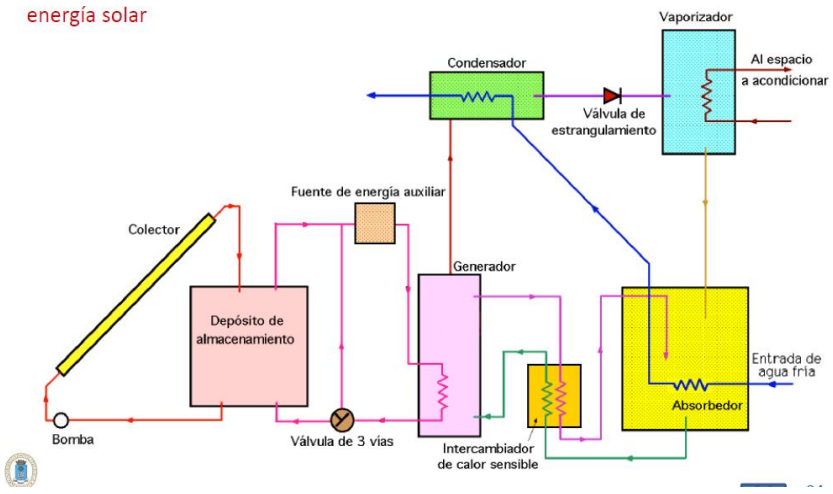

Figure 16: Absorption cooling system.

- Steam Generation

The operational sequence commences with the generation of high-temperature and high-pressure steam, serving as the primary thermal energy source for the absorption process. This steam can originate from various sources, including natural gas, industrial steam, or other heat-generating mediums. In figure 16, the source of heat is the solar energy collected by a solar collector.

- Generator

Steam is introduced into the absorption chiller's generator. Within this component, the steam interacts with a solution comprising refrigerant liquid (such as water) and a chemical absorbent (e.g., NH3). This interaction induces the evaporation of the refrigerant liquid from the solution, transforming it into vapor.

- Vapor-Liquid Separation

The refrigerant vapor is separated from the absorbent and refrigerant solution. Subsequently, this vapor undergoes cooling and condensation in the condenser.

- Condensation

The refrigerant vapor is directed to the condenser, where it undergoes cooling through contact with an external cooling fluid, such as air or water. This cooling process facilitates the vapor's condensation back into liquid form, releasing heat into the surrounding environment.

- Expansion

Here, an expansion valve is employed to further reduce the refrigerant’s pressure, facilitating pressure and temperature decrease.

- Evaporation

The expanded refrigerant liquid is then introduced into the evaporator, where it absorbs heat from the surrounding environment, typically air or water requiring cooling. This evaporation process leads to the transformation of the refrigerant liquid into vapor.

- Absorption

The refrigerant vapor generated in the evaporator enters the absorber, where it recombines with the absorbent and refrigerant solution from the generator. This recombination causes the refrigerant to re-dissolve into the absorbent solution, completing the absorption cycle.

- Return to the Generator

The absorbent and refrigerant solution, now enriched with the refrigerant, is pumped back to the generator for the commencement of a new cycle.

The main noticeable difference is that, while the adsorption chiller uses solids as the adsorbent material, the absorption chiller relies on an aqueous solution like NH3 as the absorbent. This means that the absorbent liquid can circulate, unlike the solid material in the

adsorption chiller. However, the absorbent liquid in the absorption chiller requires a secondary circuit for circulation, leading to the need for more materials and additional components compared to the adsorption process. Consequently, operating these additional systems requires more energy, which will obviously affect the value of the Coefficient of Performance of the system.

Another fundamental consideration to undertake in comparing the two systems is the disparity in the Coefficient of Performance.

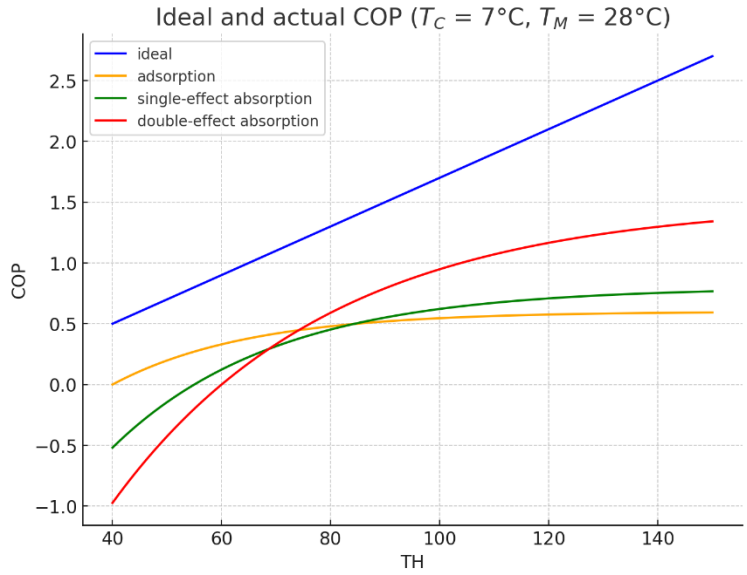

Figure 17: Comparison of the two systems COPs typical values.

As depicted in Fig. 17, a cursory examination reveals that the absorption chiller consistently demonstrates markedly higher COP values compared to those exhibited by an adsorption system, particularly when considering a multi-step absorption system, capable of achieving COP values in the order of 1.40.

Upon meticulous examination of the graph, it becomes apparent that within the operational temperature range of the refrigerant fluid, specifically between 40 and 80 Celsius degrees, easily given by Solar-thermal collectors that we are willing to use in our system, the adsorption chiller emerges as the preferred choice due to its superior COP values compared to the single-effect absorption chiller. Additionally, absorption systems necessitate surpassing a certain threshold temperature of the refrigerant fluid for effective system function and to achieve functional COP values. For the single-effect absorption chiller, the temperature threshold at which the COP surpasses the value presented by the adsorption chiller is approximately 75 Celsius degrees, while for the double-effect absorption chiller, it is around 95 Celsius degrees.

For our system, which is planned to utilize water heated by solar panels and direct solar heating of a water basin in a pool, resulting in operating fluid temperatures ranging between

45 and 80 Celsius degrees, the fact that an adsorption cooling system would offer greater functionality than the absorption one is evident.

Below is a list enumerating the advantages of the adsorption systems.

1. Long life proved to be higher than 25 years.
2. Maintenance is negligible.
3. Ultra-low electricity consumption, reduced by 99% compared to an absorption chiller's system.
4. No vibration of the system.
5. It uses green refrigerant and desiccant.
6. No crystallization, corrosion, hazardous leaks, or chemical disposal issues.
7. Compared to absorption chillers, adsorption chillers present a higher efficiency in the range of temperature pertinent to our concern.
8. Adsorption chillers do not use a toxic liquid as happens in the absorption systems.
9. Adsorption chillers do not use pumps to put the refrigerant liquid into circulation. The whole adsorption/desorption process is thermally driven.
10. Adsorption chillers are noiseless systems.

4.3 Air-Water Heat Pump

An air-to-water heat pump is a device that transfers thermal energy from the ambient outdoor air to a water-based heating system within a building. It operates on the principle of the refrigeration cycle, utilizing a small amount of electrical energy to move heat rather than generating it directly through combustion. By exploiting the thermal energy present in the outside air - a free and renewable resource - the heat pump provides efficient heating, even at lower ambient temperatures.

The system comprises four main components: an evaporator, a compressor, a condenser, and an expansion valve. A refrigerant fluid circulates through these components in a closed loop. In the evaporator, the refrigerant absorbs heat from the outdoor air, causing it to evaporate into a gas. This process occurs because the refrigerant has a boiling point lower than the ambient temperature, allowing it to extract heat energy even when it is cold outside.

The gaseous refrigerant then enters the compressor, where it is pressurized, raising its temperature significantly. This high-temperature, high-pressure gas moves to the condenser, where it releases the absorbed heat to the water circulating in the building's heating system. As the refrigerant relinquishes its heat to the water, it condenses back into a liquid. The liquid refrigerant then passes through the expansion valve, where its pressure and temperature decrease, preparing it to absorb heat once again in the evaporator, thus repeating the cycle.

By transferring heat from the environment rather than generating it solely from electrical energy, the heat pump achieves a high coefficient of performance (COP). This means that for every unit of electrical energy consumed, multiple units of heat energy are delivered to the building. For example, a COP of 4 indicates that one unit of electricity produces four units of heating energy. This efficiency results in lower operational costs and reduced environmental impact compared to conventional heating systems that rely on fossil fuels or resistive electric heating.

The utilization of "free" energy from the outdoor air aligns with sustainable energy principles. Since the thermal energy in the air is naturally replenished and abundant, the heat pump reduces reliance on non-renewable energy sources. This exploitation of ambient energy contributes to decreasing greenhouse gas emissions and supports environmental sustainability objectives.

Moreover, air-to-water heat pumps can reverse their operation to provide cooling during warmer periods, enhancing their versatility. By adjusting the cycle, the system can extract heat from the indoor environment and release it outside, effectively cooling the interior spaces.

In summary, an air-to-water heat pump harnesses renewable thermal energy from the environment to provide heating and cooling, transforming "free" ambient heat into useful thermal energy for the building. Its high efficiency and ability to exploit abundant environmental energy make it a valuable component in sustainable building design, contributing to energy efficiency goals and reducing environmental impact.

4.4 PCM: Phase Change Materials

Buildings account for nearly 41% of the world's total energy consumption, constituting approximately 30% of the annual greenhouse gas emissions. It is projected that the energy demand within the building sector will surpass 50% by the year 2050, while the demand for cooling is anticipated to triple between 2010 and 2050. It is noteworthy that well-insulated buildings have the potential to yield energy savings ranging from 5% to 30%.

Phase Change Materials (PCM) are substances that undergo a phase transition at relatively low temperature levels; in our case, the transition of particular interest is from solid to liquid state. The objective behind utilizing PCM for wall insulation is to leverage this phase transition phenomenon. Specifically, it involves storing thermal energy during the solid-liquid phase transition and harnessing the latent heat released during the transition from liquid back to solid state.

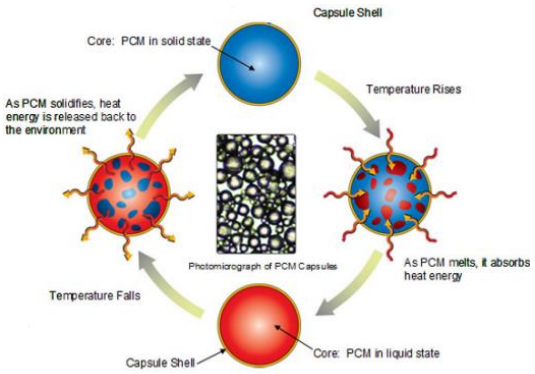

Figure 18: PCM general functioning scheme.

In figure 19 the fundamental operating principle of the PCMs can be observed: temperature is plotted along the x-axis, while heat flux is represented along the y-axis. It is evident that during the melting phase, an endothermic peak is present, and the associated heat leads to the complete transition from solid to liquid state of the material. Conversely, during the freezing phase, an exothermic peak is observed, wherein the released heat ideally matches the heat absorbed during the melting phase; subsequently, this heat is released into the environment where the PCM is deployed.

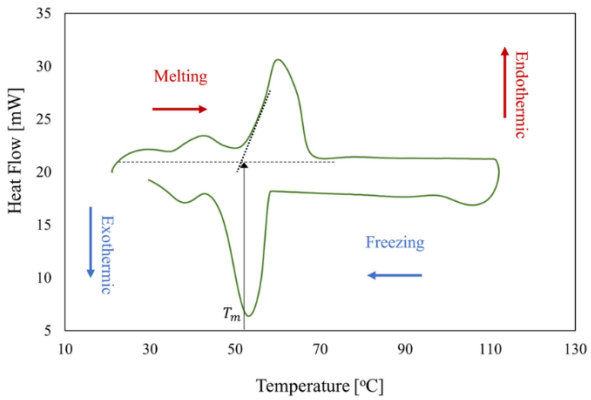

Figure 19: PCM functioning diagram.

The integration of PCMs into thermal insulation systems offers significant potential for enhancing building energy efficiency, even though the technology is still in developmental stages. One of the major challenges associated with PCMs is their limited availability and relatively high cost. In this application, a layer of PCM is incorporated within the walls of the dwelling to improve thermal regulation.

During the day, the PCM layer absorbs heat primarily from the external environment, with a lesser extent from the interior space. Initially, the absorbed thermal energy raises the temperature of the PCM until it reaches its melting point. Upon reaching this temperature, the material undergoes a phase change from solid to liquid, during which it absorbs a substantial amount of heat without a corresponding increase in temperature. This latent heat storage effectively minimizes heat transmission into the interior of the dwelling, acting as an insulating buffer that enhances thermal performance.

At night, as external temperatures decrease, the PCM begins to release the stored thermal energy. The material cools down until it reaches its solidification point, at which a phase change from liquid to solid occurs. During this transition, the PCM releases the latent heat previously absorbed, which is partially emitted back to the external environment and partially into the interior space. This controlled release of heat helps prevent the indoor environment from cooling excessively as outdoor temperatures drop, maintaining a more stable and comfortable indoor climate.

By leveraging the thermal properties of PCMs, the building's energy demand for heating and cooling can be reduced. The material acts as a thermal reservoir, absorbing excess heat during periods of high temperatures and releasing it when temperatures decrease. This passive thermal regulation contributes to improved energy efficiency and occupant comfort, aligning with sustainability objectives in building design.

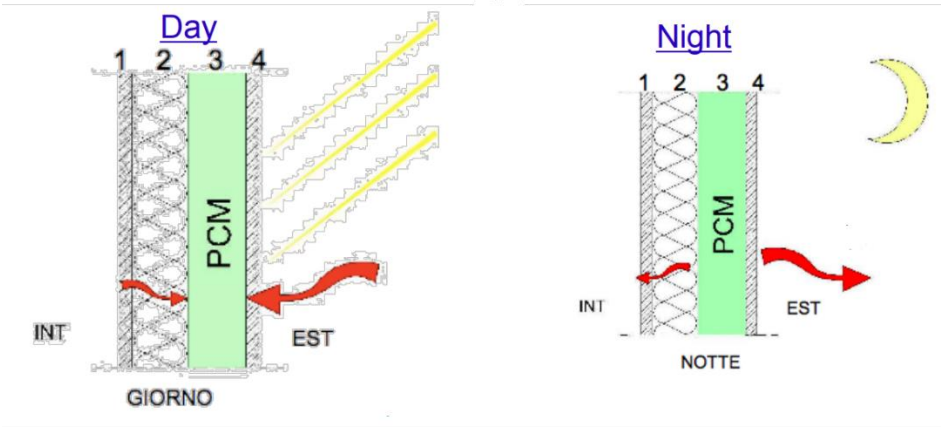

Figure 20: day and night thermal fluxes from and to PCMs.

Phase Change Materials can be integrated into the walls of residences in various forms and through various methods. Here is a list of the most economically viable approaches for achieving this objective:

- Macro-encapsulation within construction materials.

- Micro-capsules within gypsum boards. Their percentage of inclusion within the wall defines several thermal characteristics of it. Figure 21contains a table showing their influence on thermal properties. It can be readily discerned that the greater their presence within the wall, the higher its latent heat content.

Intonaco di gesso	Densità [kg/m3]	Calore specifico [kJ/kg K]	Conducibilità W/m K	Calore latente [kJ/kg]
Convenzionale	696	1.089	0.173	0
10% PCM	720	1.215	0.187	19.3
16% PCM	760	1.299	0.192	31.0
20% PCM	800	1.341	0.204	38.9
30% PCM	998	1.467	0.232	58.3

Figure 21: micro-encapsulated PCMs properties.

- Containers for PCM. In general, they are made of metal or polymeric materials

Now, it is essential to outline the specific criteria that a phase change material must meet to be effectively utilized in enhancing the building's thermal performance. These criteria ensure that the selected material not only provides the desired thermal regulation but also aligns with safety, economic, and environmental considerations.

Thermo-Physical and Chemical Requirements

The PCM must possess a melting temperature within the required operating temperature range for the building's insulation needs. This ensures that the phase change occurs at temperatures corresponding to typical indoor and outdoor conditions, maximizing the material's effectiveness in absorbing and releasing heat.

A high latent heat of fusion is crucial, as it determines the amount of thermal energy the material can store during the phase change. The higher the latent heat, the greater the energy storage capacity, enhancing the PCM's ability to regulate indoor temperatures efficiently.

Thermal conductivity is another important factor; the material should exhibit high thermal conductivity in both its solid and liquid phases. This property facilitates efficient heat transfer, enabling PCMs to quickly absorb and release heat in response to temperature fluctuations.

Minimal volume changes during phase transitions are critical to prevent structural stresses within the building envelope. Significant expansion or contraction can lead to material degradation or compromise the integrity of the insulation system. Therefore, the PCM must undergo only slight volume changes during melting and solidification—a requirement considered among the most critical.

Long-term chemical stability is essential to ensure that the PCM maintains its properties over time without degradation after repeated freeze/melt cycles. A complete reversibility of the freezing and melting cycles is required to allow the material to function effectively over many

thermal cycles. Additionally, the PCM must be non-flammable, non-toxic, and non-explosive to meet safety standards and avoid health risks or fire hazards within the building.

Kinetic Requirements

From a kinetic standpoint, the PCM should have a high nucleation rate to avoid supercooling of the liquid phase, which can delay solidification and reduce the material's ability to release stored heat when needed. A high crystallization rate is also necessary to satisfy the demands of heat recovery from the storage system. Rapid crystallization ensures that the PCM can promptly release heat, maintaining the desired indoor temperature conditions.

Economic and Environmental Requirements

Economically, PCMs should be cost-effective, with a low price point to make its integration into building insulation financially viable. Availability is important to ensure that the material can be sourced without significant delays or logistical challenges. The PCM must be non-polluting and have a low environmental impact throughout its lifecycle, including production, use, and disposal processes. Good recyclability is desirable, allowing the material to be reused or repurposed at the end of its service life, thereby reducing waste. Additionally, the PCM should be easily separable from other materials to facilitate recycling or safe disposal.

By adhering to these comprehensive criteria, the selection of an appropriate PCM can significantly enhance the thermal insulation of the building. The material's thermo-physical properties, kinetic behavior, and economic and environmental attributes collectively determine its suitability for integration into the building envelope.

In the tables provided below, the costs associated with various types of PCMs are presented, offering further insight into their economic feasibility.

Material	Type of PCM	Cost (US $/kg)
Paraffin Wax	Organic	1.88–2.00
Technical Grade Icosane	Organic	7.04
Pure Grade Icosane	Organic	53.9
Stearic Acid	Fatty Acid	1.43–1.56
Palmitic Acid	Fatty Acid	1.61–1.72
Oleic Acid	Fatty Acid	1.67–1.76
Crude Glycerine	Fatty Acid	0.22–0.29
M-27	Commercially Available Fatty Acid	14.26
M-51	Commercially Available Fatty Acid	11.13
M-91	Commercially Available Fatty Acid	10.12
Calcium Chloride	Inorganic-Salt Hydrate	0.20
Latest™29T	Commercially Available Salt Hydrate	4.95

Figure 22: PCMs properties.

Compound (M)		Phase-Change Temp (°C)	Density (kg/m^3)	Heat of Fusion (kJ/kg)	Specific Heat Capacity (kJ/kgK)	Thermal Conductivity (W/mK)
RUBITHERM GmbH, PCM SP 24 E	M1	24–35	1500	190	2	0.6
PlusICE PCM, S23	M2	23	1530	175	2.2	0.54
savENRG PCM-HS24P	M3	24	1820	185	2.26	0.5–1.09
PUR-PCM, BASF Polyurethanes GmbH	M4	22	970	365	2	0.19
PlusICE PCM, S17	M5	17	1525	160	1.9	0.43
CoolZONE23, Armstrong	M6	21–22	770	342	2	0.2
savENRG PCM-HS22P	M7	23	1540	185	3.05	0.5–1.09
ThermalCORE 23 C/ 73 F, USA	M8	22–24	770	342	2.2	0.2
Weber.murclima 23, St. Gobain-weber	M9	22–24	950	170	2.32	0.38
RUBITHERM GmbH, PCM RT 25 HC	M10	22–26	880	230	2	0.2
PlusICE PCM, PCM, A25H	M11	25	810	226	2.15	0.18
PlusICE PCM, A22H	M12	22	820	216	2.85	0.18
PlusICE PCM, A25	M13	25	785	150	2.26	0.18
PlusICE PCM, A24	M14	24	790	145	2.22	0.18
PCM-Akustikputz 23, SchreffGmbh& Co.	M15	21–22	400	196	1.7	0.08

Figure 23; PCMs properties.

Despite the considerable potential of PCMs for enhancing thermal insulation, their implementation is currently not economically advantageous. As will be detailed in subsequent sections of this thesis, the high initial costs associated with PCMs lead to payback periods that are excessively long, making it challenging to justify the investment from a financial perspective. Nonetheless, the results obtained from simulations and analyses are highly promising. The integration of PCMs shows significant potential for energy savings and improved thermal comfort. This suggests that, with future advancements in technology and anticipated reductions in material costs, PCMs could become a viable and cost-effective solution for building energy efficiency.

4.5 Hybrid Thermal – Photovoltaic Solar Panels

Hybrid solar panels are innovative systems that simultaneously generate electrical and thermal energy from solar radiation. By integrating photovoltaic cells and solar thermal collectors into a single module, these panels maximize the utilization of available solar energy, providing both electricity and heat for residential use. This dual functionality makes them particularly significant for the residential sector, where space limitations often restrict the installation of separate photovoltaic and thermal systems.

The implementation of hybrid solar panels in residential buildings can lead to exceptionally high cost-benefit ratios. By harnessing both forms of energy from a single installation, homeowners can achieve greater energy efficiency, reduce utility bills, and lower their environmental footprint. Moreover, the increased efficiency contributes to faster payback periods and enhances the overall sustainability of the building. As energy demands rise and the push for renewable solutions intensifies, hybrid solar panels hold the potential to revolutionize energy consumption in the residential sector, making them a critical component in the pursuit of sustainable living.

4.5.1 Product selection and technical specifics.

The methodology employed in the study of hybrid solar panels was entirely different from that used for other technologies. For the other technologies, priority was given to assessing the magnitude of the energy demands and determining how to meet them, including the selection of appropriate equipment and brands. In contrast, for the solar panels, the initial step involved selecting the product and determining how many units could be installed on the available roof surface. Subsequently, based on operational requirements, the appropriate number of panels was decided upon to meet the predefined objectives.

This research concluded with the discovery of an exceptional solution: the hybrid solar panel from Abora Solar.

Abora Solar, an impressive company based in Zaragoza, manufactures the panel chosen for this study. They claim to have constructed the most efficient panel in the world, a statement that appears to be highly plausible. The panel boasts a remarkable overall energy generation efficiency of 89%. In image 6 the typical disposition of the components comprising this panel is shown.

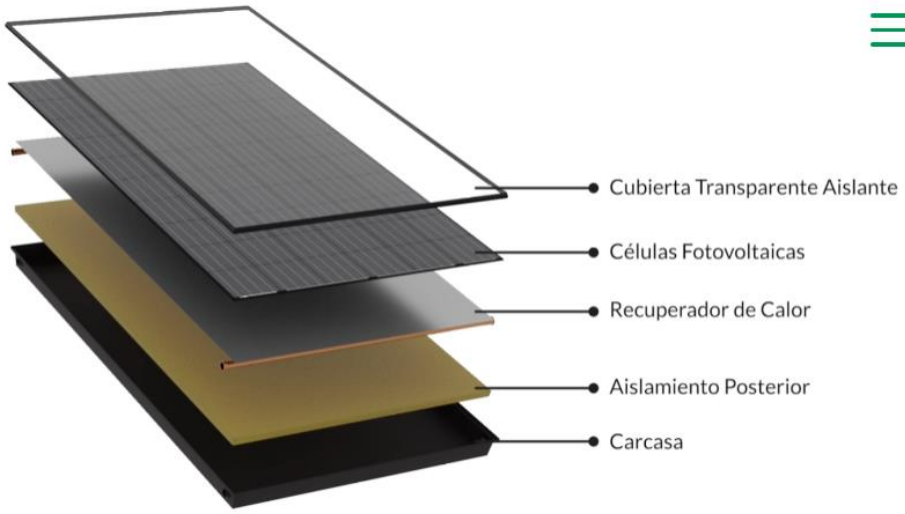

Figure 24: composition of the Abora Solar panel.

The product is offered in two different configurations: the **basic kit**, which primarily includes two hybrid solar panels, and the **basic+ kit**, which consists of two hybrid solar panels and two additional photovoltaic modules. For completeness, the technical specifications and additional details of both kits are presented in the following tables.

1. General Specifics

Table 15: General specifics of the hybrid panel

Length, width, and thickness	1970 x 995 x (85+22) mm
Gross Area	1,96 m^2
Net Area	1,88 m^2
N° cells	72
Weight	50 kg
Frontal Glass	3,2 mm tempered
Frame	Aluminum
Connection Box Protection	IP65
N° Diodes	3 diodes
Cell dimensions	156 x 156
Type of Connection FV/cables length	Solarlok PV4 / 1m

2. Electrical Specifics

Table 16: electrical specifics of the hybrid panel.

Cell Type	Mono-crystalline
Nominal Power (W)	350W
Max Power Tension (Vmpp)	39,86V
Max Power Current (Impp)	8,76A
Open circuit tension (Voc)	48,61V
Short Circuit Current (Isc)	9,16A
Module Efficiency (%)	17,8
Power Tollerance (W)	+/- 4%
Max System Tension	DC 1000 V (IEC)
Back sheet	Black
Pmpp temperature coefficient	-0,36%/°C
Voc temperature coefficient	-0,28%/°C
Isc temperature coefficient	+0,06%/°C
Max inverse Current	15A
NOCT temperature	45+/-2°C

3. Thermal Specifics

Table 17: thermal specifics of the panel.

Optical Efficiency	0,7
Thermal Losses coefficient, a1	5,98 W/(m^2*K)
Thermal Losses coefficient, a2	0,00 W/(m^2*K)
Interior Liquid Volume	1,78 L
Stagnation Temperature	126°C
Number of hydraulic connections	4 connections
Max admissible Temperature	10 bars
Nominal mass flow rate	60 L/h
Nominal Power (W)	1372

4. Efficiency of the panel based on (Tm-Ta)/G

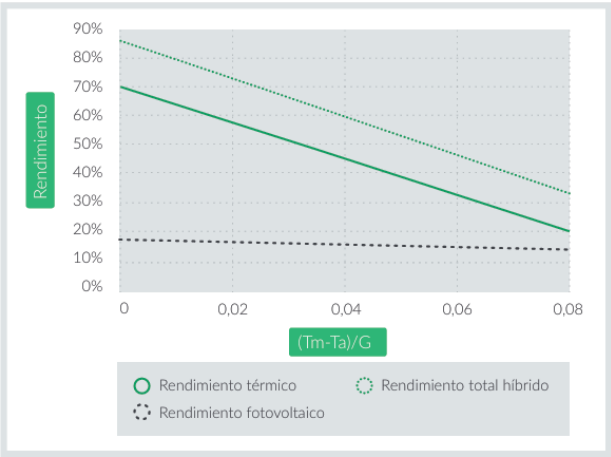

Figure 25: Efficiencies of the Panel.

Attached in image 8 is a representation of the thermal solar panel.

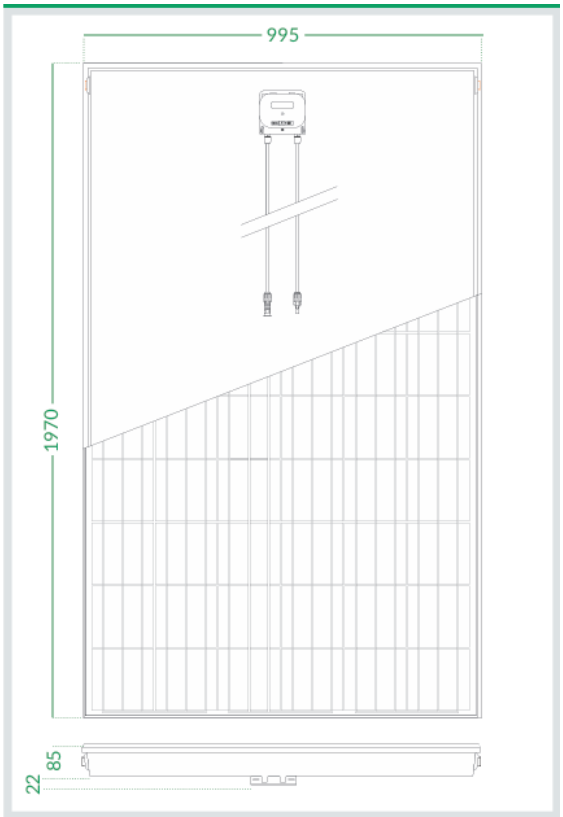

Figure 26: Dimensions of the Panel. []

5. General Specifics of the Photovoltaics' Modules coming with the BASIC+ Kit

The geometrical specifics and the electrical specifics are the same as the one indicated in tables 15 and 16. The only thing changing is the Nominal Power, which in this case is 395W per module.

6. Price of the kit and what's coming with it

What comes with the kit is indicated below, with the price at the end of table 18 and 19.

1. BASIC

Table 18: General specifics of the BASIC kit's solar panel

Number of hybrid panels	2
Connection kit for the two panels	1
Coplanar structure with profile, flashing, and panel anchors.	1
Interaccumulator tank of 150 liters with hydraulic unit, solar regulation station, and expansion vessel.	1
Double DN16 pipe insulated with probe cable for panels and fittings.	25 m
Heat transfer fluid with a high boiling point.	25 L
Solar cable 25 m X 2 and MC4 connectors.	1
360 W microinverter.	2
AC electrical protection panel.	1
Price	7.984,79 €

2. BASIC +

Table 19: General specific of the BASIC+ kit's solar panel.

Number of hybrid panels	2
Number of photovoltaic modules	8
Connection kit for the two panels	1
Coplanar structure with profile, flashing, and panel anchors.	1
Interaccumulator tank of 150 liters with hydraulic unit, solar regulation station, and expansion vessel.	1
Double DN16 pipe insulated with probe cable for panels and fittings.	25 m
Heat transfer fluid with a high boiling point.	25 L
Solar cable 25 m X 2 and MC4 connectors.	1
Inverter Fronius 3.0 kW	1
AC electrical protection panel.	1
Price	13.187,79 €

At first glance, the price of the hybrid solar panel kits may appear relatively high. However, it is important to consider that in the economic analysis, the costs of additional components such as inverters, connection cables, maintenance fluids, and the storage tank are not accounted for separately, as they are all included within a single comprehensive package. This holistic inclusion means that when assessing the CAPEX for this specific case, all these essential components are incorporated alongside the panels themselves, rather than evaluating the cost of individual panels in isolation.

As a result, the analysis of the payback period reveals that, compared to other solar panel systems available on the market, the payback time for the hybrid system is shorter. The key difference lies in the integrated approach to the initial investment, where the bundled components contribute to a more favorable economic outcome over the long term. By considering the complete set of equipment provided with the hybrid panels, the investment demonstrates enhanced cost-effectiveness and efficiency, aligning with the project's objectives of maximizing renewable energy utilization while ensuring financial viability.

4.5.2 Thermal efficiency calculation.

As shown in Image 25, the average efficiency of the panels is approximately 50%. To obtain values that more accurately reflect reality, the average monthly thermal efficiency of the panel was calculated using the following formula [18]:

$$\eta = \eta_0 - \frac{\left(\frac{T_{fi} + T_{fo}}{2}\right) - T_a}{G_T}\eta_1 - \frac{\left(\frac{T_{fi} + T_{fo}}{2}\right) - T_a}{G_T}\eta_2$$

Where:

- Ƞ is the thermal efficiency of the panel, calculated as the average monthly value per month.
- η_0 is the optical efficiency of the panel; in this case its value is 0,7 (Thermal Specifics).
- T_{fi} is the average fluid inlet temperature in the panel. In this study, it is considered equal to the temperature of the Net water, for each different month.
- T_{fo} is the average fluid outlet temperature coming from the panel. This is one of the most difficult values to obtain, so some assumptions were made to carry out all the study. In this instance, reliance was placed on observations made during academic studies and on real-life cases encountered.
- T_a is the ambient temperature. The values are monthly average values, taken from the software PVsyst.
- G_T is the average value for the monthly irradiance (the figures to carry out the calculation are taken from table 3).
- η_1 is the thermal losses coefficient, coinciding to a_1 in the thermal specifics. Its value is 5,98 $\frac{W}{m^2K}$.
- η_2 is the second thermal losses coefficient, equal to zero in this case.

In table 20 the values for most of the variables required in the equation to obtain efficiency are displayed.

Table 20: Average Ambient Temperature.

Temperatures[°C]												
	gennaio	febbraio	marzo	aprile	maggio	giugno	luglio	agosto	settembre	ottobre	novembre	dicembre
Ambient Temperature [°C]	5	7	10	12	18	24	28	27	21	16	9	6
Net water temperature [°C]	8	8	10	12	14	17	20	19	17	13	10	8
Average outlet fluid temperature [°C]	48	50	53	60	63	74	80	80	70	60	52	48
Average (outlet/inlet) fluid temperature [°C]	28	29	31,5	36	38,5	45,5	50	49,5	43,5	36,5	31	28

With all this data available, the monthly efficiencies of the panel were obtained. As can be easily observed in table 21, these values do not deviate from the actual average thermal efficiency shown in image 25, confirming the accuracy of the calculation just completed.

Table 21: Calculated thermal efficiencies.

Thermal Efficiency Estimation												
	gennaio	febbraio	marzo	aprile	maggio	giugno	luglio	agosto	settembre	ottobre	novembre	dicembre
ηwithGmax	49,8%	52,4%	53,9%	52,7%	56,0%	56,0%	57,1%	56,8%	55,8%	54,6%	50,7%	50,6%

4.5.3 Calculation for determining the maximum number of panels that can be installed on the building's rooftop.

First, it was necessary to calculate the available roof area of the building. The building consists of two interconnected identical sections, each measuring 42.95 m in length and 14 m in width (Image 9). Considering the intersection between the two wings of the building, one part is a rectangle of (42.95 x 14) m, while the other is also a rectangle of [(42.95 - 14) x 14] m. Summing these two areas, the total available roof area is 1006.6 m².

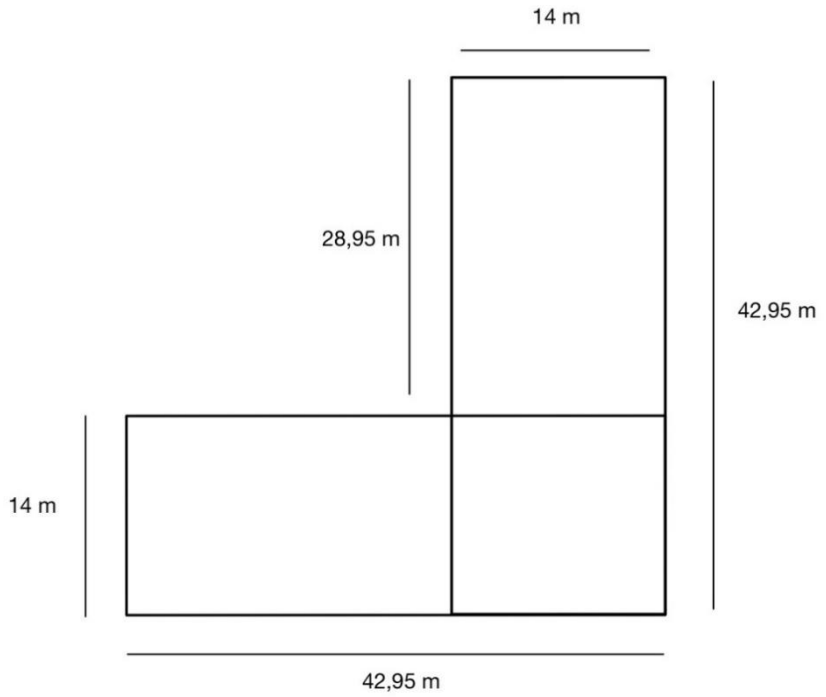

Figure 27: Building's rooftop dimensions.

Given these dimensions, an assumption is made: only 85% of the total roof surface is considered usable. Therefore, the available area for panel installation is 855.61 m².

The maximum number of panels that can be installed on the roof needs to be calculated. To determine this, the minimum distance between modules in different rows must first be found. This is obtained by considering the tilt angle, the panel dimensions and the solar altitude angle. To ensure validity throughout the year without shading effects, the worst solar altitude

value was considered, which occurs towards the end of December, when the minimum angle is approximately 26° (Obtained with PVsyst).

Assumptions made:

- Panels are positioned with their longer side of 1.97 m vertically to maximize panel density in the horizontal direction.
- Solar altitude = α = 26°, worst condition.
- Tilt Angle = β =36°.

The formula for obtaining the minimum distance between the solar panels is the following:

$$d_{min} = \frac{m * \sin \beta}{\tan \alpha}$$

Where:

- m=panel's height=1,97m.

In image 28 it can be visualized the method to obtain this value:

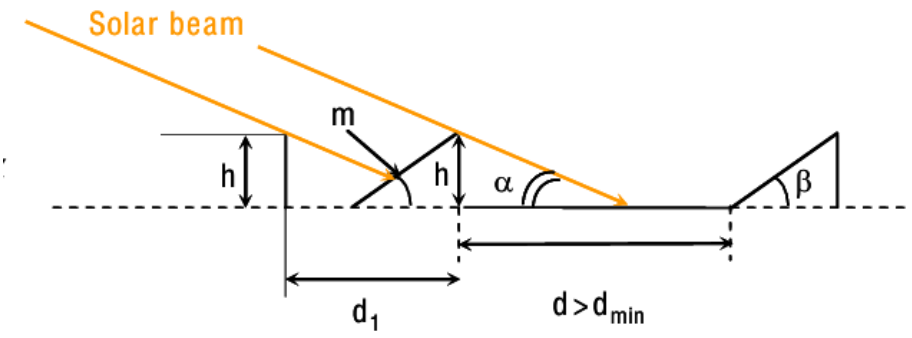

Figure 28: Minimum inter distance between panels.

Considering all the values mentioned above and rounding up, the result is 2.45 m. There must be a distance of at least 2.45 meters between one panel and the next.

Considering also the footprint of each panel, which is equal to the length multiplied by the cosine of the tilt angle, $1{,}97 \cos \beta = 1{,}58\ m$. This means that each panel occupies a space along the length equal to $4{,}03\ m$.

The final maximum layout calculated is as follows: On the wider wing of the house, measuring 42,95x14, 3x3 arrays of 12 panels each are installed; On the longer wing of the house, measuring 14x28,95, 7 arrays of 12 panels each are installed. This results in a maximum number of panels that can be installed on the building of 192 panels.

The final layout is shown in image 29.

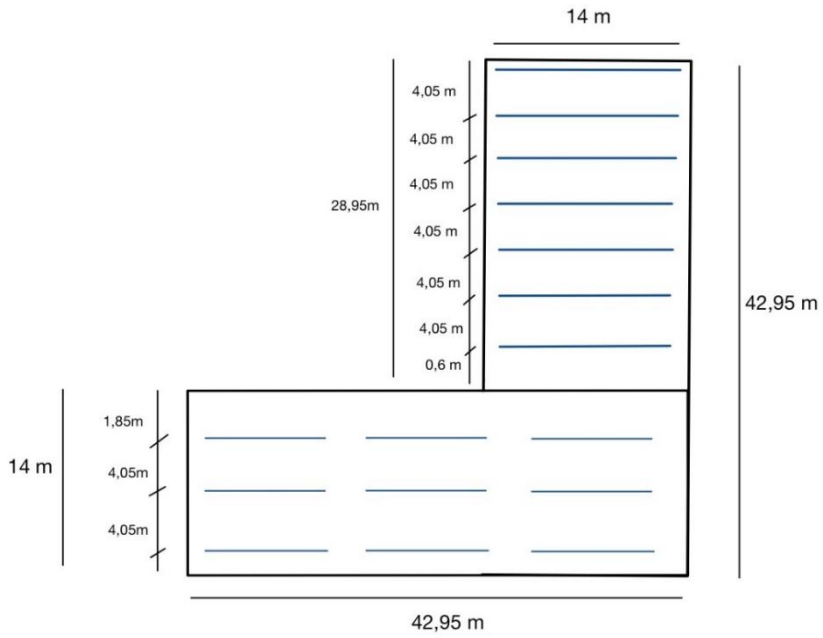

Figure 29: Final layout of the solar panels' installation.

Additionally, all panels must be oriented towards the southeast direction, as shown in Image 30.

Figure 30: Optimal orientation of the panels, on AutoCAD.

Additionally, table 22 presents some noteworthy figures regarding the price of this installation, considering only BASIC kit types, the total area occupied by the panels, and other relevant details.

Table 22: Specifics of the maximum number of panels configuration.

Height of the single panel	1,97 m
Length of the single panel	0,995 m
Optimal tilt angle β	37°
Solar altitude, worst condition, α	26°
Minimum distance between panels	2,45 m
Total Roof Area	1006,6 m^2
Total USABLE roof Area	855,61 m^2
Max number of installable panels	192
Max number of installable kits	96
Total Net modules Area	360,96 m^2
Total Price	766.539,80 €
Tank Volume	20.0 liters

5. Definition of Energy System Configuration.

This chapter presents the development of various energy system configurations designed to meet the thermal and electrical demands of the building under study. All configurations incorporate the use of hybrid solar panels, as previously detailed. The primary objective is to maximize the utilization of solar energy by integrating advanced technologies for heating, cooling, and domestic hot water (DHW) production.

5.1 Proposed system combinations.

1. Enhanced Solar System with Adsorption Chiller and Heat Pump

The first configuration involves implementing a large-scale solar energy system, coupled with an extensive thermal storage unit. This system is designed to fully satisfy the building's DHW requirements, provide the necessary thermal energy to operate an adsorption chiller for cooling production, and supply the heat required for warming the swimming pool during the summer months.

The adsorption chiller is selected for its capability to utilize thermal energy efficiently while consuming minimal electrical power. Operating on the principles of adsorption refrigeration cycles, it uses thermal energy from the solar collectors to drive the adsorption-desorption processes, producing chilled water for cooling applications. The chiller operates in a thermal tracking mode, adjusting its operation based on the availability of heat from the solar system. This ensures optimal utilization of the thermal energy harvested during periods of high solar irradiance.

During the winter season, the reduced solar energy availability necessitates supplementary heating sources to meet the building's thermal demands. Any residual heating demand not met by the solar system is addressed by a reversible air-to-water heat pump, utilized exclusively in heating mode. This heat pump is meticulously sized to optimize performance according to the specific thermal loads required, considering factors such as the building's heat loss characteristics and ambient temperature profiles.

In instances where the heat pump cannot fully meet the demand, particularly during peak load periods or extreme weather conditions, an electric boiler is employed as a supplementary system to ensure continuous thermal comfort. The electric boiler serves as a backup heating source, providing additional flexibility and reliability to the overall heating system.

To optimize the performance of the heat pump, a combination of scheduled operation and thermal tracking is implemented. A detailed timetable is defined for different months of the year, considering solar energy production patterns and the building's thermal needs. This program schedules the operation of the heat pump during periods when it can operate most

efficiently, such as during off-peak electricity tariff periods or when ambient temperatures are favorable for heat pump operation. Thermal tracking allows the system to adjust its operation in real time based on actual thermal demands and energy availability.

The adsorption chiller consistently operates in thermal tracking mode, aligning its operation with the thermal energy supplied by the solar collectors. This synchronization ensures that the chiller's operation is directly correlated with solar energy availability, maximizing the use of renewable energy and minimizing reliance on grid electricity.

2. Optimized Utilization of the Reversible Heat Pump

The second configuration emphasizes greater exploitation of the reversible air-to-water heat pump, leveraging its capability to operate in both heating and cooling modes. In this scenario, the solar system is configured to cover the DHW demand and the heating of the swimming pool during the summer. By focusing the solar energy system on these thermal loads, the heat pump's capacity can be dedicated to meeting the building's cooling requirements during the summer months.

This configuration allows the heat pump to focus exclusively on cooling during the summer, utilizing its full potential in cooling mode. The heat pump operates by extracting heat from the building's interior and rejecting it into the outdoor air, providing a comfortable indoor environment during hot periods. The sizing of the heat pump is optimized to handle the cooling loads efficiently, considering factors such as internal heat gains, occupancy patterns, and local climatic conditions.

Any residual summer heating demand not covered by the solar system, such as additional DHW needs or pool heating shortfalls, is supplied by the electric boiler. Throughout the rest of the year, the heat pump operates in heating mode, fully meeting the building's heating requirements. It extracts heat from the ambient air and transfers it to the building's heating system, providing space heating and contributing to DHW production as needed.

This configuration simplifies the energy system by eliminating the need for the adsorption chiller and consolidating the heating and cooling functions within the heat pump. By relying on a single piece of equipment for both heating and cooling, system complexity is reduced, potentially lowering maintenance requirements and operational costs. The objective is to optimize energy efficiency through a streamlined system that is easier to manage and maintain, while still capitalizing on the benefits of renewable energy utilization through the solar system.

3. Integration of Phase Change Materials and Optimal System Selection

The third configuration introduces the application of Phase Change Materials (PCMs) on the external walls of the building, aiming to reduce the overall energy demand by enhancing the thermal inertia of the building envelope. PCMs have the unique ability to absorb and release latent heat during phase transitions, thereby stabilizing indoor temperatures and reducing peak thermal loads for both heating and cooling.

The integration of PCMs into the building's construction involves incorporating PCM layers within the wall assemblies. These materials absorb excess heat during periods of high ambient temperatures, undergoing a phase change from solid to liquid, and store this thermal energy. When temperatures decrease, the PCMs release the stored heat as they solidify, contributing to maintaining a stable indoor temperature. This passive thermal regulation reduces reliance on active heating and cooling systems, leading to energy savings and improved occupant comfort.

To satisfy the remaining energy demands of the building, the most efficient configuration among the first two is selected based on detailed analysis. The reduction in thermal loads achieved by using PCMs allows for potential downsizing of heating and cooling equipment, further enhancing energy efficiency and cost-effectiveness. The integration of PCMs significantly decreases reliance on active heating and cooling systems, contributing to improved energy efficiency and environmental sustainability of the project.

5.2 Preliminary comparative analysis and expected results.

These three configurations offer distinct strategies for integrating renewable energy technologies and optimizing the building's energy performance. In general, the selection among these solutions depends on various factors, including the specific requirements of the building, local climatic conditions, economic considerations and the sustainability objectives established for the project.

In the subsequent chapters, each configuration will be analyzed in detail, examining their energy performance, economic viability, and environmental impact. The analysis will include simulations of system operation under typical and extreme conditions, assessment of energy savings, calculation of payback periods, and evaluation of greenhouse gas emission reductions. This comprehensive analysis aims to identify the most suitable solution for the case study, aligning with the overarching goal of achieving a highly efficient and sustainable energy system for the residential complex.

By exploring these configurations, the potential of combining advanced renewable energy technologies with innovative energy management strategies is demonstrated. The use of

hybrid solar panels across all configurations underscores the commitment to maximizing solar energy utilization. The incorporation of an adsorption chiller in the first configuration leverages thermal energy for cooling, reducing electrical consumption and enhancing system efficiency. This approach aligns with the principles of utilizing renewable energy sources to meet energy demands, thereby reducing reliance on fossil fuels and contributing to environmental sustainability.

The focus of the second configuration on the reversible heat pump's full capabilities exemplifies a pragmatic approach to energy management, capitalizing on the heat pump's versatility to meet both heating and cooling demands effectively. Simplifying the system by relying solely on the heat pump for active thermal control streamlines operations and may offer advantages in terms of maintenance and operational costs. This configuration also takes advantage of the heat pump's ability to exploit ambient air as a renewable energy source, further enhancing the sustainability credentials of the system.

The integration of PCMs in the third configuration highlights the benefits of passive energy-saving technologies. By enhancing the building's thermal mass, PCMs reduce fluctuations in indoor temperatures and diminish demand on active heating and cooling systems. This approach not only contributes to energy savings but also improves occupant comfort by maintaining more consistent indoor conditions. The use of PCMs represents an innovative strategy for energy efficiency, complementing the active systems employed in the other configurations.

Each configuration presents unique advantages and challenges. The first configuration may offer superior performance in terms of renewable energy utilization but may involve higher initial investment and system complexity due to the inclusion of the adsorption chiller and larger thermal storage. The economic viability of this configuration depends on factors such as the cost of equipment, installation expenses, and potential incentives for renewable energy systems.

The second configuration offers a more straightforward system that may be more cost-effective and easier to manage but relies more heavily on electrical consumption for cooling. The performance of the heat pump in cooling mode depends on ambient temperature conditions, and its efficiency may be affected during periods of high outdoor temperatures. Additionally, reliance on electricity for cooling may have implications for operational costs and environmental impact, depending on the source of the electricity.

The third configuration provides significant energy demand reduction through passive means but requires assessment of the cost-effectiveness and feasibility of PCM integration. The initial costs of PCMs can be high, and their availability may be limited. The long-term benefits in terms of energy savings and improved comfort must be weighed against the investment required for their implementation.

The aim is to identify a solution that delivers optimal energy performance while balancing economic viability and sustainability objectives. The selected configuration should demonstrate a favorable balance between initial investment and long-term benefits, contributing to reduced energy consumption, lower greenhouse gas emissions, and enhanced occupant comfort.

Ultimately, selection of the most appropriate configuration will be based on a comprehensive analysis that aligns with the project's goals of maximizing renewable energy use, enhancing energy efficiency, and minimizing environmental impact. Findings from this analysis will contribute to the development of best practices for integrating advanced energy systems in residential buildings, offering valuable insights for future projects seeking to achieve similar sustainability outcomes. The results may also inform policy recommendations and guide stakeholders in making informed decisions regarding sustainable building design and energy system integration.

6. Energy Simulations and Sizing.

This chapter presents the modeling methodologies employed for the three configurations described in Chapter 5. Building upon the prior simulation conducted using the HULC software, all relevant parameters of the case study - illustrated in Figure 4 and 5 - are input into the model. These parameters encompass the building's architectural features, material properties, occupancy schedules, and the ventilation rate determined in Chapter 2 and 3. Additionally, the solar control systems, discussed in Chapter 3, are incorporated into the model to accurately simulate their influence on the building's thermal performance.

6.1 Energy Demands of the Building.

A simulation in HULC is executed to determine the building's energy demands, specifically for domestic hot water, heating, and cooling. These demands are calculated based on the floor area of the residential units, with detailed computations provided in Figure 31. The results offer a comprehensive understanding of the building's energy consumption patterns throughout the year, which are essential for the subsequent sizing and design of the energy systems.

These are the results obtained by the simulation. All the figures are per unit of square meters.

		Calefacción	Refrigeración	A.C.S.	Ventilación	Iluminación	Otros
Demanda, D	kWh/m²año	25,57	9,71	20,02	-	-	-
Energía Final, C_ef	kWh/m²año	27,97	3,46	20,02	3,56	0,00	-
Energía Primaria Total, C_ep;tot	kWh/m²año	33,61	7,40	21,97	7,62	0,00	-
Energía Primaria No Renovable, C_ep;nren	kWh/m²año	23,83	5,63	2,78	5,80	0,00	-
Energía Primaria Renovable,C_ep;ren	kWh/m²año	9,78	1,77	19,18	1,82	0,00	-
Emisiones, E_CO2	kgCO2/m²año	4,91	0,95	0,47	0,98	0,00	-

Figure 31: First simulation's results.

For the swimming pools, the energy requirements are derived from the calculations presented in Chapter 2.3.

Table 23 presents the total energy demands, based on the total living surface of the building. The values are obtained multiplying the numbers shown in Figure 31 by 5144,95 m^2.

Table 23: Total energy demands of the building.

Need	*Energy Demand*
Living Area	5.144,95 m^2
Heating Demand	131.556,37 kWh
Cooling Demand	49.957,46 kWh
ACS Demand	103.001,90 kWh
Swimming Pool Heating Demand	43.657,96 kWh

The energy demand obtained for both the residential units and the swimming pools serve as the foundational basis for designing Configurations 1 and 2. In these configurations, the full energy demands are addressed through the proposed energy systems, which include hybrid solar panels, heat pumps, and thermal storage solutions. In contrast, Configuration 3 incorporates phase change materials (PCMs) into the building envelope, which are anticipated to reduce the overall energy demands due to their thermal energy storage capabilities and passive temperature regulation.

With the established baseline energy demands, the subsequent sections detail the sizing and design processes for the three proposed configurations. The methodologies involve selecting appropriate system components, determining optimal capacities, and analyzing system performance under varying operational conditions.

By systematically evaluating each configuration, the study aims to identify the optimal energy system design that meets the building's requirements while maximizing efficiency, sustainability, and cost-effectiveness. The integration of advanced modeling techniques ensures that the proposed solutions are both technically feasible and aligned with the project's objectives.

The analysis and sizing of the system components were conducted by examining the building's energy demand behavior on an hourly basis, adhering to standard energy sizing methodologies. In the absence of actual hourly demand profiles for the building, certain assumptions were established to facilitate the analysis:

1. Division of the Year into Thermal Periods:

The year was segmented into two distinct thermal periods:

- Summer Thermal Period: From May 1st to September 30th. During this period, it is assumed that the building's heating demand is zero due to higher ambient temperatures.
- Winter Thermal Period: From October 1st to April 30th. In this period, the building's cooling demand is considered zero owing to lower ambient temperatures.

This division reflects the seasonal variation in thermal demands, simplifying the analysis by focusing on the predominant energy needs in each period.

2. Domestic Hot Water (DHW) Demand:

No division into thermal periods was applied for DHW demand. It is assumed that the requirement for domestic hot water remains relatively constant throughout the year, independent of seasonal changes. This constant demand is accounted for in the sizing calculations without temporal segmentation.

3. Assumed Hourly Demand Curves:

To compensate for the lack of detailed hourly consumption data, assumed hourly percentage demand curves were developed for both a typical winter day and a typical summer day. These curves stand for the estimated distribution of heating and cooling demands over a 24-hour period. By applying these percentage profiles to the total daily energy demands, it was possible to distribute the energy requirements hour by hour. This approach enables a more correct sizing of the system components by aligning the capacity with the temporal fluctuations in demand.

Note: These percentage values are not completely assumed: inspiration from other studies in the same sector and in the same city were analyzed. These values are likely to be real.

In the tables and figures below, the assumed charge curve considered are shown.

Table 24: Hourly winter day thermal energy charges.

Winter day	
Hour	**% hourly charge**
0,00	1,0%
1,00	1,0%
2,00	1,0%
3,00	1,0%
4,00	1,0%
5,00	2,5%
6,00	4,5%
7,00	8,0%
8,00	9,5%
9,00	8,0%
10,00	5,5%
11,00	4,0%
12,00	3,0%
13,00	3,5%
14,00	3,5%
15,00	2,5%
16,00	2,5%
17,00	3,5%
18,00	8,0%
19,00	10,0%
20,00	8,0%
21,00	4,5%
22,00	3,0%
23,00	1,0%

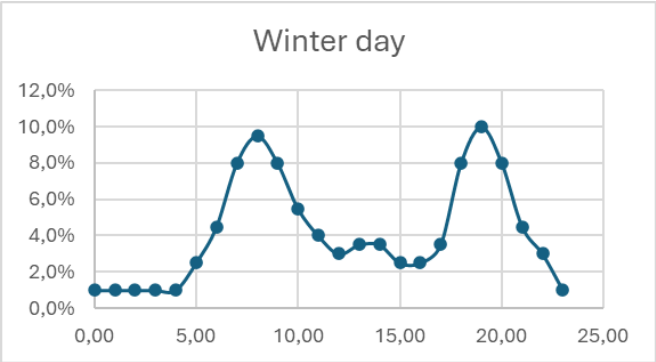

Figure 32: Daily winter day % thermal charge variation.

Table 25: Hourly summer day thermal energy charges.

Summer day	
Hour	**% hourly charge**
0,00	0,5%
1,00	0,5%
2,00	0,5%
3,00	0,5%
4,00	0,5%
5,00	1,5%
6,00	2,5%
7,00	4,0%
8,00	5,0%
9,00	6,5%
10,00	8,5%
11,00	10,0%
12,00	11,0%
13,00	11,5%
14,00	10,5%
15,00	8,0%
16,00	7,0%
17,00	4,5%
18,00	2,5%
19,00	2,0%
20,00	1,0%
21,00	0,5%
22,00	0,5%
23,00	0,5%

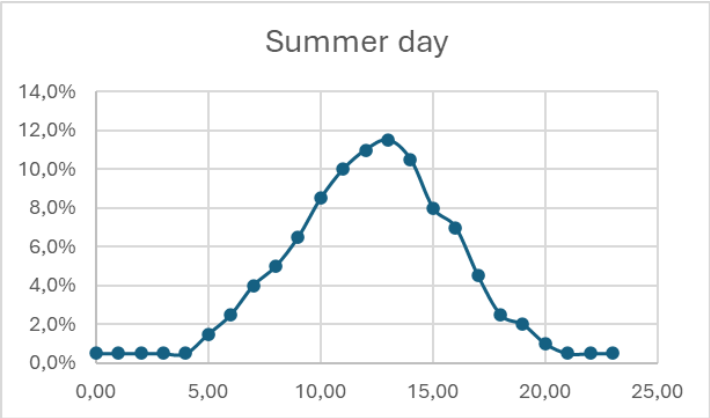

Figure 33: Summer Day daily % thermal charge.

Table 26: Hourly DHW charges.

DHW hourly demand	
Hour	**% hourly charge**
0,00	0,5%
1,00	0,5%
2,00	0,5%
3,00	0,5%
4,00	0,5%
5,00	1,0%
6,00	3,5%
7,00	9,5%
8,00	10,0%
9,00	6,0%
10,00	4,5%
11,00	2,5%
12,00	3,5%
13,00	5,0%
14,00	5,0%
15,00	2,0%
16,00	2,0%
17,00	2,5%
18,00	5,5%
19,00	7,5%
20,00	11,5%
21,00	8,0%
22,00	5,0%
23,00	3,0%

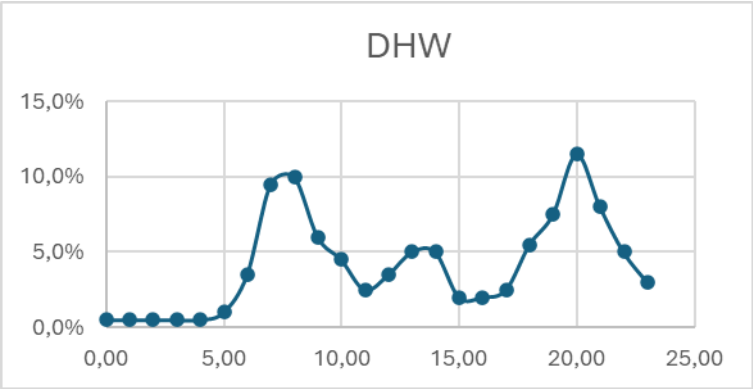

Figure 34: Daily DHW % charge.

4. Swimming Pool Energy Demand:

Based on the data presented in Chapter 2.3, a load curve was defined for the swimming pool's energy demand for both a typical winter day and a typical summer day. This curve accounts for factors such as operational hours, occupancy patterns, and thermal losses specific to the pool. Incorporating these load profiles ensures that the swimming pool's thermal requirements are accurately integrated into the overall energy demand model of the building.

Following the assumptions in chapter 2.3, these curves are obtained:

Table 27: Winter Day % thermal energy needed from the swimming pool.

Winter day	
Hour	**% hourly charge**
0	0,0%
1	0,0%
2	0,0%
3	0,0%
4	0,0%
5	0,0%
6	0,0%
7	0,0%
8	0,0%
9	0,0%
10	0,0%
11	12,5%
12	12,5%
13	12,5%
14	12,5%
15	12,5%
16	12,5%
17	12,5%
18	12,5%
19	0,0%
20	0,0%
21	0,0%
22	0,0%
23	0,0%

Table 28: Summer Day % thermal energy needed from the swimming pool.

Summer day	
Hour	**% hourly charge**
0	0,0%
1	0,0%
2	0,0%
3	0,0%
4	0,0%
5	0,0%
6	0,0%
7	0,0%
8	0,0%
9	8,3%
10	8,3%
11	8,3%
12	8,3%
13	8,3%
14	8,3%
15	8,3%
16	8,3%
17	8,3%
18	8,3%
19	8,3%
20	8,3%
21	0,0%
22	0,0%
23	0,0%

By implementing these assumptions, the analysis could proceed with a structured methodology, allowing for the effective sizing of the energy system components despite the absence of detailed consumption data. The development of hourly demand curves is essential for designing systems that can respond to the dynamic nature of energy usage, ensuring that ability is matched to demand throughout the day. This method provides a robust foundation for optimizing system performance and achieving energy efficiency objectives.

6.2 Technical sizing, configuration 1

Configuration 1 involves sizing a large-scale hybrid solar panel system designed to cover the summer energy demands for operating the adsorption chiller, producing domestic hot water, and heating the swimming pool. The adsorption chiller uses thermal energy collected by the solar panels to generate cooling, operating on adsorption-desorption cycles with minimal electrical consumption.

To meet heating demands during the rest of the year, an air-to-water heat pump is incorporated. This heat pump exploits ambient thermal energy from the surrounding environment to provide space heating and supplement DHW production. It works by extracting heat from outdoor air and transferring it into the building's heating system, utilizing a renewable and "free" energy source.

In situations where the heat pump cannot fully satisfy the heating demand - such as during peak load periods or extremely low ambient temperatures - an electric boiler serves as an auxiliary heating source to ensure consistent thermal comfort throughout the building.

To optimize the utilization of solar energy, considering that production and demand are often out of phase, a thermal storage system with accumulation tanks supplied by Abora Solar, the manufacturer of the panels, is planned. These tanks store excess thermal energy produced during peak solar periods for use when demand exceeds production. Additionally, to maximize the efficiency of the heat pump, an on-off scheduling program is implemented to cover the daily thermal deficit as effectively as possible. This time-based control strategy ensures that the heat pump works during optimal periods, aligning its function with the building's heating requirements and minimizing energy waste.

- **Selection of the Adsorption Chiller.**

Due to the limited availability and prohibitive costs of adsorption chillers in the current market, the selection process was constrained to models that are commercially accessible and compatible with the system's design requirements. This type of equipment is not widely distributed, making options scarce and often economically challenging to obtain.

After a thorough market analysis, the adsorption chiller chosen for this configuration is the eCoo 40X model manufactured by FAHRENHEIT. The technical specifications of this unit, provided in Figure X, align well with the project's thermal load demands and operational parameters. The eCoo 40X offers performance characteristics that are suitable for the intended application, facilitating efficient integration into the proposed energy system. Its compatibility with the system's sizing ensures optimal utilization of the thermal energy supplied by the hybrid solar panels, thereby contributing to the overall efficiency and sustainability of the configuration.

Table 29: Specifics of the Adsorption Chiller.

MODEL: eCoo 40X		
PERFORMANCE		
Cooling Capacity	Up to 100	kW
COP_{TH}	Up to 0,65	
APPLICATION RANGE		
Hot water temperature	50-95	°C
Re-cooling water temperature	22-40	°C
Chilled water temperature	8-21	°C
Max operating pressure	4	bar
DIMENSIONS		
W x D x H	875 x 2930 x 2500	mm
Footprint	2,56	m^2
Empty Weight	2300	kg
ELECTRICAL POWER	CONSUMPTION/SUPPLY	
At typical pressure drop	2,064	kW
Power Supply	230V, 50/60 Hz	
HOT WATER CIRCUIT		
Volume flow rate	15,00	m^3/h
Available Delivery head	280	mbar
Connection	DN 65	
RE-COOLING CIRCUIT		
Volume flow rate	30,60	m^3/h
Available delivery head	271	mbar
Connection	DN 80	
CHILLED WATER CIRCUIT		
Volume flow rate	17,40	m^3/h
Available delivery head	472	mbar
Connection	DN 65	

The selected adsorption chiller offers excellent characteristics, particularly its ability to run without a lower threshold below which the machine ceases to function. Furthermore, it can work with a minimal electrical supply, effectively approaching zero, which enhances its efficiency and suitability for integration into the system. As shown in Table 24, the thermal coefficient of performance (COP) of the chiller is 0.65. A key assumption in this analysis is that COP stays constant at this value throughout the operating range. This assumption enables the transformation of the cooling demand specified in Table 23 into the corresponding heat demand required by the adsorption chiller. Consequently, the sizing calculations consider the chiller's heat input necessary to meet the building's cooling requirements, rather than directly using the building's cooling demand.

Following this assumption, the new required heat input for the adsorption chiller is found by dividing the cooling demand by the COP of 0.65.

$$E_{\text{th for cooling}} = \frac{E_{\text{cooling}}}{COP} = \frac{49.957{,}46\ \text{kWh}}{0{,}65} = 76.857{,}64\ \text{kWh}$$

The price of this component is not public. FARHENHEIT request is 95.000€.

- **Technical dimensioning of the solar panels' system.**

The hybrid solar panel system was meticulously sized to meet the summer thermal energy demand, which encompasses three primary components:

1. Heat Required by the Adsorption Chiller: The thermal energy necessary for the adsorption chiller to operate effectively, converting thermal input into cooling output to satisfy the building's cooling demand during the summer months.

2. Heat for Swimming Pool Heating: The energy needed to keep the swimming pool at the desired temperature, as previously calculated (chapter 2.3).

3. Heat for DHW Production: The thermal energy needed to supply hot water for domestic use, which stays relatively constant but is particularly significant during the summer due to increased usage patterns.

To accurately distribute these total summer demands over time, the load curves developed in Chapter 6.1 were applied.

Regarding the solar irradiance data, the global solar radiation values were obtained from the historical records for the year 2023, sourced from the PVGIS software.

The panels' efficiencies were incorporated based on the parameters specified in Chapter 4.2.4.1, which detail the electrical and thermal performance characteristics of the hybrid panels under various operating conditions.

The thermal energy production of the hybrid solar panels was calculated using the standard formula for thermal collectors, adjusted for the specific properties of the panels:

$$E_{\text{thermal}} = \eta_{\text{thermal}} * G_{T_{\text{optimalangle}}} * (2 * A_{\text{net}})$$

Where:

- E_{thermal} is the thermal energy generation in kWh.
- η_{thermal} values are displayed in Table 21. It is taken as a constant value for each day of the month.
- $G_{T_{\text{optimalangle}}}$ hourly values are taken from PVGIS.
- A_{net} =1,88 m^2, multiplied by 2 to obtain the thermal energy produced by 1 kit.

By applying this calculation on an hourly basis, it was possible to estimate the thermal energy output throughout the day and across the summer period.

To address the mismatch between energy production and demand - since the peak thermal energy production typically occurs when the building's thermal demand is lowest - a thermal storage system was integrated into the design.

This system consists of accumulation tanks provided by Abora Solar, the panel manufacturer. The storage tanks were sized in liters to accommodate the maximum thermal energy produced by the solar panel system during peak production periods. This ensures that excess energy generated is not wasted but stored for use when demand exceeds production, such as in the early morning or evening hours.

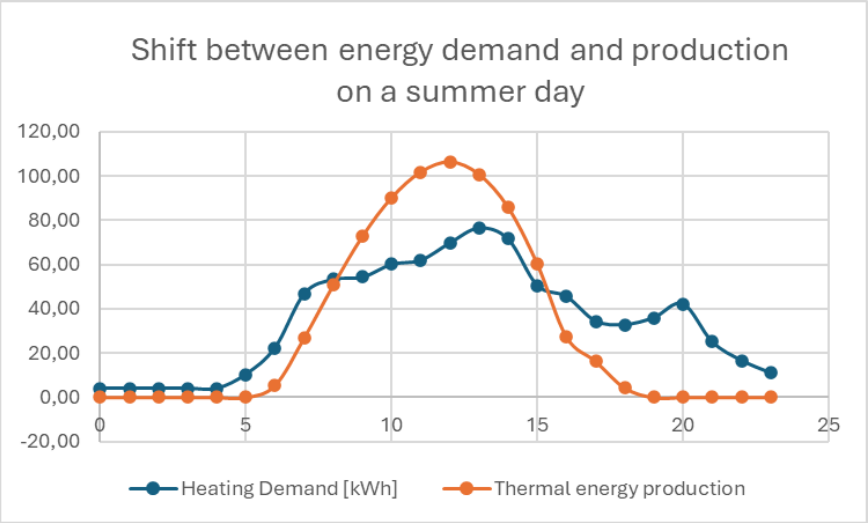

Figure 35: Shift between thermal energy production and demand, without a storage system.

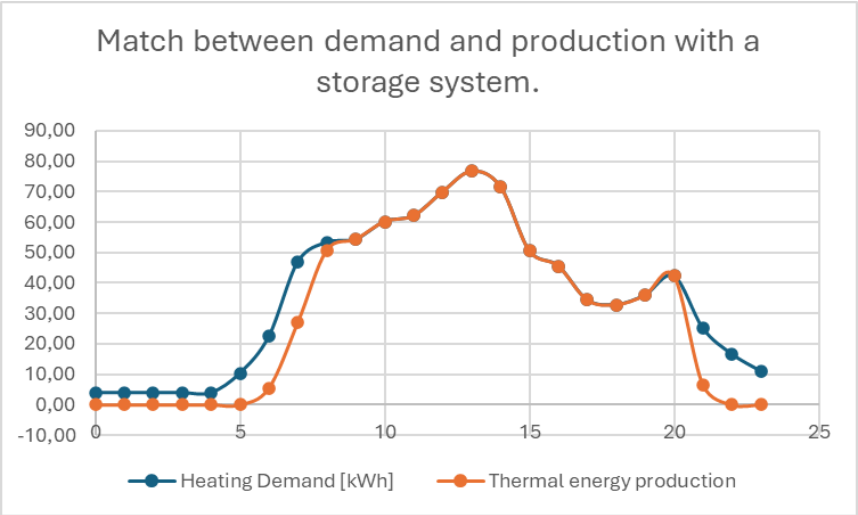

Figure 36: Match between Thermal energy production and demand with a storage tank.

The sizing of the storage tanks was determined by calculating the maximum surplus thermal energy that could not be immediately consumed, in order to always store the whole energy produced by the panels system.

An important factor in the sizing process is the consideration of thermal losses associated with the storage system. These losses occur due to heat transfer from the storage tanks to the surrounding environment and can impact the overall efficiency of the system. For simplicity, and as will be detailed in subsequent chapters, these losses were set at a value of 2% of the hourly thermal load stored.

By incorporating these losses into the sizing calculations, the system ensures that the net stored energy, together with the solar panels' production, is sufficient to meet the building's demands.

The primary objective of sizing the panels and the storage tank was to cover between **70% and 80% of the summer thermal demand** through their production and storage capabilities. Achieving this coverage level reduces reliance on auxiliary heating systems during the summer months, such as electric boilers and heat pumps, thereby enhancing energy efficiency and reducing operational costs.

This goal was met by determining the optimal number of hybrid solar panel kits required, together with the correct dimensioning of the storage tank. This is key.

Note: storage tank capacity is "free", is saying that Abora Solar gives 150 liters of storage systems per bought kit; As will be seen, the available capacity will be way higher than what is actually needed. Part of this capacity will be shifted to the heat pump.

The simulation model was implemented using **Excel**, enabling detailed analysis and optimization of the system components. The model achieved a coverage of 75% of the total

summer thermal energy demand by jointly optimizing the number of hybrid solar panel kits and the size of the thermal storage tank. The tank size was calculated retrospectively to ensure it could accumulate all the peak energy output produced by the solar panels. This approach allows for the storage of excess thermal energy generated during periods of high solar irradiance. The energy accumulated in the tank is defined as:

$$E_{\text{stored(hour n)}} = (98\% \times E_{\text{stored(hour n}-1)}) + E_{\text{excess from the solar panels}} - E_{\text{given}}$$

Where:

- Each E is energy, in kWh.
- 98% because an hourly 2% of stored energy is considered to be wasted.
- E in excess from the solar panels is the part of energy overproduced form the solar panels, which is not "feeding" the building's energy demand directly.
- E given is the energy needed from the storage tank in a precise hour, because the panels system is not capable of giving energy to satisfy the building's demand.

Based on the calculations and demand profiles, it was found that a total of **52 Basic kits** would be sufficient to meet the desired coverage percentage.

With this number of kits, a peak thermal energy production of 170 kWh is achieved. Correspondingly, Abora Solar would supply a total storage capacity of 7.800 liters, which at first glance appears excessive compared to what might actually be required by the panel system. Therefore, assuming the peak production is indeed 170 kWh, the necessary storage volume to properly accumulate all the energy produced by the panels is calculated as:

$$l = {E_{\text{stored peak}} \times 3{,}6 \times 10^6} \Big/ {4186 \times \Delta T}$$

Where:

- ΔT is the difference between the inlet and the outlet temperature of the tank, considered to be equal to 50°C.
- *l* is the size of the tank in liters.

The result leads to a value of approximately **3.000 liters.**

This configuration yields excellent results. Out of a total summer thermal demand of 128,833.78 kWh, the system **self-consumes 97,212.85 kWh**, corresponding to **75% of the total demand**. The remaining unmet demand is satisfied by a combination of the heat pump and the electric boiler, which will be appropriately sized in the subsequent sections.

The same system without the storage tank would lead to a self-consumption equal to 82.796,40 kWh, a significant 17,5% less than the defined configuration. Another important fact is that a total of 14.416.45 kWh would be wasted without the storage tank.

By strategically sizing both the hybrid solar panel system and the thermal storage, the configuration effectively uses renewable energy resources to meet the building's thermal demands during summer, including the energy cooling demand. This strategy enhances the sustainability of the building's energy system and reduces environmental impact by decreasing greenhouse gas emissions associated with fossil fuel consumption.

- **Technical dimensioning of the deficit heating's supply system: Air-Water heat pump and electrical boiler.**

The next phase involves sizing the system components necessary to meet the remaining heating demand throughout the whole year, specifically the heat pump and the electric boiler.

The selected heat pump is an air-to-water type, previously described in detail. The electric boiler's role is to satisfy any heating demand that the heat pump alone cannot fulfill. It is recognized that heat pumps have a minimum thermal load threshold below which they cease to work efficiently.

To mitigate this limitation, a thermal storage system will be designed. This storage system allows the heat pump to work according to a well-defined time schedule, which considers the heat produced by the solar panels. The time program is thus a function of external climatic conditions and is defined differently for each month. By scheduling the operation of the heat pump during different periods, the system maximizes the utilization of available renewable energy while ensuring the heat pump operates within its efficient operating range.

The thermal storage system is calculated using the same equations and criteria outlined for the solar panel system's storage, including the 2% allowance for energy dissipation. This approach ensures consistency in the modeling of thermal losses and storage capacities across the system.

In conclusion, the model addresses unmet heating demand through the following mechanisms:

- Electric Boiler Activation: If the heating demand is below the heat pump's minimum rated thermal power, the electric boiler is engaged to supply the required heat.

- Heat Pump in Thermal Tracking Mode: If the heating demand exceeds the energy available from the thermal storage tank, the heat pump works in thermal tracking mode to meet the additional demand.

This strategy ensures that the heating requirements are met efficiently throughout the year by refining the use of renewable energy sources and appropriately using auxiliary systems when necessary.

The steps of the dimensioning procedure are described below:

1. Definition of a frequence curve.

Defining a frequency curve is a primary and fundamental step in designing a system of this nature. The frequency curve is constructed based on the annual hourly energy deficit data, where the deficit is defined as the building's energy demand after subtracting the thermal production and storage provided by the solar panel system. This deficit is the residual energy requirement that must be met by auxiliary systems such as the heat pump and electric boiler.

The energy deficit data are compiled and put into Excel in a single column. These values are then sorted in descending order, from the largest to the smallest deficit. Sorting the data in this manner allows for the identification of the largest peak deficit recorded throughout the year, which is critical for sizing the capacity of the supplementary heating systems.

Subsequently, another column is created, holding a series of threshold values ranging from zero up to the largest peak deficit, incremented by a defined interval of one-unit. This set of threshold values stands for potential capacities of the heat pump system.

In an adjacent column, a count is performed to find the number of occurrences where the actual energy deficit exceeds each threshold value. This involves iterating through the sorted deficit data and telling the instances where the deficit is greater than each threshold level. The frequency for each threshold is then calculated using the formula:

$$\text{Frequency}_{\text{treshold x}} = 1 - \frac{\text{Number of occurrences above treshold x}}{\text{Total number of Data Points}}$$

This calculation yields the cumulative frequency distribution, which effectively represents the percentage of time that the energy deficit is below each threshold level. In other words, it says that the proportion of the year during which a heat pump with a specific peak power capacity would be sufficient to meet the residual heating demand.

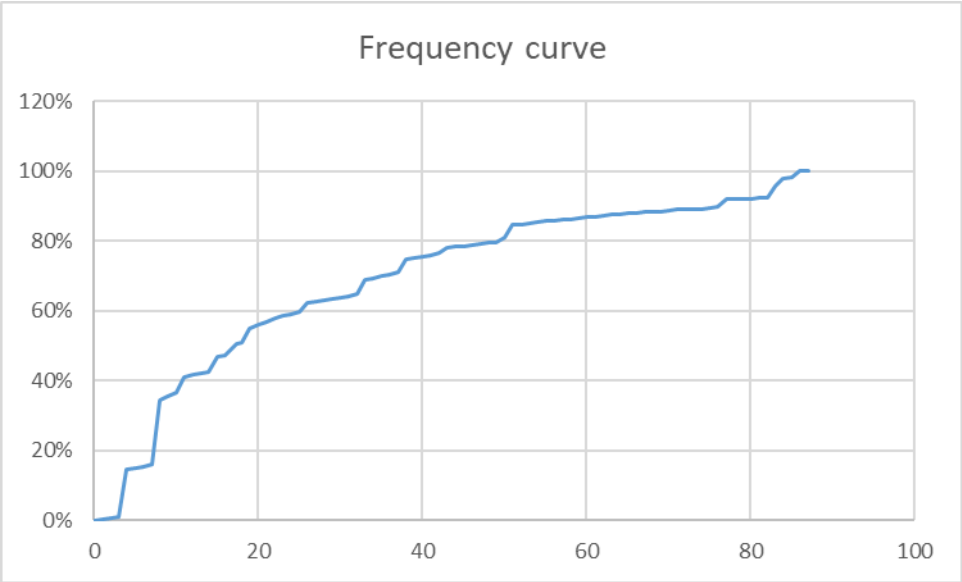

Figure 37: frequency curve for dimensioning the heating supply system.

- **Definition of the heat pump's type.**

By analyzing the frequency curve, it is possible to find the optimal sizing of the heat pump to achieve the desired level of coverage.

In this case, the strategy adopted involved finding a commercially available product capable of meeting the maximum thermal demand recorded during the year, which is 87.10 kW, and analyzing its suitability for integration into the system. After a comprehensive selection process, the **TRANE CUBE CXB** air-to-water heat pump was chosen. The technical details of this model are provided in Figure 38.

CXB

	Pc (1) kW	Pec (1) kW	EER (1)	SEER (2)	ηsc (2) %	Ph (3) kW	Peh (3) kW	COP (3)	Ph (4)	Peh (4) kW	COP (4) kW	SCOP (5)	ηsh (5) %	LwO (6) dB(A)	Refrigerant	L (7) mm	W (7) mm	H (7) mm	OW (4) kg
CXB 017	15,1	5,8	2,60	-	-	17,4	5,4	3,23	17,8	4,4	4,06	3,73	146,0	74	R410A	1807	779	1687	328
CXB 020	17,0	6,9	2,47	-	-	20,1	6,1	3,29	20,5	4,9	4,18	3,73	146,0	74	R410A	1807	779	1687	331
CXB 025	22,0	8,4	2,62	-	-	26,5	8,0	3,32	27,2	6,6	4,15	3,70	145,0	77	R410A	1807	779	1687	365
CXB 028	25,2	9,9	2,55	-	-	31,0	9,1	3,40	31,5	7,3	4,30	3,65	143,0	76	R410A	2061	779	1687	385
CXB 033	28,5	11,9	2,39	-	-	35,7	10,5	3,40	36,6	8,7	4,20	3,78	148,0	77	R410A	2061	779	1687	396
CXB 036	31,1	14,0	2,22	-	-	39,6	12,0	3,30	40,6	9,8	4,13	3,80	149,0	78	R410A	2061	779	1687	396
CXB 039	33,3	15,5	2,15	-	-	42,5	12,9	3,30	43,8	10,8	4,04	3,78	148,0	78	R410A	2061	779	1687	398
CXB 045	40,4	16,6	2,44	-	-	48,6	15,0	3,24	50,1	12,3	4,08	3,93	154,0	79	R410A	2061	779	1687	580
CXB 050	45,0	19,7	2,29	-	-	54,4	17,0	3,20	56,0	13,9	4,02	3,80	149,0	79	R410A	2061	779	1687	590
CXB 055	50,1	17,8	2,82	-	-	57,1	17,5	3,27	59,4	14,4	4,12	3,38	132,0	81	R410A	2524	1038	1995	726
CXB 065	57,8	21,8	2,65	-	-	66,5	21,3	3,13	69,2	17,4	3,97	3,49	137,0	82	R410A	2524	1038	1995	737
CXB 080	71,2	25,1	2,84	-	-	79,0	24,9	3,17	82,3	20,7	3,98	3,24	127,0	84	R410A	2524	1038	1995	809
CXB 090	78,4	28,5	2,75	-	-	87,4	27,9	3,13	91,3	23,2	3,93	3,33	130,0	85	R410A	2524	1038	1995	815

Pc: Cooling capacity
Pec: Total power input in cooling
EER: Energy Efficiency Ratio (cooling)
SEER: Seasonal Energy Efficiency Ratio
ηsc: Seasonal space cooling energy efficiency
Ph: Heating capacity
Peh: Total power input in heating
COP: Coefficient Of Performance (heating)
SCOP: Seasonal Coefficient Of Performance
ηsh: Seasonal space heating energy efficiency
LwO: A-weighted sound power level outside
Refrigerant: Refrigerant type
L: Length
W: Width
H: Height
OW : Operating Weight

Figure 38: technical specifics of the heat pump.

The selected heat pump is reversible, capable of operating in both heating and cooling modes. Its thermal characteristics align precisely with the requirements of the case study. Specifically, it has a maximum thermal output capacity of 87.4 kW and a lower operational limit of 17.4 kW, below which the unit ceases to function. To address this limitation and ensure full coverage of the building's thermal demand, an electric boiler with a peak power output of 18 kW is incorporated into the system. This boiler supplements the heat pump by providing thermal energy when the demand falls below the heat pump's lower operating threshold, thereby guaranteeing consistent thermal comfort throughout the building.

To enhance the accuracy of the calculations and make them more representative of real-world simulations, the COP (Coefficient of Performance) values of the heat pump provided in Figure 38 - which correspond only to specific load conditions - have been interpolated. This interpolation allows for the determination of the COP at any given operating load of the machine, enabling a more precise analysis of the heat pump's performance across its entire operational range.

Note:

- A reversible heat pump capable of operating in both heating and cooling modes was selected. This choice provides an emergency backup in situations where the adsorption chiller may not function properly.

- The product's price is not publicly listed or commercially available in standard catalogs. For the purposes of this project, a dedicated price of €80.000 was provided.

- **Definition of the thermal storage tank maximum capacity.**

The dimensioning process was not based on complex reasoning but on using existing resources to minimize capital expenditures, given the substantial monetary investment already planned.

The primary design principle was to avoid relying on the thermal storage tank of the solar panel system. Instead, a secondary, decoupled storage tank was created to separate the two systems, simplifying both the sizing calculations and the control mechanisms for each.

Using the residual storage capacity provided by Abora Solar, amounting to 5.000 liters, a second decoupled storage tank was proved. The following formula was applied to find the maximum storable energy value:

$$l \times 4186 \times \Delta T / 3{,}6 \times 10^{6} = E_{\text{stored peak}}$$

In which:

- ΔT is set to be equal to 75°C.

Note: the considered value of temperature level is higher than the imposed one for the solar panels' system. This is because the temperature level of the produced hot water is much higher than the one provided by the solar panels.

In this case study, the calculated peak for the thermal energy stored will be 525 kWh.

- **Definition of a scheduled time program for the functioning of the heat pump.**

Analyzing the previously constructed frequency curve and applying it to the selected heat pump reveals a significant issue. If the heat pump was to operate solely in thermal tracking mode, it would be active for **49%** of the total usage time, while the electric boiler would operate for the remaining **51%**. Since the main objective of this sizing is to maximize the utilization of the heat pump's capabilities over the electric boiler - especially considering their different efficiency values and the electrical input required for their operation - it is imperative to establish a thermal storage system and define an hourly operating schedule for the heat pump. This schedule should be a function of external climatic conditions and the building's thermal demand. By an optimized operation program, the heat pump can be used more effectively, reducing reliance on the less efficient electric boiler and enhancing the overall efficiency of the heating system.

After a manual optimization process, the results obtained are shown in the table below. The criteria used in this iterative process were to minimize the use of the electric boiler and to not overtake the threshold given for too many hours by the maximum capacity of the thermal storage tank, to minimize the wasted energy.

Note: not only a schedule time was chosen, but also the % of working charge of the unit. It is as fundamental as the scheduled time program, because it also depends on this data the energy consumption of the unit.

	Jan; 50% of the nominal charge	Febr, 50% of the nominal charge	Mar, 50% of the nominal charge	Apr, 50% of the nominal charge	May, 65% of the nominal charge	Jun, 65% of the nominal charge	Jul, 65% of the nominal charge	Aug, 65% of the nominal charge	Sep, 65% of the nominal charge	Oct, 65% of the nominal charge	Nov, 50% of the nominal charge	Dec, 50% of the nominal charge
00:00	1	1	1	1	1	1	1	1	1	1	1	1
01:00	1	1	1	1	1	1	1	1	1	1	1	1
02:00	1	1	1	1	1	1	1	1	1	1	1	1
03:00	1	1	1	1	0	0	0	0	0	0	1	1
04:00	1	1	1	1	0	0	0	0	0	0	1	1
05:00	1	1	1	0	0	0	0	0	0	0	1	1
06:00	1	1	1	0	0	0	0	0	0	0	1	1
07:00	0	0	0	0	0	0	0	0	0	0	0	0
08:00	0	0	0	0	0	0	0	0	0	0	0	0
09:00	0	0	0	0	0	0	0	0	0	0	0	0
10:00	0	0	0	0	0	0	0	0	0	0	0	0
11:00	0	0	0	0	0	0	0	0	0	0	0	0
12:00	0	0	0	0	0	0	0	0	0	0	0	0
13:00	0	0	0	0	0	0	0	0	0	0	0	0
14:00	0	0	0	0	0	0	0	0	0	0	0	0
15:00	0	0	0	0	0	0	0	0	0	0	0	0
16:00	1	1	1	0	0	0	0	0	0	0	1	1
17:00	1	1	1	0	0	0	0	0	0	0	1	1
18:00	1	1	1	0	0	0	0	0	0	0	1	1
19:00	1	1	1	0	0	0	0	0	1	1	1	1
20:00	1	1	1	1	0	0	0	0	1	1	1	1
21:00	1	1	1	1	0	0	0	0	1	1	1	1
22:00	1	1	1	1	0	0	0	0	1	1	1	1
23:00	1	1	1	1	0	0	0	0	1	1	1	1

Figure 39: Scheduled time program for the functioning of the heat pump.

- **Dimensioning of the electrical boiler.**

The electric boiler is selected with a peak power rating of 18 kW. Its purpose is to activate when the heat pump alone is unable to provide thermal power below its lower operational threshold of 17.4 kW.

In this context, a specific boiler model is not chosen based on detailed individual characteristics. Instead, the thermal performance and cost of modern, new-generation electric boilers are considered. An efficiency of 98% and a total price of €5.000 are assumed for the boiler of this case study. The electric boiler will work within the energy collection system defined for the heat pump, not within the tank chosen for the solar panel array.

- **Thermal storage tank's coating.**

It is necessary to conduct a more detailed analysis of the storage tank. In the current energy balance calculations, thermal losses from the tank have not been considered. Given the size and dimensions of the storage tanks, it is unacceptable to assume that these losses are negligible. Therefore, a strategy has been adopted that involves insulating the storage tanks to minimize thermal losses and enhance the overall efficiency of the system.

More precisely, one of the products from the company **roVa** has been analyzed, as they produce materials suitable for the intended purpose. The selected product is the **roVa Shield Aerogel Insulating Coating**, which is sold in liquid form and must subsequently be applied manually or sprayed.

Aerogels, despite their high cost, are ideal for applications requiring coatings to prevent thermal losses. Their exceptional insulating properties, resulting from a nanoporous structure that significantly reduces heat conduction and convection, make them superior to traditional insulation materials. This makes aerogels particularly suitable for insulating thermal storage tanks, where minimizing heat loss is critical for overall system efficiency.

The thermal conductivity of this material is excellent for our purposes, with a value of 0.044 W/mK. The detailed technical specifications of this material are provided in Table 30.

Table 30: Technical features of the roVa shield.

Category	Feature
Coating Type	Water-based Acrylic
Color	White (eggshell finish)
Size	4L. 18L (1.05. 4.76 Gallon)
Relative Density	0.52 ~ 0.62
Viscosity	10.000 ~ 18.000 cPs
VOCs	0.9 g/L
Theoretical coverage	0.68 m^2/L (1mm thickness) 28 sq.ft./gallon (0.04" thickness)
Solids by Volume	68%
Dilution Agent	Water (only if necessary. up to 10wt%)
Recommended Thickness	Sprayer: 1~2 Brush. Roller: 3~4
Number of coats	1.0 mm (2 ~ 3 coats) ; minimum 0.04" (2 ~ 3 coats) 40 mils (2 ~ 3 coats)
Dry to touch time	40 minutes (25°C. 77°F. Brush)
Cure time	24 hours (25°C. 77°F. Brush. 1mm. 0.04" thickness)
Recoat time	Brush. Roller: 4 hours @ 350um thickness
Recoat time	Sprayer: 8 hours @ 800um thickness per coat with 10% dilution (2 coats necessary)
Recoat time	Sprayer: Single coat possible @ 1500um thickness with no dilution
Application	Brush. Roller. Sprayer (airless. pneumatic. spray gun)
Thermal Conductivity	0.044 W/m·k
Application Temperature	5 ~ 35°C 41 ~ 95°F
Operation Temperature	-50 ~ 120°C -58 ~ 248°F

This material can be easily purchased on Amazon. A container holding 18 liters of the product is priced at $450, as shown in image 40.

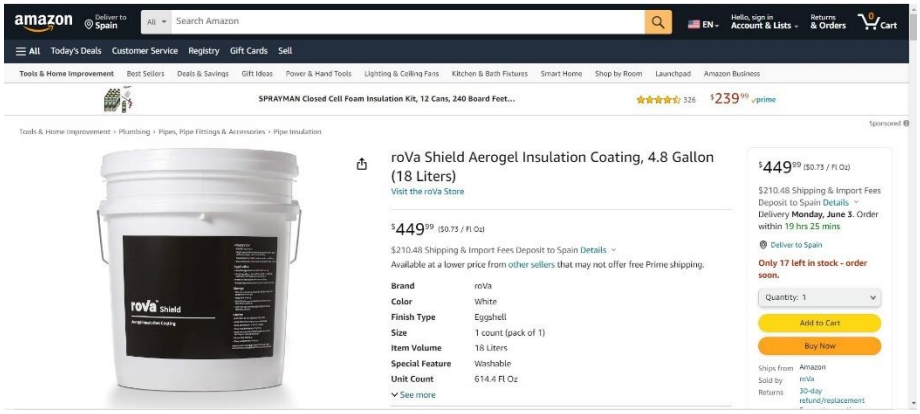

Figure 40: roVa shield price.

To calculate the required volume of product, the following procedure was implemented:

First, the external surface of the tank was determined. As a rule of thumb, the collection tank should have an aspect ratio, which is the ratio between its height and diameter, of approximately 3 [X]. With this ratio set, and given the total volume of the two tanks, both the solar panels' and the heat pump's one, which is simply the volume of the collected water, so 8 m^3, it was straightforward to calculate the tank's diameter and height using Excel's solver function, doing the equivalence between the real volume and the "calculated volume", which is the one obtained with the formulas. The procedure is presented in table 55. The tank is considered cylindric. The table also contains the values for the lateral surface and the top and bottom surfaces, leading to the calculation of the total external tank surface.

Table 31: Tank's surfaces values.

h/D	3	
Volume	8000	l
Volume	8	m^3
D	1,50	m
h	4,51	m
Volume calculated	8,00	m^3
Top and bottom surface	3,55	m^2
Lateral Surface	21,29	m^2
Total external surface	24,84	m^2

In order to calculate the heat losses from the tank, it is necessary to know the thickness of the insulating material. It is assumed that the required thickness of the insulating material is 2 cm. Using the following equation, the value of the heat lost is obtained:

$$q = \frac{k * A * \Delta T}{dx} = 2{,}75kW$$

In which:

- k is the thermal conductivity of the isolating material (table 30).

- A is the total external surface of the tank (table 31).

- $\Delta T = T_w - T_{ambient}$ =50K; These two values are considered as averages of the temperature inside the tank and as average on the ambient temperature.

- dx is the thickness of the coating, set to be 20mm.

With 20mm, the heat loss is 2,73 kW, so a figure that can be accepted.

For a lack of simplicity, in the Energy balance this value is set to be the 2% of the total hourly stored heat.

In table 30, the theoretical coverage is represented. It is the number of square meters that can be covered with a liter of product, considering a 1mm coating. It is equal to 0,68 m^2/L. To find the total number of liters required to cover the whole tank, its total external area is divided for the theoretical coverage, leading to a value of 36,5 liters. Multiplying this figure for the actual thickness, the total amount of liters needed in this analysis is obtained, and it is equal to 730,5 liters. Dividing this result by 18 liters, which is the volume of the product available on the market, the number of products needed results being 41, bringing the total cost to 18.500 $.

- **Technical conclusions.**

Note: these conclusions are NOT intended as final conclusions, but only as additional conclusions to the ones already given in the earlier part of this chapter. Other considerations will be made in the next part of the thesis.

- With the implemented strategy the whole energy demand of the building is satisfied; The combination of the solar panels system and the storage tank associated with it, the heat pump together with its storage tank and with the electrical boiler are a good strategy in terms of reaching the goal of thermal self-sustainability.

- The implementation of the scheduled time program has led to significant improvements. The electric boiler, which was initially predicted to work for 51% of the total time based on preliminary analysis, now functions for only 328 hours out of the 5,975 hours during which an energy deficit is detected. This adjustment means that the heat pump now satisfies 95% of the energy deficit, compared to the previously expected 49% coverage. This outcome is noteworthy because a greater part of the total thermal energy deficit is met using a more energy-efficient strategy, leading to a substantial reduction in the electrical energy required by the production system.

- The electric boiler is activated only when the energy available from the thermal storage system falls below 17,4 kWh. In situations where the thermal demand cannot be satisfied by the energy already stored, the system responds by activating the heat pump, which operates in thermal tracking mode to meet the entire required heating load. These instances occur outside the predefined time schedule for the heat pump's operation, as the heat pump's primary goal during scheduled periods is to supply as much energy as possible to the storage tank without exceeding its maximum storage capacity.

- The total electrical energy needed for the normal operation of the system, including the heat pump and the electric boiler, amounts to 45.500 kWh annually. Considering that all the electrical energy necessary for the operation of these components is purchased from the grid, and simultaneously, all the electrical energy produced by the solar panels - totaling 74.000 kWh - is sold back to the grid at the same price, it can be confidently asserted that the designed system is entirely self-sustaining from an electrical standpoint. Furthermore, the system cuts electrical energy consumption typically associated with conventional cooling production methods, enhancing overall energy efficiency and contributing to a reduction in operational costs.

6.3 Economic Analysis, Configuration 1.

In this subchapter, the viability of the investment is analyzed using the Weighted Average Cost of Capital (WACC) theory. The assessment focuses on determining the payback period for the invested capital, evaluating how effectively the investment can recoup the initial expenditure over time. By applying WACC, the analysis accounts for the cost of financing and the expected returns, providing a comprehensive understanding of the investment's financial performance and sustainability.

- **Total monetary investment.**

Table 32 presents the listed prices of the selected equipment, which have been extensively discussed throughout this thesis. The materials encompass all the components previously mentioned, including those preliminarily considered for enhancing the building's solar control.

Note:

- *The proposed materials include most of the necessary connections for their installation; therefore, no additional cash flows have been allocated for installation materials.*
- *The costs associated with the labor required for installation and commissioning have not been budgeted and are not considered as separate cash flows. However, to render the economic analysis more realistic, the operational expenditure (OPEX) have been overestimated in the WACC analysis presented in the following chapter.*

Table 32: total monetary investment of the configuration 1.

Name		N° units	Price per unit, €	Total price, €
Control solar				
PASTEL COLOR OUTDOOR SHUTTERS (V 1750X1150 mm)	UD	104	216,84 €	22.551,36 €
PASTEL COLOR OUTDOOR SHUTTERS (V 700X1150 mm)	UD	20	128,40 €	2.568,00 €
WHITE COLOR INDOOR CURTAINS (P 2500X2200 mm)	UD	40	180,89 €	7.235,60 €
WHITE COLOR INDOOR CURTAINS (P 1750X2200 mm)	UD	8	126,63 €	1.013,04 €
Heating installation				
Heat Pump, TRANE	UD	1	80.000,00 €	80.000,00 €
Electrical Heater	UD	1	4.000,00 €	4.000,00 €
Adsorption chiller, Fahrenheit eCoo x40	UD	1	95.000,00 €	95.000,00 €
Solar Panels				
Abora Solar, BASIC kit	UD	52	7.894,79 €	410.529,08 €
Tank and other stuff included in the price				
roVa, aerogel coating shield	UD	41	450,00 €	18.450,00 €
Total investment				**641.347,08 €**

- **WACC Theory for calculating the payback time of the investment, general definition.**

In this section, the focus is on the payback time related to the economic investment.

An economic analysis with the WACC theory will be executed for each part of the energy system, namely the solar field, the heat pump, the adsorption chiller, and a final global analysis for the whole investment.

To determine the payback time, which is defined as the number of years required for the balance between the costs and benefits of an investment to reach zero, the following assumptions have been considered, basing on the WACC theory:

- The CAPEX is the initial investment. So, the total amount of money that was spent to buy the equipment.
- The yearly OPEX coincides with the operational yearly cost. In this analysis it is considered equal a defined % of the CAPEX, and it is a constant amount of money that has to be spent each year for the maintenance of the analyzed system.
  Note: this percentage will be overestimated, due to consider also the installation costs.
- The SAVINGS are the price you would receive considering selling the whole energy that is produced. It is in fact the total amount of energy that is being saved. This is valid for the year in which the investment is made.
  From the second year, also the rate of increase of energy cost **must be considered**.
  The formula for obtaining the savings for each year is as follows:

$$\text{Savings}_{\text{year(x)}} = \text{Savings}_{\text{year(X-1)}} * (1 + \text{r}\%)$$

Where r % is the rate of increase of energy cost. Considering the high fluctuation period in which we are living, in this analysis it was set to a 4% value.

Note: This is merely a projection based on historical data from recent years. This figure could change significantly in the coming years due to the current unstable global geopolitical situation.

- $\text{CashFlow}_{\text{year(x)}} = \text{Savings}_{\text{year(x)}} + \text{OPEX}_{\text{year(x)}}$

Observation: for the first year, also the CAPEX as to be considered.

- $\text{DiscountedCashFlow}_{\text{year(X)}} = \frac{\text{CashFlow}_{\text{year(X)}}}{(1+\text{d}\%)^{\text{x}}}$

In this formula:

- X is the year taken in analysis.
- d% is the discount rate (WACC theory). Considering the need for bank financing, the discount rate is nothing more than the interest rate on the bank loan, which increases

the amount owed to the bank year after year. In this analysis, a discount rate of 2% has been considered.
Note: this value is a strong assumption.

- The thermal energy cost is set equal to 88€/MWh. This value is equal to the natural gas price, registered as its average value in the year 2023 [ ]
- The electricity cost is set equal to 119€/MWh [ ], set to be equal to its average market price registered in the year 2023.

- **Carbon tax definition and value.**

The carbon tax is a governmental fee imposed on the carbon dioxide emissions from burning fossil fuels. By putting a price on carbon emissions, it incentivizes companies and individuals to reduce their environmental impact. This tax makes investments in energy requalification - such as energy-efficient renovations and renewable energy installations, more attractive financially. Investors can save money by lowering their energy costs and reducing or avoiding carbon tax payments. Consequently, the carbon tax encourages the adoption of cleaner technologies and energy practices, offering both economic benefits to investors and positive contributions to environmental sustainability.

In Madrid, in 2023, its value was set to 80 $\frac{€}{ton_{CO2}}$.

The value of the carbon tax for this investment is considered a positive cash flow, effectively serving as an incentive that is included in the calculation of savings. Regarding the electrical energy produced, the carbon tax savings on the generated or unused electricity are calculated as if it had been derived from non-renewable sources, using the following formula:

$$CO_{2\,\text{production}} = 0{,}2\,[\,{}^{\text{ton}_{CO_2}}/_{\text{MWh}}\,] \times E_{el}[\text{MWh}]$$

For thermal energy, the same principle applies: the thermal energy produced or saved by the operation of our high-efficiency system results in a saved carbon tax, which is included in the calculation of savings. This is calculated using the following formula, based on the production of thermal energy from non-renewable sources:

$$CO_{2\,\text{production}} = 0{,}202[\,{}^{\text{ton}_{CO_2}}/_{\text{MWh}}\,] \times \frac{E_{th}[\text{MWh}]}{0{,}9}$$

The 0,9 factor is considered as the average efficiency of the heat producing systems, 90%.

6.4 Economic analysis of the solar power plant.

Table 34 presents the economic analysis conducted using the WACC methodology for the solar production system. Some parameters and the formulas used for the calculations have been defined in Chapter 6.3, while additional input parameters are provided in Table 33. These are the resulting figures from the simulations conducted with the previously implemented Excel model discussed in the chapters above.

Table 33: Solar Panels field's parameters for the WACC theory analysis.

N° of BASIC kits	52
Thermal Energy Produced	198 MWh
Electrical Energy Produced	75 MWh
CAPEX parameter for a single BASIC kit	7.894,89 €

The savings are calculated as follows:

$$Savings_{panels\ system}[€] = E_{th,produced\ by\ the\ panels}\,[MWh] \times Gas\ Price\ \left[\frac{€}{MWh}\right] + E_{e,produced\ by\ the\ panels}[MWh] \times EE\ Price\ \left[\frac{€}{MWh}\right] + Carbon\ Tax\ [€]$$

The thermal energy produced is multiplied by the price of the Gas. This assumption is made in order to compare classic heat producing systems to this technology analyzed.

In table 34 the results obtained from the WACC theory are shown.

Table 34: WACC theory for the Solar Panels field.

Year	Capex	Opex	Savings	Cash flow	Discounted cash flow	Cum cash flow	NPV
0	-328.423,68 €	-2.627,39 €	34.917,20 €	-296.133,87 €	-296.133,87 €	-296.133,87 €	-296.133,87 €
1		-2.627,39 €	36.313,89 €	33.686,50 €	33.025,98 €	-262.447,37 €	-263.107,89 €
2		-2.627,39 €	37.766,44 €	35.139,05 €	33.774,56 €	-227.308,32 €	-229.333,33 €
3		-2.627,39 €	39.277,10 €	36.649,71 €	34.535,84 €	-190.658,60 €	-194.797,49 €
4		-2.627,39 €	40.848,19 €	38.220,80 €	35.310,11 €	-152.437,81 €	-159.487,38 €
5		-2.627,39 €	42.482,11 €	39.854,72 €	36.097,65 €	-112.583,09 €	-123.389,73 €
6		-2.627,39 €	44.181,40 €	41.554,01 €	36.898,77 €	-71.029,08 €	-86.490,96 €
7		-2.627,39 €	45.948,65 €	43.321,26 €	37.713,77 €	-27.707,81 €	-48.777,19 €
8		-2.627,39 €	47.786,60 €	45.159,21 €	38.542,95 €	17.451,40 €	-10.234,24 €
9		**-2.627,39 €**	**49.698,06 €**	**47.070,67 €**	**39.386,63 €**	**64.522,07 €**	**29.152,39 €**
10		-2.627,39 €	51.685,99 €	49.058,60 €	40.245,14 €	113.580,67 €	69.397,53 €
11		-2.627,39 €	53.753,43 €	51.126,04 €	41.118,78 €	164.706,70 €	110.516,31 €
12		-2.627,39 €	55.903,56 €	53.276,17 €	42.007,90 €	217.982,87 €	152.524,21 €
13		-2.627,39 €	58.139,70 €	55.512,32 €	42.912,83 €	273.495,19 €	195.437,03 €
14		-2.627,39 €	60.465,29 €	57.837,90 €	43.833,90 €	331.333,09 €	239.270,94 €
15		-2.627,39 €	62.883,90 €	60.256,52 €	44.771,48 €	391.589,61 €	284.042,41 €
16		-2.627,39 €	65.399,26 €	62.771,87 €	45.725,91 €	454.361,48 €	329.768,32 €
17		-2.627,39 €	68.015,23 €	65.387,84 €	46.697,55 €	519.749,32 €	376.465,87 €
18		-2.627,39 €	70.735,84 €	68.108,45 €	47.686,77 €	587.857,77 €	424.152,64 €
19		-2.627,39 €	73.565,27 €	70.937,88 €	48.693,95 €	658.795,66 €	472.846,59 €
20		-2.627,39 €	76.507,89 €	73.880,50 €	49.719,46 €	732.676,15 €	522.566,04 €

It is evident that the Net Present Value, NPV, is set to be 9 years.

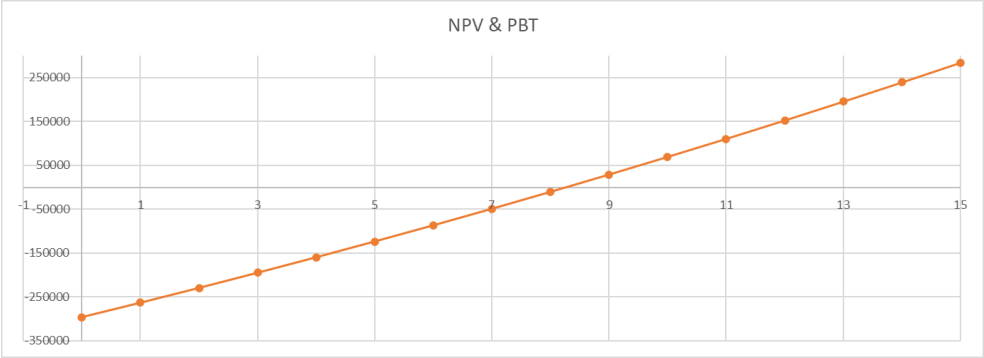

Figure 41: NPV and PBT of the solar panels field.

In the calculation to determine the savings, the amount of savings related to the carbon tax is equal to a 4.755,20 €/year. This helps the investment a lot, making it more sustainable.

In general, public incentives help a lot.

Notes and considerations:

- *In CAPEX calculations, the cost of the hybrid solar panels has been discounted by 20%. This adjustment is made because the analysis focuses exclusively on the payback time of the solar panels themselves, rather than the entire system. The monetary investment considered in this chapter for the solar panels includes the price of the storage tank, the necessary connections, and all components provided with the Abora*

Solar basic kit. In the comprehensive economic analysis to be conducted subsequently, these elements will be incorporated into the overall CAPEX evaluation.

- *The operational expenditure (OPEX) is estimated at 0.8% of the CAPEX. This estimation is since the price quoted by Abora Solar already covers the installation costs of the panels.*

- *The payback time (PBT) of 9 years is longer than the typical PBT for conventional solar systems, whether photovoltaic or thermal collectors. This extended payback period is attributed to the nascent stage of hybrid solar panel technology. As market demand for these panels increases, it is expected that their production costs and market prices will decrease accordingly. This anticipated reduction in price will enhance the competitiveness of hybrid solar panels, positioning them favorably against other products available in the market.*

- *All previous considerations regarding energy prices, the rate of increase, and the discount rate remain applicable.*

6.5 Economic analysis of the heat pump and the electrical boiler.

The economic analysis of the investment in the heat pump and electric boiler adheres to the same considerations and base values utilized in the analysis of the solar panel investment (WACC). For these two systems, the following values are considered:

Table 35: Heat Pump and electrical Boiler economic parameters for the WACC theory.

CAPEX Heat Pump	80.000,00 €
CAPEX Electrical Boiler	5.000,00 €
Previously used Gas	182 MWh
Electrical Energy used by the system	45,5 MWh
OPEX	4%*CAPEX

The OPEX is set at 4% of the CAPEX. This high OPEX percentage accounts for the requirement of a specialized maintenance contract for the heat pump, which is more detailed and comprehensive than standard maintenance programs.

Additionally, as previously mentioned, the installation costs for these components are not included in the CAPEX. Instead, these costs are directly incorporated into OPEX, ensuring that installation expenses are not entirely overlooked but are instead distributed over the total investment period. This methodology ensures that the financial implications of installation and maintenance are adequately captured in the overall economic evaluation, providing a more accurate reflection of the investment's cost structure and long-term sustainability.

By integrating these factors into the OPEX, the analysis maintains a comprehensive approach to evaluating the economic viability of the heat pump and electric boiler, aligning with the project's objectives of maximizing energy efficiency and minimizing operational costs.

In table 36 the main results are resumed.

Table 36: NPV and PBT of the heat pump and boiler investment.

Year	Capex	Opex	Savings	Cash flow	Discounted cash flow	Cum cash flow	NPV
0	-85.000,00 €	-3.400,00 €	19.218,92 €	-69.181,08 €	-69.181,08 €	-69.181,08 €	-69.181,08 €
1		-3.400,00 €	19.987,67 €	16.587,67 €	16.262,42 €	-52.593,41 €	-52.918,66 €
2		-3.400,00 €	20.787,18 €	17.387,18 €	16.712,01 €	-35.206,23 €	-36.206,65 €
3		-3.400,00 €	21.618,67 €	18.218,67 €	17.167,86 €	-16.987,57 €	-19.038,79 €
4		**-3.400,00 €**	**22.483,41 €**	**19.083,41 €**	**17.630,12 €**	**2.095,85 €**	**-1.408,67 €**
5		**-3.400,00 €**	**23.382,75 €**	**19.982,75 €**	**18.098,99 €**	**22.078,60 €**	**16.690,32 €**
6		-3.400,00 €	24.318,06 €	20.918,06 €	18.574,64 €	42.996,65 €	35.264,96 €
7		-3.400,00 €	25.290,78 €	21.890,78 €	19.057,24 €	64.887,44 €	54.322,21 €
8		-3.400,00 €	26.302,41 €	22.902,41 €	19.546,99 €	87.789,85 €	73.869,19 €
9		-3.400,00 €	27.354,51 €	23.954,51 €	20.044,06 €	111.744,36 €	93.913,26 €
10		-3.400,00 €	28.448,69 €	25.048,69 €	20.548,65 €	136.793,05 €	114.461,91 €
11		-3.400,00 €	29.586,64 €	26.186,64 €	21.060,94 €	162.979,69 €	135.522,85 €
12		-3.400,00 €	30.770,10 €	27.370,10 €	21.581,14 €	190.349,79 €	157.103,99 €

It can be easily noticed that the PBT for this investment is between 4 and 5 years.

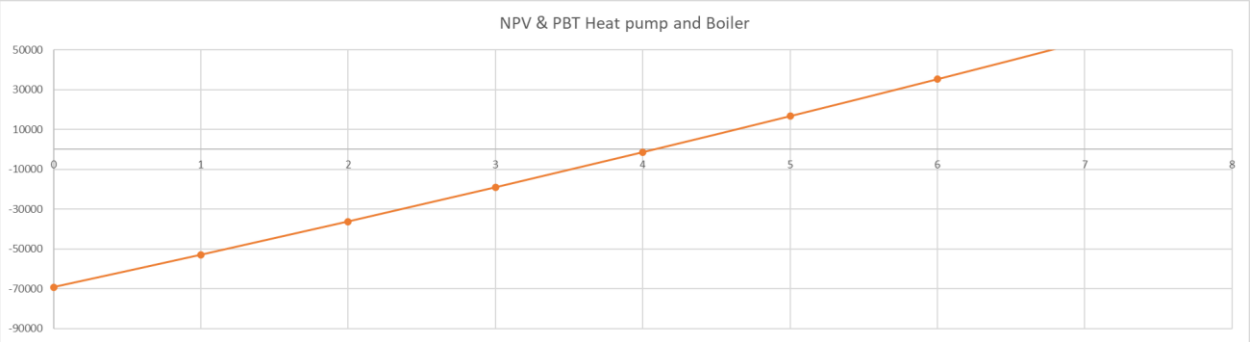

Figure 42: NPV for the heating supply system.

In the calculation to determine the savings, the amount of savings related to the carbon tax is equal to a 1.535,00 €/year. This is the result of 36,81 tons/year of CO2 emissions saved avoiding using Natural Gas and 17,60 ton/year of CO2 emissions produced by using the electrical energy input required by the two systems.

The savings are defined as:

$$\text{Savings}[€] = \text{Carbon tax } [€] + \text{Saved Gas } [\text{MWh}] \times \text{Gas Price } \left[\frac{€}{\text{MWh}}\right] - \text{Used Electricity } [\text{MWh}] \times \text{Electricity Price } \left[\frac{€}{\text{MWh}}\right]$$

In which:

- Used Electricity is the driving electricity of the two systems, equal to 45,60 MWh/year.
- Saved Gas is the amount of Natural Gas avoided, considering producing all the heat demand with classic thermal producing systems. It is determined as:
-

$$Saved\ Gas\ [MWh] = \frac{Heating\ Demand[MWh]}{0{,}9} = \frac{164MWh}{0{,}9} = 182\ MWh$$

Where the Efficiency of this classic producing system is set to be 90%.

This leads to the values for the savings detected in table 36.

Note:

- *The price for the thermal storage tank is not considered. This is because the storage system is considered "free", since it is coming from Abora Solar with the hybrid panels.*

6.6 Economic analysis of the adsorption chiller.

The economic analysis of the adsorption chiller follows the same principles and base values established for the WACC theory applied to the previously discussed systems. However, specific considerations pertinent to the adsorption chiller must be noted:

- Savings Calculation: The savings associated with the adsorption chiller are determined by recognizing that the energy saved corresponds to the building's cooling demand divided by a conventional Coefficient of Performance value typical of current market refrigeration machines, set at 1,6. This approach effectively reduces the electrical energy requirement of the existing energy production system that the adsorption chiller is intended to replace. By calculating savings in this manner, the analysis accurately reflects the efficiency improvements and the consequent reduction in electrical energy consumption.
  This assumption leads to an Electrical energy saving equal to **30 MWh/year.**

- Operational Expenditure (OPEX): Due to the inherent characteristics of adsorption chillers, minimal maintenance is required. Consequently, the OPEX for this component can be considered negligible. The low maintenance demand contributes to the overall cost-effectiveness of the adsorption chiller, as operational costs do not significantly impact the financial performance of the investment.

- Energy Consumption: The electrical energy utilized by the adsorption chiller is assumed to be zero. This assumption is based on the system's configuration, where the thermal input required for the chiller's operation is provided free of charge by the solar panel system. Additionally, the electrical input necessary for the chiller's functionality is deemed negligible, further enhancing the economic viability of the system by eliminating associated electrical energy costs.

- The amount of CO2 emissions saved is 6 tons/year, leading to a positive monetary income of 480,00€/year.

Based on these assumptions, the results of the WACC analysis are detailed in Table X.

Table 37: Economic analysis of the adsorption chiller.

Year	Capex [€]	Opex[€]	Savings[€]	Cash flow[€]	Discounted cash flow[€]	Cum cash flow[€]	NPV[€]
0	-95.000,00 €	-95,00 €	3.120,00 €	-91.975,00 €	-91.975,00 €	-91.975,00 €	-91.975,00 €
1		-95,00 €	3.244,80 €	3.149,80 €	3.088,04 €	-88.825,20 €	-88.886,96 €
2		-95,00 €	3.374,59 €	3.279,59 €	3.152,24 €	-85.545,61 €	-85.734,72 €
3		-95,00 €	3.509,58 €	3.414,58 €	3.217,63 €	-82.131,03 €	-82.517,09 €
4		-95,00 €	3.649,96 €	3.554,96 €	3.284,23 €	-78.576,07 €	-79.232,86 €
5		-95,00 €	3.795,96 €	3.700,96 €	3.352,07 €	-74.875,12 €	-75.880,79 €
6		-95,00 €	3.947,80 €	3.852,80 €	3.421,17 €	-71.022,32 €	-72.459,61 €
7		-95,00 €	4.105,71 €	4.010,71 €	3.491,56 €	-67.011,61 €	-68.968,05 €
8		-95,00 €	4.269,94 €	4.174,94 €	3.563,27 €	-62.836,68 €	-65.404,78 €
9		-95,00 €	4.440,73 €	4.345,73 €	3.636,31 €	-58.490,95 €	-61.768,47 €
10		-95,00 €	4.618,36 €	4.523,36 €	3.710,73 €	-53.967,58 €	-58.057,74 €
11		-95,00 €	4.803,10 €	4.708,10 €	3.786,55 €	-49.259,49 €	-54.271,19 €
12		-95,00 €	4.995,22 €	4.900,22 €	3.863,79 €	-44.359,27 €	-50.407,40 €
13		-95,00 €	5.195,03 €	5.100,03 €	3.942,49 €	-39.259,24 €	-46.464,91 €
14		-95,00 €	5.402,83 €	5.307,83 €	4.022,67 €	-33.951,41 €	-42.442,24 €
15		-95,00 €	5.618,94 €	5.523,94 €	4.104,37 €	-28.427,46 €	-38.337,87 €
16		-95,00 €	5.843,70 €	5.748,70 €	4.187,62 €	-22.678,76 €	-34.150,25 €
17		-95,00 €	6.077,45 €	5.982,45 €	4.272,44 €	-16.696,31 €	-29.877,81 €
18		-95,00 €	6.320,55 €	6.225,55 €	4.358,88 €	-10.470,76 €	-25.518,93 €
19		-95,00 €	6.573,37 €	6.478,37 €	4.446,95 €	-3.992,39 €	-21.071,98 €
20		-95,00 €	6.836,30 €	6.741,30 €	4.536,70 €	2.748,91 €	-16.535,27 €

Observations:

- Payback Time (PBT) Concerns: The analysis indicates that a payback time (PBT) for the investment in the adsorption chiller is not achievable within the typical warranty period provided by the manufacturer. Specifically, the PBT extends to the 25th year, which exceeds the standard product warranties. This discrepancy poses significant risks regarding long-term reliability and support for the chiller, potentially undermining the financial viability of the investment.
- Economic Viability of the Adsorption Chiller: The selection of an adsorption chiller appears to be a questionable design decision under current market conditions. The high cost of this component is primarily due to its limited demand, resulting in elevated prices. This economic inefficiency suggests that the adsorption chiller may not be the most cost-effective cooling solution compared to alternative technologies available in the market. The substantial initial investment required for the adsorption chiller detracts from the overall financial feasibility of the project, making it less attractive from an economic perspective.
- Future Market Considerations: Despite the current economic challenges, the analysis acknowledges the potential for improved viability of the adsorption chiller under future market conditions. If the price of adsorption chillers were to decrease by 50%, the PBT would become significantly more favorable, aligning with investment objectives. Such a reduction in cost would enhance the economic attractiveness of the adsorption chiller, making it a more competitive and sustainable choice for energy-efficient cooling solutions.

Table 38: Economical analysis of an hypothetical 50% reduction of the adsorption chiller price.

Year	Capex [€]	Opex[€]	Savings[€]	Cash flow[€]	Discounted cash flow[€]	Cum cash flow[€]	NPV[€]
0	-47.500,00 €	-47,50 €	3.120,00 €	-44.427,50 €	-44.427,50 €	-44.427,50 €	-44.427,50 €
1		-47,50 €	3.244,80 €	3.197,30 €	3.134,61 €	-41.230,20 €	-41.292,89 €
2		-47,50 €	3.374,59 €	3.327,09 €	3.197,90 €	-37.903,11 €	-38.095,00 €
3		-47,50 €	3.509,58 €	3.462,08 €	3.262,39 €	-34.441,03 €	-34.832,60 €
4		-47,50 €	3.649,96 €	3.602,46 €	3.328,11 €	-30.838,57 €	-31.504,49 €
5		-47,50 €	3.795,96 €	3.748,46 €	3.395,09 €	-27.090,12 €	-28.109,40 €
6		-47,50 €	3.947,80 €	3.900,30 €	3.463,35 €	-23.189,82 €	-24.646,05 €
7		-47,50 €	4.105,71 €	4.058,21 €	3.532,91 €	-19.131,61 €	-21.113,13 €
8		-47,50 €	4.269,94 €	4.222,44 €	3.603,81 €	-14.909,18 €	-17.509,32 €
9		-47,50 €	4.440,73 €	4.393,23 €	3.676,06 €	-10.515,95 €	-13.833,26 €
10		-47,50 €	4.618,36 €	4.570,86 €	3.749,70 €	-5.945,08 €	-10.083,56 €
11		-47,50 €	4.803,10 €	4.755,60 €	3.824,75 €	-1.189,49 €	-6.258,81 €
12		-47,50 €	4.995,22 €	4.947,72 €	3.901,24 €	3.758,23 €	-2.357,57 €
13		**-47,50 €**	**5.195,03 €**	**5.147,53 €**	**3.979,21 €**	**8.905,76 €**	**1.621,64 €**
14		-47,50 €	5.402,83 €	5.355,33 €	4.058,67 €	14.261,09 €	5.680,31 €
15		-47,50 €	5.618,94 €	5.571,44 €	4.139,66 €	19.832,54 €	9.819,97 €
16		-47,50 €	5.843,70 €	5.796,20 €	4.222,22 €	25.628,74 €	14.042,19 €
17		-47,50 €	6.077,45 €	6.029,95 €	4.306,36 €	31.658,69 €	18.348,56 €
18		-47,50 €	6.320,55 €	6.273,05 €	4.392,13 €	37.931,74 €	22.740,69 €
19		-47,50 €	6.573,37 €	6.525,87 €	4.479,56 €	44.457,61 €	27.220,25 €
20		-47,50 €	6.836,30 €	6.788,80 €	4.568,67 €	51.246,41 €	31.788,92 €

These observations highlight the critical need for careful consideration of market dynamics and technological advancements when selecting components for energy systems. While the current economic landscape presents challenges for the adoption of adsorption chillers, anticipated price reductions could substantially improve their viability, supporting more sustainable and cost-effective energy solutions in the future.

A significant advantage of this system is the integration of a component that seamlessly collaborates with a system designed to harness and optimize the most abundant and cost-effective thermal energy source available today—solar energy. By effectively utilizing solar thermal energy, the system maximizes the exploitation of renewable resources, thereby reducing reliance on conventional and more expensive energy sources. This synergy not only enhances the overall efficiency and performance of the energy system but also contributes to sustainability objectives by leveraging a widely accessible and environmentally friendly energy source. Consequently, the system benefits from lower operational costs and a reduced environmental footprint, making it a highly advantageous solution in the context of modern energy management and sustainable building practices.

6.7 Global system's Economic Analysis.

Before analyzing the detailed results obtained from the economic analysis, several key considerations regarding the calculation methodologies applied in this study must be addressed. These considerations ensure the accuracy and reliability of the economic and environmental assessments conducted for the integrated energy systems.

- CAPEX: The CAPEX encompasses the total investment incurred for the acquisition of the selected machinery. In this case, the cost of the hybrid solar panels has been discounted by 20%, as the analysis focuses solely on the payback period of the solar panels themselves. So, in this analysis, CAPEX includes the proportionate cost of the thermal storage tank, connections, and all components provided with the Abora Solar basic kit.

- OPEX: The OPEX is calculated as the sum of the individual operational expenditures associated with each of the analyzed systems.

- Savings: The savings metric represents the cumulative sum of all identified savings across the various components of the energy system. The formula employed to calculate the savings is as follows:

$$
\begin{aligned}
&Savings_{global}[€] \\
&= Saved\ Gas_{heatpump}\ [MWh] \times Gas\ Price\ \left[\frac{€}{MWh}\right] \\
&+ Saved\ EE_{adsorptionchiller}[MWh] \times EE\ Price\ \left[\frac{€}{MWh}\right] \\
&+ E_{th,produced\ by\ the\ panels}\ [MWh] \times Gas\ Price\ \left[\frac{€}{MWh}\right] \\
&+ E_{e,produced\ by\ the\ panels}[MWh] \times EE\ Price\ \left[\frac{€}{MWh}\right] \\
&+ Global\ Carbon\ Tax\ [€]
\end{aligned}
$$

- CO_2 Emissions Avoided: The avoided CO_2 emissions are included in the savings calculation. This is achieved by summing the avoided emissions from each individual component of the system, resulting in a total avoidance of 102,25 tons/year. This reduction translates into a positive financial impact, generating an income of 8.180 € through carbon tax savings.

Subsequently, Table 39 presents comprehensive results derived from economic, and environmental, analysis. Also, the values for the units presented above are reported.

Table 39: Global Economic Analysis of the system.

Year	Capex [€]	Opex[€]	Savings[€]	Cash flow[€]	Discounted cash flow[€]	Cum cash flow[€]	NPV[€]
0	-590.529,60 €	-7.274,39 €	58.664,12 €	-539.139,87 €	-539.139,87 €	-539.139,87 €	-539.139,87 €
1		-7.274,39 €	61.010,68 €	53.736,29 €	52.682,64 €	-485.403,58 €	-486.457,24 €
2		-7.274,39 €	63.451,11 €	56.176,72 €	53.995,31 €	-429.226,87 €	-432.461,93 €
3		-7.274,39 €	65.989,15 €	58.714,76 €	55.328,23 €	-370.512,10 €	-377.133,70 €
4		-7.274,39 €	68.628,72 €	61.354,33 €	56.681,92 €	-309.157,77 €	-320.451,78 €
5		-7.274,39 €	71.373,87 €	64.099,48 €	58.056,87 €	-245.058,30 €	-262.394,91 €
6		-7.274,39 €	74.228,82 €	66.954,43 €	59.453,62 €	-178.103,87 €	-202.941,29 €
7		-7.274,39 €	77.197,97 €	69.923,58 €	60.872,69 €	-108.180,28 €	-142.068,60 €
8		-7.274,39 €	80.285,89 €	73.011,50 €	62.314,62 €	-35.168,78 €	-79.753,99 €
9		-7.274,39 €	83.497,33 €	76.222,94 €	63.779,95 €	41.054,16 €	-15.974,04 €
10		**-7.274,39 €**	**86.837,22 €**	**79.562,83 €**	**65.269,23 €**	**120.616,99 €**	**49.295,19 €**
11		-7.274,39 €	90.310,71 €	83.036,32 €	66.783,04 €	203.653,31 €	116.078,24 €
12		-7.274,39 €	93.923,14 €	86.648,75 €	68.321,95 €	290.302,06 €	184.400,18 €
13		-7.274,39 €	97.680,06 €	90.405,68 €	69.886,53 €	380.707,74 €	254.286,71 €
14		-7.274,39 €	101.587,27 €	94.312,88 €	71.477,37 €	475.020,62 €	325.764,09 €
15		-7.274,39 €	105.650,76 €	98.376,37 €	73.095,09 €	573.396,99 €	398.859,18 €
16		-7.274,39 €	109.876,79 €	102.602,40 €	74.740,29 €	675.999,38 €	473.599,47 €
17		-7.274,39 €	114.271,86 €	106.997,47 €	76.413,59 €	782.996,86 €	550.013,05 €
18		-7.274,39 €	118.842,73 €	111.568,34 €	78.115,62 €	894.565,20 €	628.128,68 €
19		-7.274,39 €	123.596,44 €	116.322,05 €	79.847,04 €	1.010.887,25 €	707.975,71 €
20		-7.274,39 €	128.540,30 €	121.265,91 €	81.608,48 €	1.132.153,17 €	789.584,19 €

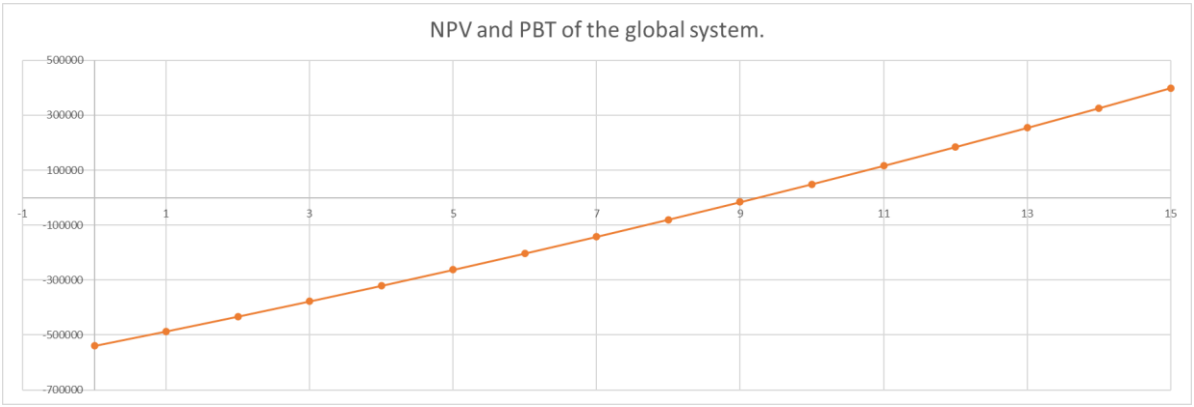

Figure 43: NPV and PBT of global investment.

- **Conclusions:**

- **High Investment Requirement**: The necessary investment is substantial and does not include installation costs. The total investment must be undertaken by an investment company, such as an Energy Service Company (ESCo), which could enable building owners to incur no direct expenses by assuming the savings share or being assigned to the building's residents. Under the latter scenario, the investment per family would amount to approximately €9.400, which is significantly high compared to current standards.

- **Enhanced System Efficiency and Autonomy**: Despite the elevated investment cost, the system improvements are considerable. The implementation would result in a thermally and electrically self-sufficient system, which is exceptionally rare in contemporary buildings. This autonomy allows the building to operate independently from market fluctuations in raw material prices, ensuring consistent energy reliability and reducing vulnerability to energy supply disruptions. Such self-sufficiency not only enhances operational stability but also contributes to long-term cost savings and resilience against external economic pressures.

- **Minimal CO_2 Emissions**: The new system would achieve a substantial reduction in CO_2 emissions, thereby classifying the building as environmentally sustainable. This adaptation aligns the building with potential future regulations on acceptable emission limits in the residential sector, providing significant environmental and ancillary benefits. Reduced carbon emissions contribute to mitigating climate change and improving air quality, while also enhancing the building's marketability and compliance with increasingly stringent environmental standards.

- **Maximized Utilization of Solar Energy**: The system optimally harnesses solar energy, the world's most abundant primary energy source. The chosen systems are ideally suited to solar availability, thereby maximizing renewable energy utilization and enhancing overall system efficiency. By effectively capturing and converting solar energy, the system reduces reliance on non-renewable energy sources, lowers operational costs, and supports sustainable energy practices. This strategic utilization of solar power not only improves the building's energy performance but also reinforces its commitment to renewable energy integration and sustainability goals.

These considerations highlight the significant environmental advantages of the proposed investment, and the fact that the building would become an Energetically independent system, underscoring its potential to deliver substantial energy savings, environmental benefits, and

long-term financial viability despite the initial high costs. The integration of advanced energy systems fosters a sustainable and resilient building infrastructure, positioning it favorably in the evolving landscape of energy efficiency and environmental stewardship.

6.8 Technical sizing, configuration 2.

In this sizing process, many calculation steps are omitted as they are identical to those performed for Configuration 1. Therefore, this chapter directly refers to the previous chapter for detailed formulations that led to specific results.

Configuration 2 aims to evaluate the outcomes of modifying what could be perceived as a premature and suboptimal decision in Configuration 1, the use of an adsorption chiller. This choice in Configuration 1 appears to lack thorough consideration and may not be the most economically viable option.

Instead, Configuration 2 proposes a sizing approach that focuses on maximizing the utilization of the reversible air-to-water heat pump selected previously, to produce both heating and cooling with it, maximizing its investment.

Additionally, this configuration seeks to significantly reduce the investment required for the solar panel system, addressing the high economic burden observed in Configuration 1. The hybrid solar panel system in Configuration 2 is specifically designed to meet the thermal energy demands for domestic hot water (DHW) generation and swimming pool heating during the summer months. By narrowing the scope of the solar panel system to these specific applications, the overall investment cost is reduced while maintaining essential energy functions.

Subsequent sections will present the detailed sizing performed for Configuration 2, highlighting both the advantages and potential challenges associated with this revised approach. This analysis will demonstrate how optimizing the heat pump usage and limiting the solar panel system's objectives can lead to a more cost-effective and efficient energy solution for the building, thereby enhancing the system's overall performance and economic feasibility.

Note:

In this chapter, the same considerations and assumptions over the division of the year in two thermal seasons are made, including what was established for the % hour charge during a type day of summer and winter; Nothing changes.

Also, the thermal demands remains the same, in particular the swimming pool's one, critical for this dimensioning of configuration 2.

- **Technical dimensioning of the hybrid solar panels field.**

As extensively outlined in the introduction, the primary objective of the hybrid solar panel system is to fulfill the DHW and the thermal demand required for swimming pool heating.

The sizing process employs the same calculation methodology utilized for the solar panel system in Configuration 1, albeit with distinct objectives.

Specifically, **the aim is to cover between 70% and 80% of the total thermal demand for DHW and heating of the swimming pool in the summer period**. This involves accurately sizing the thermal storage tank to ensure optimal performance and efficiency.

The thermal storage tank, as previously mentioned, is provided by the manufacturer of the selected hybrid solar panels. By adhering to this structured approach, the system is designed to effectively meet a significant portion of the building's thermal energy requirements, thereby enhancing overall energy efficiency and reducing reliance on auxiliary heating sources.

For the dimensioning of the storage tank dimensions the same criteria of the dimensioning of configuration 1 is adopted.

The results are shown in table 40.

Table 40:technical specifics of the solar panels' field and of the storage tank.

N° of Basic kits	22
CAPEX of 1 basic kit	7.984,79 €
% of coverage of the thermal demand	76%
Thermal energy self-consumed	39.591,34 kWh
Total demand	51.976,14 kWh
imensions of the tank	2.500 liters
ximum storage capacity	150 kWh

In table 41 the geometrical dimensions of the storage tank are shown.

Note: also here, the same selection criteria as configuration 1 was used.

Table 41: Geometrical dimensions of the solar field thermal storage tank.

h/D	3	
Volume	2500	l
Volume	2,5	m3
D	1,02	m
h	3,06	m
Volume calculated	2,50	m^3
Top and bottom surface	1,63	m^2
Lateral Surface	9,80	m^2
Total external surface	11,44	m^2

- **Technical dimensioning of the heating back-up system for the summer's energy deficit.**

In this section, the backup methodology is discussed for providing the additional heat required to meet the remaining energy deficit, despite the integration of a solar panel system and its thermal storage. For Configuration 2, unlike the first configuration, only the electric boiler is designated as the auxiliary heating source. The selected electric boiler is the same as that used in Configuration 1, with a capacity of 18 kW.

Upon iterating and analyzing this specific case in detail, it became evident that the optimal configuration - meeting both the requirement of fully covering the thermal deficit and minimizing the system's electrical energy consumption - involves implementing a scheduled time program for the operation of the electric boiler. This program is designed to work in coordination with the thermal storage system of the solar panels.

A key distinction from Configuration 1 lies in using the electric boiler as a direct support to the solar panel system, rather than as a complement to the heat pump, specifically for the summer months.

The scheduled time program for the electric boiler is set to activate every summer evening for three hours, from midnight to 2 a.m., operating at full capacity and generating 18 kWh. This targeted usage strategy optimizes the system's efficiency by precisely addressing the anticipated thermal requirements while reducing unnecessary energy expenditure, aligning with the design objectives for Configuration 2.

With a combination of the solar panels field and the electrical boiler, the whole summer thermal energy demand has been covered.

At the end, the amount of electrical energy needed by the electrical boiler is 8.400 kWh, while in the same functioning period the amount of electricity produced by the hybrid panels was 15.000 kWh.

- **Technical dimensioning of the heating supplying system for the winter: dimensioning of the heat pump, functioning and strategy.**

To ensure the correct operation and sizing of the heat pump for Configuration 2, a calculation and simulation methodology identical to that applied in the previous configuration was used.

Within this model, the thermal output of the solar panels is integrated, and the thermal storage system is monitored to prevent exceeding its maximum storage capacity (table 40).

Based on this setup, a frequency curve was then developed to assess the range of energy deficits encountered. This curve reveals that the peak energy deficit reached in Configuration 2 is equivalent to that observed in Configuration 1.

This outcome is not unexpected; even with the substantial thermal production of Configuration 1's solar panel system, in fact, there may still be unusual days where the panels cannot provide the required energy.

With this result, it can be concluded that the heat pump model which best suits Configuration 2's requirements is, in fact, the same as that selected for Configuration 1: the TRANE CXB Cube.

The technical specifications and operational characteristics of this heat pump, as previously detailed in the preceding chapter, include interpolated COP values corresponding to all load conditions necessary to meet the building's energy demand.

Through a comprehensive and detailed analysis, it became evident that the most effective strategy for the optimal operation of the heat pump was to implement thermal tracking.

This decision was driven by the significantly reduced thermal contribution from the hybrid solar panel system compared to Configuration 1, resulting in consistently higher energy deficit values.

The primary rationale for this choice is the impracticality of sizing a thermal storage system to accommodate such elevated deficit levels, as the required storage capacities would be excessively large and economically unjustifiable.

Consequently, the appropriate strategy involves utilizing both the electric boiler and the heat pump in thermal tracking mode. The heat pump operates within its designated operational range, encompassing its maximum thermal output and the lower power limit of 17.4 kW.

When the energy deficit drops below 17.4 kWh, the electric boiler activates to supply the necessary thermal energy.

This configuration leads to a total electrical energy demand of 70.000 kWh for the two components during the winter season, compared to a total electrical energy production of 16.000 kWh from the solar panels within the same analysis period.

At first sight, this second configuration seems worse than the first one in terms of self-sustainability.

- **Technical dimensioning of the heat pump in reversed mode: cooling production**.

The sizing of the heat pump in reverse mode, designated for cooling production, does not constitute a distinct sizing process.

The capacity of the heat pump was previously determined during the sizing of the heating supply system for the winter months, necessitating adherence to its technical specifications for cooling operations as well.

Utilizing the data provided in the technical datasheet, an interpolation of the various Energy Efficiency Ratio (EER) values was performed. This interpolation allows for a more detailed definition of the EER corresponding to each required operating load.

Fundamentally, the approach adheres to the principle of utilizing available resources efficiently. Given the heat pump's rated capacity and the absence of a backup system to accommodate scenarios where the required energy falls below the heat pump's minimum operational limit, a comprehensive time program is essential.

This program includes the allocation of load percentages and the determination of operating hours for the heat pump, tailored to each month and the specific cooling demand of the building. By implementing this scheduled time program, the heat pump operates within its optimal range, ensuring effective cooling performance while minimizing electrical energy consumption.

This strategy aligns with the overall objective of maximizing system efficiency and reliability, thereby enhancing the economic and operational feasibility of the cooling configuration.

This strategy must strictly adhere to the maximum storage capacity defined by the dimensions of the collection tank, ensuring that energy production does not exceed these limits. By doing so, the system avoids surpassing the storage threshold and minimizes the risk of dissipating a significant portion of the generated energy.

The optimization of the sizing process thus depends on two key parameters: the size of the thermal storage tank and the time program deemed most appropriate for generating cooling energy. Accurately determining the optimal tank size is essential to ensure that the system operates within the defined storage capacity limits, thereby preventing the excess dissipation of generated energy. Simultaneously, the establishment of an effective time program is crucial for scheduling the heat pump's operation to align with the building's cooling demand and

external climatic conditions. By carefully balancing these two factors, the system can achieve maximum efficiency in cooling energy production while maintaining energy conservation.

This dual-parameter optimization approach ensures that the energy system operates reliably and efficiently, providing the necessary cooling performance without surpassing the storage capacity, thereby enhancing the overall economic and operational feasibility of the configuration.

The primary variable under consideration is the amount of thermal energy designated for storage. An analysis of the hourly thermal demand values reveals that storing approximately 100 kWh of thermal cooling energy would sufficiently cover the building's thermal demand over an extended number of hours.

Consequently, the thermal storage tank is sized to accommodate a maximum thermal cooling power of 93 kW. The sizing calculation is performed using the following formula:

$$E_{stored} = {V \times 4186 \times \Delta T}/{3{,}6 \times 10^6}$$

In which:

- ΔT is set to be equal to 16°C.
- V is the volume in liters.

By applying the inverse formula, volume V of the tank is found to be 5.000 liters.

This will impact a lot on the CAPEX of the investment, but it is a mandatory prerogative to have an efficient functioning of the system.

To achieve the desired outcome and effectively store cooling energy, a Puffer-type thermal flywheel is employed.

Based on the calculated volume requirements, the market price for such a thermal flywheel is approximately €5,000.

The selection of a Puffer-type thermal flywheel is due to its proven efficiency in managing thermal energy storage, providing reliable performance in maintaining the system's thermal balance.

This investment ensures that the thermal storage capacity aligns with the system's operational demands, thereby enhancing the overall efficiency and reliability of the energy management strategy.

The incorporation of the Puffer-type thermal flywheel facilitates optimal energy utilization, minimizing energy losses and supporting the sustained performance of the cooling system under varying load conditions.

The second variable under consideration is the scheduled time program. A fundamental requirement for defining this program is to ensure that the thermal storage system's peak capacity is never exceeded.

The scheduled time program is the one that follows:

Each month of the summer period has the same heat pump's functioning; It works from 00:00 a.m. to 02:00 a.m. and 16:00 p.m. to 20:00 p.m. - to help in the most critical hours of the day - at 60% of its nominal capacity.

This value is not random: it is the value, in the range from 50% to 100%, that has the best value for EER.

Also, working always at the same charge % value leads to the most efficient strategy.

With this functioning configuration, the total of the electrical energy consumed from the heat pump is 22.300 kWh, compared to a total electricity production of the panels of 15.000 kWh.

These results show that the system, also for the second system, is not self-sufficient.

- **Sizing the insulating coating for the storage tanks.**

Reference is made directly to the methodology applied in Configuration 1, as the calculation method is identical.

For both the storage tank of the solar panel system and the thermal cooling system, an aerogel insulation (roVa, same as the one previously chosen), the following values are obtained:

Table 42:aerogel coating's technical dimensioning.

h/D	3	
Volume	7500	l
Volume	7,5	m^3
D	1,47	m
h	4,41	m
Volume calculated	7,50	m^3
Top and bottom surface	3,40	m^2
Lateral Surface	20,39	m^2
Total external surface	23,79	m^2

Note: as in configuration 1, an isolating shield of 20 mm is considered.

This leads to the need for 39 packs of products.

6.9 Economic Analysis, Configuration 2.

In this section, the total monetary investment and the economic analyses based on the WACC theory, which were extensively defined for Configuration 1, will be examined.

For the sake of simplicity, only the tables illustrating the results for each system component and their respective investment characteristics will be presented.

Subsequently, conclusions will be drawn to summarize the economic viability and overall financial performance of the integrated energy system.

This structured approach ensures a clear and concise presentation of the financial aspects, facilitating a comprehensive understanding of the investment's implications within the context of the proposed configurations.

- **Total monetary investment.**

  In table 43 the figures related to the investment can be easily found.

Table 43: total monetary investment, configuration 2.

Name		N° units	Price per unit, €	Total price, €
Control solar				
PASTEL COLOR OUTDOOR SHUTTERS (V 1750X1150 mm)	UD	104	216,84 €	22.551,36 €
PASTEL COLOR OUTDOOR SHUTTERS (V 700X1150 mm)	UD	20	128,40 €	2.568,00 €
WHITE COLOR INDOOR CURTAINS (P 2500X2200 mm)	UD	40	180,89 €	7.235,60 €
WHITE COLOR INDOOR CURTAINS (P 1750X2200 mm)	UD	8	126,63 €	1.013,04 €
Heating installation				
Heat Pump, TRANE	UD	1	80.000,00 €	80.000,00 €
Solar Panels				
Abora Solar, BASIC kit	UD	22	7.894,79 €	173.685,38 €
Tank and other stuff included in the price				
roVa, aerogel coating shield	UD	39	450,00 €	17.550,00 €
Cooling Storage Tank				
Thermal Flywheel 5000 l	UD	1	5.000,00 €	5.000,00 €
Total investment				**309.603,38 €**

Also, for the second configuration, the costs related to the installation are not considered, and neither in the value proposed for the CAPEX.

This is because it is difficult to have monetary esteem of these values.

To overcome this problem, the values proposed for the OPEX value are overestimated.

6.10 Economic Analysis of the hybrid solar panels' field.

In table 44 the input data for the WACC analysis are presented.

Table 44; Input data for the WACC analysis of the second configuration.

Natural Gas price	88 €/MWh
Electrical Energy price	119 €/MWh
rate of increase	4%
Discount rate	2%
CAPEX of 1 basic kit	7.894,80 €
N° of panels kits	22
Thermal Energy produced	80 MWh/year
Electrical Energy produced	31,3 MWh/year
Avoided CO2 emissions	22,65 tons/year
Carbon tax (included in the savings)	1.812 €

Note: the OPEX is equal to the value considered for configuration 1, so a 0,8% of the CAPEX value.

Table 45 presents the results and output of the WACC theory.

Table 45: Solar field's WACC analysis.

Year	Capex [€]	Opex[€]	Savings[€]	Cash flow[€]	Discounted cash flow[€]	Cum cash flow[€]	NPV[€]
0	-138.948,48 €	-1.111,59 €	14.086,44 €	-125.973,62 €	-125.973,62 €	-125.973,62 €	-125.973,62 €
1		-1.111,59 €	14.649,90 €	13.538,31 €	13.272,86 €	-112.435,31 €	-112.700,77 €
2		-1.111,59 €	15.235,90 €	14.124,31 €	13.575,85 €	-98.311,00 €	-99.124,92 €
3		-1.111,59 €	15.845,33 €	14.733,75 €	13.883,94 €	-83.577,25 €	-85.240,98 €
4		-1.111,59 €	16.479,15 €	15.367,56 €	14.197,25 €	-68.209,69 €	-71.043,73 €
5		-1.111,59 €	17.138,31 €	16.026,73 €	14.515,90 €	-52.182,97 €	-56.527,83 €
6		-1.111,59 €	17.823,85 €	16.712,26 €	14.840,01 €	-35.470,71 €	-41.687,83 €
7		-1.111,59 €	18.536,80 €	17.425,21 €	15.169,70 €	-18.045,50 €	-26.518,13 €
8		-1.111,59 €	19.278,27 €	18.166,68 €	15.505,09 €	121,19 €	-11.013,04 €
9		**-1.111,59 €**	**20.049,40 €**	**18.937,81 €**	**15.846,32 €**	**19.059,00 €**	**4.833,28 €**
10		-1.111,59 €	20.851,38 €	19.739,79 €	16.193,50 €	38.798,79 €	21.026,78 €
11		-1.111,59 €	21.685,43 €	20.573,85 €	16.546,78 €	59.372,64 €	37.573,56 €
12		-1.111,59 €	22.552,85 €	21.441,26 €	16.906,29 €	80.813,90 €	54.479,85 €
13		-1.111,59 €	23.454,97 €	22.343,38 €	17.272,16 €	103.157,28 €	71.752,01 €
14		-1.111,59 €	24.393,16 €	23.281,58 €	17.644,53 €	126.438,86 €	89.396,54 €
15		-1.111,59 €	25.368,89 €	24.257,30 €	18.023,53 €	150.696,16 €	107.420,07 €
16		-1.111,59 €	26.383,65 €	25.272,06 €	18.409,33 €	175.968,22 €	125.829,40 €
17		-1.111,59 €	27.438,99 €	26.327,40 €	18.802,05 €	202.295,62 €	144.631,44 €
18		-1.111,59 €	28.536,55 €	27.424,96 €	19.201,85 €	229.720,59 €	163.833,29 €
19		-1.111,59 €	29.678,01 €	28.566,43 €	19.608,87 €	258.287,01 €	183.442,16 €
20		-1.111,59 €	30.865,13 €	29.753,55 €	20.023,28 €	288.040,56 €	203.465,45 €

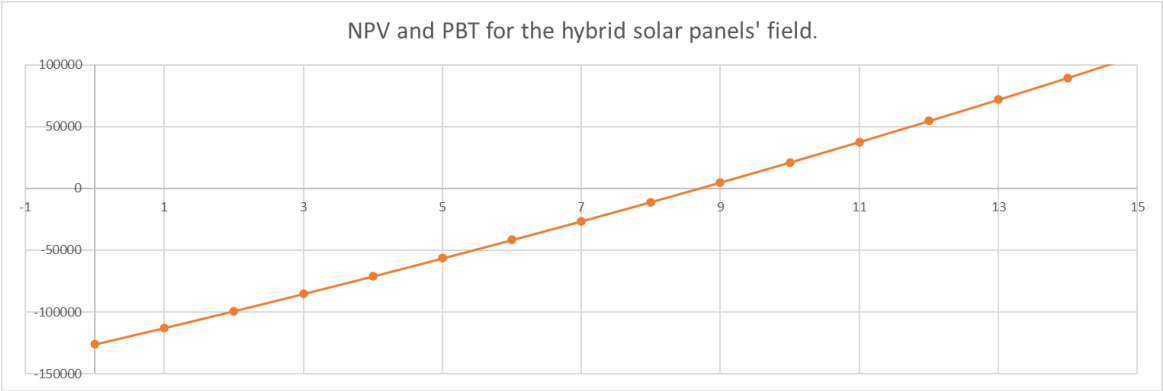

Figure 44: NPV and PBT for the hybrid solar panels' field.

Technical Observations:

- *The payback period for this system aligns with the results observed in Configuration 1. This consistency is attributed to the investment involving the same type of product, analyzed over an identical time frame and under comparable production conditions. Given these similarities, it is expected that financial performance remains consistent across both configurations.*

- *Like the previous configuration, CAPEX has been discounted by 20%, based on the assumption that the cost of the storage tank constitutes 20% of the total investment.*

- *The CO2 emissions savings are way lower than configuration 1's registered value. This has a big economic impact on the definitions of the savings, and a worse ambient impact compared to the 1 system.*

- *This discounting approach is employed to isolate and analyze the payback period specifically for the solar panels, ensuring that the financial assessment focuses solely on the return on investment for the panels themselves.*

6.11 Economic analysis of the Heat Pump and the Electrical Boiler.

In table 46 the input data for the second configuration's WACC analysis are proposed.

Table 46: Input data for the WACC analysis of configuration 2.

Natural Gas price	88 €/MWh
Electrical Energy price	119 €/MWh
rate of increase	4%
Discount rate	2%
CAPEX of the Electrical Boiler	5.000 €
CAPEX of the Heat Pump	80.000,00 €
Previously used EE for the cooling production	30 MWh/year
Used EE for the cooling production	22,3 MWh/year
Previously used gas	182 MWh/year
Electrical Energy used	93 MWh/year
Total avoided CO2 emissions	18,5 ton/year
Carbon tax fee	1.470 €

Note:

- *As in Configuration 1, the pre-intervention conditions for heat production are assumed to be entirely supplied by gas boilers operating at an efficiency of 90%.*

- *The OPEX value is equal to the configuration 1's value, so a 4% of the CAPEX.*

Table 47 presents the output of the WACC analysis.

Table 47: output of the WACC analysis, configuration 2.

Year	Capex [€]	Opex[€]	Savings[€]	Cash flow[€]	Discounted cash flow[€]	Cum cash flow[€]	NPV[€]
0	-85.000,00 €	-3.400,00 €	15.303,56 €	-73.096,44 €	-73.096,44 €	-73.096,44 €	-73.096,44 €
1		-3.400,00 €	15.915,70 €	12.515,70 €	12.270,29 €	-60.580,75 €	-60.826,15 €
2		-3.400,00 €	16.552,33 €	13.152,33 €	12.641,60 €	-47.428,42 €	-48.184,55 €
3		-3.400,00 €	17.214,42 €	13.814,42 €	13.017,64 €	-33.614,00 €	-35.166,91 €
4		-3.400,00 €	17.903,00 €	14.503,00 €	13.398,53 €	-19.111,01 €	-21.768,39 €
5		-3.400,00 €	18.619,12 €	15.219,12 €	13.784,42 €	-3.891,89 €	-7.983,96 €
6		**-3.400,00 €**	**19.363,88 €**	**15.963,88 €**	**14.175,47 €**	**12.071,99 €**	**6.191,50 €**
7		-3.400,00 €	20.138,44 €	16.738,44 €	14.571,82 €	28.810,42 €	20.763,32 €
8		-3.400,00 €	20.943,97 €	17.543,97 €	14.973,61 €	46.354,40 €	35.736,93 €
9		-3.400,00 €	21.781,73 €	18.381,73 €	15.381,01 €	64.736,13 €	51.117,94 €
10		-3.400,00 €	22.653,00 €	19.253,00 €	15.794,17 €	83.989,13 €	66.912,11 €
11		-3.400,00 €	23.559,12 €	20.159,12 €	16.213,24 €	104.148,25 €	83.125,34 €
12		-3.400,00 €	24.501,49 €	21.101,49 €	16.638,38 €	125.249,73 €	99.763,72 €
13		-3.400,00 €	25.481,54 €	22.081,54 €	17.069,75 €	147.331,28 €	116.833,47 €
14		-3.400,00 €	26.500,81 €	23.100,81 €	17.507,52 €	170.432,09 €	134.341,00 €
15		-3.400,00 €	27.560,84 €	24.160,84 €	17.951,86 €	194.592,92 €	152.292,86 €
16		-3.400,00 €	28.663,27 €	25.263,27 €	18.402,93 €	219.856,20 €	170.695,78 €
17		-3.400,00 €	29.809,80 €	26.409,80 €	18.860,89 €	246.266,00 €	189.556,67 €
18		-3.400,00 €	31.002,20 €	27.602,20 €	19.325,94 €	273.868,20 €	208.882,61 €
19		-3.400,00 €	32.242,28 €	28.842,28 €	19.798,23 €	302.710,48 €	228.680,84 €
20		-3.400,00 €	33.531,97 €	30.131,97 €	20.277,96 €	332.842,45 €	248.958,80 €

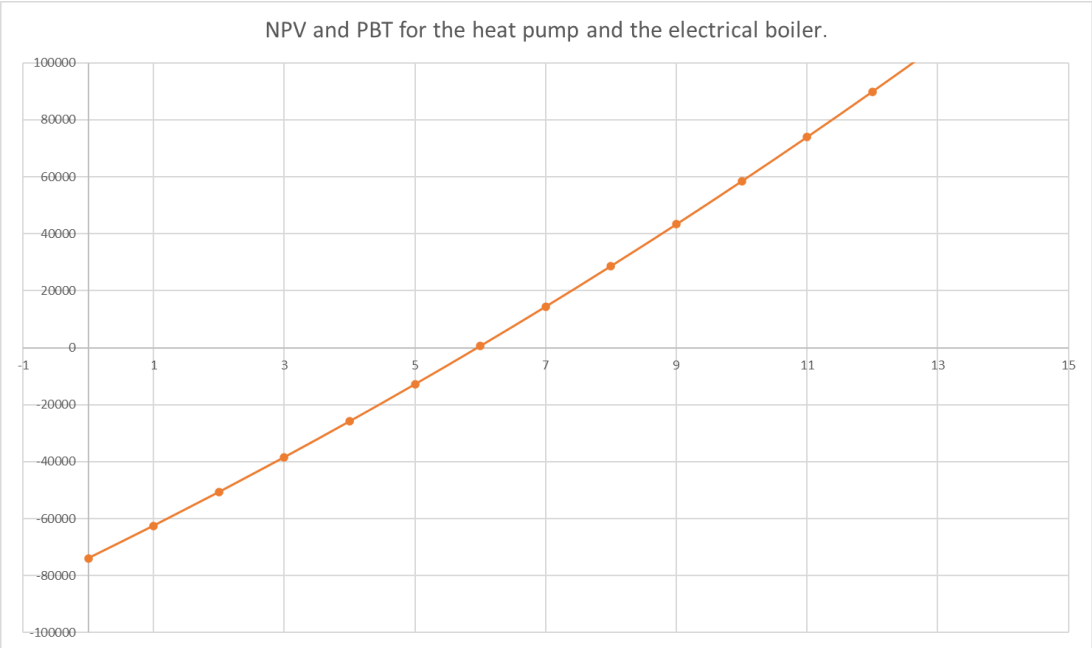

Figure 45: NPV and PBT, configuration 2.

Technical Notes:

- *The CO_2 emission values remain consistent with those previously observed, ensuring that the environmental performance of the system aligns with earlier findings.*
- *PBT conditions are less favorable compared to Configuration 1.*
  This decline is primarily due to the high electrical energy consumption recorded, particularly in the production of cooling energy.

The Energy Efficiency Ratio (EER) values of the heat pump do not significantly differ from the standard values observed in currently marketed cooling systems. This indicates that the increased electrical consumption is inherent to the system's operational characteristics rather than a result of inefficiencies in the equipment. Consequently, while the environmental impact remains controlled, the economic return on investment is adversely affected by the elevated energy usage required to meet the cooling demands.

6.12 Economic Analysis of the global system.

In this chapter the WACC analysis for the totality of the system is conducted.

As previously done, only tables showing the input and output data will be presented, with all the essential notes.

Table 48: Input for the global WACC analysis.

Natural Gas price	88 €/MWh
Electrical Energy price	119 €/MWh
rate of increase	4%
Discount rate	2%
CAPEX of the Electrical Boiler	5.000 €
CAPEX of the Heat Pump	80.000,00 €
Previously used EE for the cooling production	30 MWh/year
Used EE for the cooling production	22,3 MWh/year
Previously used gas	182 MWh/year
Electrical Energy used	93 MWh/year
CAPEX panels	7.894,80 €
N° of basic kits	22
Thermal energy produced	80 MWh
EE produced	31,3 MWh
Total avoided CO2 emissions	45 ton/year
Carbon tax fee	3.600 €

Note:

- *All the technical considerations made for chapter 1's global economic analysis stay the same. So, the CAPEX, the OPEX and the CO2 emission factor are determined in the same way.*

In table 49 the WACC theory's results are shown.

Table 49: output from the WACC analysis for the global system.

Year	Capex [€]	Opex[€]	Savings[€]	Cash flow[€]	Discounted cash flow[€]	Cum cash flow[€]	NPV[€]
0	-258.685,60 €	-6.112,54 €	28.361,60 €	-236.436,54 €	-236.436,54 €	-236.436,54 €	-236.436,54 €
1		-6.112,54 €	29.496,06 €	23.383,53 €	22.925,03 €	-213.053,01 €	-213.511,51 €
2		-6.112,54 €	30.675,91 €	24.563,37 €	23.609,54 €	-188.489,64 €	-189.901,96 €
3		-6.112,54 €	31.902,94 €	25.790,41 €	24.302,88 €	-162.699,23 €	-165.599,09 €
4		-6.112,54 €	33.179,06 €	27.066,52 €	25.005,28 €	-135.632,71 €	-140.593,80 €
5		-6.112,54 €	34.506,22 €	28.393,69 €	25.717,04 €	-107.239,02 €	-114.876,77 €
6		-6.112,54 €	35.886,47 €	29.773,94 €	26.438,40 €	-77.465,09 €	-88.438,36 €
7		-6.112,54 €	37.321,93 €	31.209,39 €	27.169,66 €	-46.255,69 €	-61.268,71 €
8		-6.112,54 €	38.814,81 €	32.702,27 €	27.911,07 €	-13.553,42 €	-33.357,63 €
9		-6.112,54 €	40.367,40 €	34.254,86 €	28.662,94 €	20.701,44 €	-4.694,70 €
10		**-6.112,54 €**	**41.982,10 €**	**35.869,56 €**	**29.425,53 €**	**56.571,00 €**	**24.730,84 €**
11		-6.112,54 €	43.661,38 €	37.548,84 €	30.199,15 €	94.119,85 €	54.929,98 €
12		-6.112,54 €	45.407,84 €	39.295,30 €	30.984,08 €	133.415,15 €	85.914,06 €
13		-6.112,54 €	47.224,15 €	41.111,61 €	31.780,61 €	174.526,76 €	117.694,67 €
14		-6.112,54 €	49.113,11 €	43.000,58 €	32.589,06 €	217.527,34 €	150.283,74 €
15		-6.112,54 €	51.077,64 €	44.965,10 €	33.409,73 €	262.492,44 €	183.693,47 €
16		-6.112,54 €	53.120,74 €	47.008,21 €	34.242,93 €	309.500,65 €	217.936,40 €
17		-6.112,54 €	55.245,57 €	49.133,04 €	35.088,98 €	358.633,69 €	253.025,38 €
18		-6.112,54 €	57.455,40 €	51.342,86 €	35.948,19 €	409.976,55 €	288.973,57 €
19		-6.112,54 €	59.753,61 €	53.641,08 €	36.820,89 €	463.617,63 €	325.794,45 €
20		-6.112,54 €	62.143,76 €	56.031,22 €	37.707,41 €	519.648,85 €	363.501,86 €

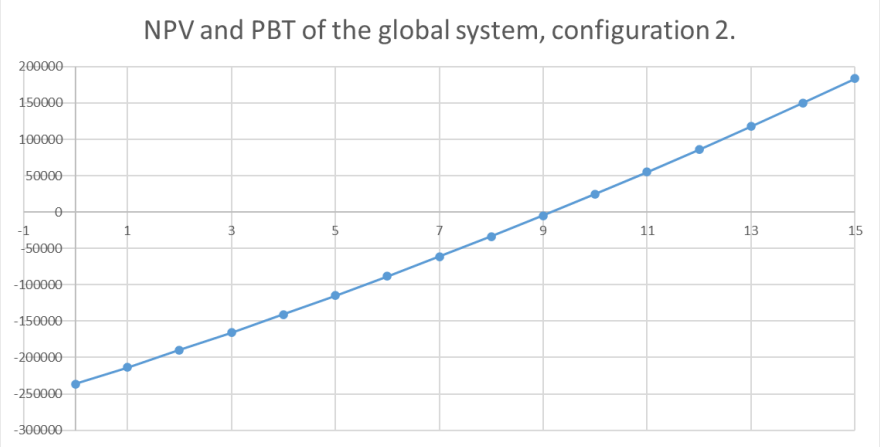

Figure 46: NPV and PBT for global investment.

6.13 Comparison between configurations and selection of the most viable option.

This paragraph presents comprehensive evaluations of the two proposed configurations, encompassing both technical and economic aspects.

These assessments build upon the extensive analyses conducted during the sizing processes detailed in the preceding chapters.

By integrating these considerations, the evaluation aims to identify the most advantageous option among the proposed configurations.

The synthesis of technical performance metrics and economic feasibility assessments will culminate in determining the optimal solution. This chosen configuration will represent the most viable path forward, demonstrating superior technical efficiency and economic sustainability compared to the alternative.

Consequently, the selected option is poised to offer the best balance of performance and cost-effectiveness, aligning with the project's objectives of maximizing energy efficiency and ensuring financial viability.

- One of the most critical parameters in the sizing of an energy supply system, which has been significantly underestimated for an extended period but is now indispensable, is the quantity of CO_2 emissions.
  In Configuration 1, this value amounts to a total of 103 tons per year of CO_2 emissions avoided, whereas in Configuration 2, the value decreases to 45 tons per year.
  The disparity is substantial and is primarily due to Configuration 1 being equipped with a considerably larger solar panel system compared to Configuration 2. As a result, the electrical energy consumed by the system, and consequently the associated CO_2 emission factor, are significantly reduced.
  This difference in emission factors between the two configurations also has a pronounced impact on the economic return. Specifically, Configuration 1 generates a monetary income of 8.200€ from the carbon tax, while Configuration 2 yields 3.600€.
  The substantial reduction in avoided CO_2 emissions in Configuration 2 underscores the enhanced environmental performance of Configuration 1, which leverages a more extensive solar energy system to achieve greater emissions reductions. Consequently, the economic benefits derived from carbon tax savings are markedly higher in Configuration 1, reflecting the superior environmental and financial advantages of a more robust solar panel deployment.

- The Capital Expenditure of the two systems exhibits a significant disparity.
  The first configuration requires an investment of 590.500€, whereas the second configuration requires 259.000€, which is slightly less than half of the first configuration's amount.

When considering the per capita investment for each of the 63 occupants of the building, the first system entails a cost of 9.400€ per individual, compared to 4.100€ for the second system.
Given the paramount importance of financial considerations in investment decisions, if monetary criteria were the sole determining factor, the second configuration would represent the more economically prudent choice.
This substantial reduction in CAPEX makes the second configuration a more attractive option from a purely financial standpoint, highlighting its potential for broader economic feasibility and accessibility.

- Contrary to what might be expected when evaluating only the CAPEX values, the payback time is identical for both configurations.
  This outcome is extraordinary, as it indicates an economic return period of ten years even for the system incorporating an adsorption chiller, which remains relatively uncommon in the current market.
  This result demonstrates that Configuration 1 is optimally sized, ensuring that the production systems are fully aligned with the primary objective of effectively harnessing and maximizing solar energy utilization.
  Additionally, this exceptional result is attributable to the significantly higher savings generated by Configuration 1 compared to Configuration 2.
  These enhanced savings enable the investment to be recouped in the shortest possible time, underscoring the financial viability and efficiency of the first configuration despite the inclusion of the less widespread adsorption chiller technology.
  Consequently, Configuration 1 not only meets but exceeds the economic performance expectations, validating its design and integration strategy in leveraging solar energy to achieve substantial energy and cost savings.

- To substantiate the previous observation, the Net Present Value (NPV) of the two configurations at year 11, designated as the end-of-life year for the production systems of both configurations, is determined to be 116.000€ and 55.000€ for Configuration 1 and Configuration 2, respectively.
  This substantial difference further underscores the economic advantage of Configuration 1 over Configuration 2, highlighting its superior financial performance and greater long-term value within the context of the investment analysis.

- Another critical factor to consider is the utilization of solar energy. Configuration 1 achieves an annual production of 75 MWh of electrical energy and 198 MWh of thermal energy, compared to Configuration 2, which generates 31.3 MWh of electrical energy and 80 MWh of thermal energy from its solar panel system.
  This substantial difference significantly influences the evaluation of the two systems, as one of the primary objectives was to render the building self-sustaining and to maximize the exploitation of solar energy as the predominant energy source.
  The higher energy production in Configuration 1 not only enhances the building's energy autonomy but also contributes to greater environmental sustainability by

reducing reliance on external energy inputs. Consequently, Configuration 1 demonstrates superior performance in meeting the building's energy demands through optimized solar energy utilization, reinforcing its viability as the more effective and sustainable energy solution compared to Configuration 2.

- The dependency on the energy sales market differs markedly between the two system configurations. Configuration 1 draws a total of 45 MWh of electrical energy from the grid to produce thermal energy through the heat pump and boiler, and 0 MWh for cooling energy production using the adsorption chiller.
  In contrast, Configuration 2 requires a total of 93 MWh from the grid for heating production and 22.3 MWh for cooling production.
  These figures are particularly significant as they highlight a critical distinction: with Configuration 2, the building becomes substantially more exposed to fluctuations in energy prices on the market.
  This increased dependency means that any volatility in energy costs could have a more pronounced impact on the overall operational expenses of the building. Conversely, Configuration 1, with its lower reliance on grid-supplied energy, offers greater financial stability and reduces vulnerability to market price changes.
  This difference underscores the importance of considering energy market dynamics when selecting and designing energy supply systems, as it directly affects the economic resilience and sustainability of the building's energy infrastructure.

Figure 47 graphically presents all the values extensively discussed in this chapter, thereby providing a visual representation of the data.

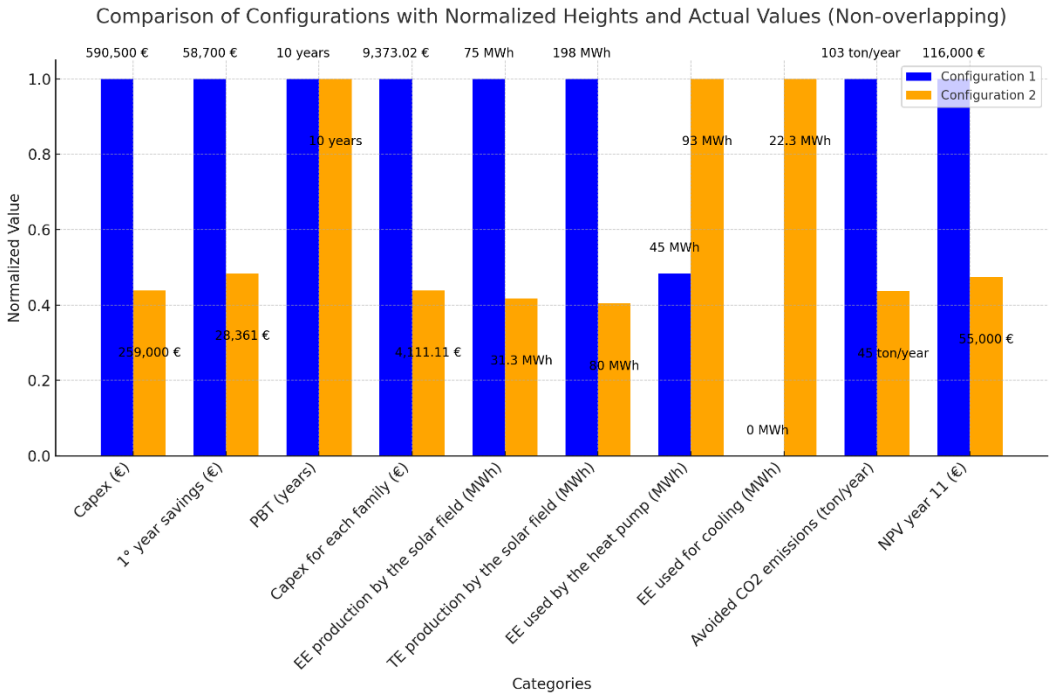

Figure 47: Recap of the most valuable figures of the chapter.

In conclusion, if the primary objective is to minimize the initial financial outlay, Configuration 2 emerges as the more cost-effective option.

However, considering the broader implications of investment, Configuration 1 presents a more prudent choice.

Configuration 1 is significantly more environmentally friendly, offering substantial reductions in CO_2 emissions and leveraging a larger solar energy system to enhance sustainability.

Additionally, Configuration 1 is less susceptible to fluctuations in the energy market due to its greater self-sufficiency, thereby providing greater financial stability and reducing dependency on external energy sources.

Furthermore, Configuration 1 delivers superior overall benefits, including higher energy savings and a more favorable environmental impact, compared to Configuration 2.

Therefore, despite the higher initial investment, Configuration 1 is the more sensible option for investors seeking long-term sustainability, environmental responsibility, and resilience against energy market volatility.

For this reason, incorporating these considerations, the sizing of the third configuration, which involves the application of Phase Change Materials on the building's lateral walls, will be conducted to evaluate the investment's viability and its impact on the building's energy consumption. The analysis will continue using Configuration 1 as a prototype.

6.14 Configuration 3, technical and economic analysis.

For the technical and economic analysis of Configuration 3, the study commences with Configuration 1, which has been identified as the superior option among the initial two presented.

In this sizing process, the adaptability of installing Phase Change Materials (PCM) on the lateral surfaces of the building under investigation is examined within an energy supply system composed of hybrid solar panels. These panels can provide all the necessary heating required during the summer months, without the need for additional systems except for backup components, including a reversible air-to-water heat pump, an adsorption chiller, and thermal energy storage tanks. These elements work in tandem to manage energy efficiently, ensuring its availability whenever demanded by the building.

As detailed in the dedicated chapter on PCM, these materials have the capacity to store substantial amounts of energy in the form of latent heat by undergoing phase transitions, typically between solid and liquid states. This property makes PCMs exceptionally suitable for achieving the primary objective of this thesis, which is to dimension the building's energy production system in the most efficient and economically viable manner.

By integrating PCM, the system enhances thermal regulation, stabilizing indoor temperatures and reducing the reliance on active heating and cooling systems.

However, practical considerations must be addressed. Despite the significant reduction in the building's energy demand achieved using PCM, their current market price remains prohibitively high.

This economic barrier poses a challenge to the widespread adoption of PCM, as the initial investment required does not yet align with cost-effective standards.

Therefore, while PCMs offer substantial technical benefits in terms of energy storage and efficiency, their financial feasibility must be carefully evaluated to determine whether the long-term energy savings justify the upfront costs.

This analysis underscores the need for continued advancements in PCM technology and cost reduction to fully realize their potential in sustainable energy systems.

Notes:

This analysis has proven to be the most complex component of the entire thesis. Numerous attempts were made, unsuccessfully, to obtain detailed quotations both economically and technically for the characterization of these materials' properties.

Ultimately, to streamline the process and ensure the study remains as generalizable as possible, enabling a comprehensive overview of the materials' technical performance and economic investment implications, a strategic decision was made to utilize listed prices and

average technical properties based on currently available market products. This approach facilitates a broader applicability of the findings, providing valuable insights into the practical behavior of Phase Change Materials without being constrained by the limitations of unavailable or highly specialized data.

By adopting standardized pricing and typical technical specifications, the study effectively balances methodological rigor with practical relevance, ensuring that the economic and technical evaluations of PCM integration remain both realistic and representative of current market conditions.

ASSUMPTIONS:

- The price per square meter of the material is between three and five times that of standard construction materials used for building walls. Therefore, a unit price of €200 per square meter is adopted, based on the current market average.
- In the absence of detailed technical specifications, a general reduction of 25% in the building's thermal demand is assumed, reflecting the average benefits provided by current market-available materials.

NOTE: The thermal demand of the swimming pool remains unchanged. Only the building's sizing is affected.

- **Technical sizing of the building's PCM coating.**

As previously outlined, a unit price of €200 per square meter of product is projected, with the implementation of Phase Change Materials expected to achieve a 25% reduction in the building's thermal demand for both heating and cooling.

The initial phase of the analysis involved determining the external surface area of the building designated for PCM application according to the project specifications. This information was obtained from the technical documents provided. A total lateral surface area of 2750 m² was considered, of which 350 m² pertains to windows and is therefore excluded from the current sizing calculations.

As a result, the first outcome of the sizing process is reflected in the values presented in Table 50 presented below:

Table 50: technical results of PCM's sizing process.

Energy Demand's reduction	25%
m^2 of total lateral building's surface	2.750 m^2
Heating's savings	32.750 kWh/year
Cooling's savings	12.500 kWh/year
Gas' savings	36.400 kWh/year
New heating demand	98.250 kWh/year
New cooling demand	37.500 kWh/year
m^2 of PCMs needed	2.400 m^2
PCM's price	200 €/m^2
Total investment on PCMs	480.000,00 €

Without excessive complexity, it is evident that the reduction in thermal demand can lead to significant savings across subsequent economic components related to the energy supply system, while also offering notable environmental benefits from this installation. However, the total investment cost of €480,000 remains substantial and may pose a financial challenge. This high upfront expenditure necessitates a careful evaluation of the long-term economic returns and environmental advantages to determine the overall feasibility and sustainability of integrating Phase Change Materials (PCM) into the building's energy infrastructure. Balancing these factors is crucial to ensure that the investment yields both financial savings and environmental improvements, justifying the initial capital outlay.

Note: as previously mentioned, the thermal demands of the swimming pool remain the same as for the configurations 1 and 2. For all the specifics here missing, they can be found in the previous chapters.

- **Technical sizing of the hybrid panels' solar field.**

As previously indicated, the sections pertaining to the technical sizing of the additional system components will not include detailed descriptions of the calculation processes.

Instead, the results will be presented, accompanied by the most pertinent considerations. This approach ensures a clear and concise presentation of the outcomes, focusing on the key findings and their implications for the overall energy supply system. By highlighting the essential results and their significance, this methodology facilitates a comprehensive understanding of the system's performance without delving into the intricate computational details.

Table 51: technical sizing of the solar panles field results.

N° of basic kits	40
Storage tank'sn volume	2.500 l
Maximum storage capacity	145 kW
Thermal demand in summer	109.700 kWh
Thermal Energy self-consumed	76.000 kWh
Thermal deficit	33.700 kWh
Covered %	70%

Note: The number of kits required in Configuration 2 decreases by 12 units compared to Configuration 1.

This outcome is noteworthy, considering the substantial economic savings that can be achieved by adopting a configuration that delivers the same performance results as the reference configuration. The reduction in the number of kits not only lowers the initial capital investment but also enhances the overall cost-effectiveness of the energy system.

- **Technical sizing, adsorption chiller.**

As previously reiterated in the various sizing analyses conducted for adsorption chillers, their market presence remains significantly limited. Consequently, reference will be made to the same product evaluated during the design of the two preceding configurations.

This decision does not result in any savings in Capital Expenditure compared to the earlier configurations. However, the primary distinction lies in the impact this choice has on the sizing of the solar panel system.

Specifically, when the solar panels are intended to cover the summer demand for Domestic Hot Water, swimming pool heating, and the operation of adsorption chillers, the

implementation of Phase Change Materials reduces the operational frequency of the adsorption chiller. Consequently, the thermal demand for the adsorption chiller decreases.

The results of the technical analysis are not presented here, as they are identical to those previously discussed.

- **Technical dimensioning of the heat pump and electrical boiler.**

The sizing of the heat pump was conducted using a methodology identical to that employed for Configurations 1 and 2.

The thermal contribution provided by the solar panels was integrated into the Excel simulation model, resulting in the determination of the building's annual hourly thermal deficit values.

This thermal deficit was analyzed using the same approach as in the previous configurations, involving the creation and subsequent analysis of a frequency curve for these values, leading to the following conclusions.

Firstly, the heat pump's minimum rated power must be equal to the maximum recorded deficit, which is 73 kW.

Secondly, by operating in thermal tracking mode and adhering to the heat pump's rated power values, the heat pump would function for 64% of the total thermal demand period.

To implement this operational requirement, a thermal storage system was specifically sized to be decoupled from that of the solar panels.

Consequently, a heat pump with a maximum rated power of 75 kW and a minimum power of 10 kW was selected. This selection process also necessitated the further selection of an electric boiler with a minimum nominal power of 10 kW.

These design choices ensure that the energy system operates efficiently within the defined thermal storage capacity, optimizing energy utilization and maintaining consistent thermal comfort for the building.

Note: As the objective of this analysis is to provide a general overview of a hypothetical investment in Phase Change Materials, the rated values of the heat pump in question, along with its thermal specifications and cost, have been derived from those of the heat pump selected for the preceding configurations. Consequently, this analysis presents fictitious values to facilitate a comprehensive evaluation. By utilizing these standardized parameters, the study ensures consistency and comparability across different configurations, allowing for an effective assessment of the potential benefits and economic implications associated with PCM integration. This approach enables the exploration of PCM's impact on the overall energy system without being constrained by the limitations of specific, real-world product data, thereby offering a broader perspective on its feasibility and performance within the context of sustainable energy management.

To accurately size the system for achieving minimal external energy consumption, a scheduled time program is implemented, consistent with the approaches used in previous configurations. This program defines the percentage of operation for the heat pump and establishes distinct hourly activation schedules for each month of the year, tailored to the external climatic conditions specific to each period.

Initially, the dimensioning of the thermal storage tank must be established. Based on the residual capacity provided by Abora Solar, a complimentary storage tank with a volume of 5.000 liters and a peak storage capacity of 380 kW is planned. This allocation ensures that the thermal storage system can effectively manage and store the energy produced, optimizing the availability of stored energy when required by the building.

By integrating this appropriately sized thermal storage tank, the system enhances its ability to maintain energy efficiency and reliability, thereby minimizing the reliance on external energy sources and reducing overall operational costs.

Table 52: scheduled time program for the heat pump's functioning.

	JAN, 50%	FEB, 50%	MAR, 50%	APR, 50%	MAY, 65%	JUN, 65%	JUL, 65%	AUG, 65%	SEPT, 65%	OCT, 65%	NOV, 50%	DEC, 50%
00:00	1	1	1	1	1	1	1	1	1	1	1	1
01:00	1	1	1	1	1	1	1	1	1	1	1	1
02:00	1	1	1	1	1	1	1	1	1	1	1	1
03:00	1	1	1	1	1	1	1	1	1	1	1	1
04:00	1	1	1	1	0	0	0	0	0	0	1	1
05:00	1	1	1	0	0	0	0	0	0	0	1	1
06:00	1	1	1	0	0	0	0	0	0	0	1	1
07:00	0	0	0	0	0	0	0	0	0	0	0	0
08:00	0	0	0	0	0	0	0	0	0	0	0	0
09:00	0	0	0	0	0	0	0	0	0	0	0	0
10:00	0	0	0	0	0	0	0	0	0	0	0	0
11:00	0	0	0	0	0	0	0	0	0	0	0	0
12:00	0	0	0	0	0	0	0	0	0	0	0	0
13:00	0	0	0	0	0	0	0	0	0	0	0	0
14:00	0	0	0	0	0	0	0	0	0	0	0	0
15:00	0	0	0	0	0	0	0	0	0	0	0	0
16:00	1	1	1	0	0	0	0	0	0	0	1	1
17:00	1	1	1	0	0	0	0	0	0	0	1	1
18:00	1	1	1	0	0	0	0	0	0	0	1	1
19:00	1	1	1	0	0	0	0	0	1	1	1	1
20:00	1	1	1	1	0	0	0	0	1	1	1	1
21:00	1	1	1	1	0	0	0	0	1	1	1	1
22:00	1	1	1	1	0	0	0	0	1	1	1	1
23:00	1	1	1	1	0	0	0	0	1	1	1	1

To address the remaining thermal deficit, the system configuration incorporates a heat pump and an electric boiler operating in thermal tracking mode. This approach ensures that the residual energy demand is met efficiently by dynamically adjusting the operation of both components based on real-time thermal requirements. Consequently, this configuration results in a total annual electrical energy consumption of 36 MWh.

- **Technical dimensioning of the storage tank coating.**

Following the same directives established for the previous configurations, the storage tank insulation has been implemented to ensure that hourly thermal losses remain approximately 2% of the stored load.

The results are that 38 packages of the roVa aerogel for coatings are needed in order to reach the goal.

- **Total investment, configuration 3.**

Table 53; Total investment, configuration 3.

Name		N° units	Price per unit, €	Total price, €
Control solar				
PASTEL COLOR OUTDOOR SHUTTERS (V 1750X1150 mm)	UD	104	216,84	22.551,36 €
PASTEL COLOR OUTDOOR SHUTTERS (V 700X1150 mm)	UD	20	128,4	2.568,00 €
WHITE COLOR INDOOR CURTAINS (P 2500X2200 mm)	UD	40	180,89	7.235,60 €
WHITE COLOR INDOOR CURTAINS (P 1750X2200 mm)	UD	8	126,63	1.013,04 €
PCM	m^2	2400	200	576.000,00 €
Heating installation				
Heat Pump, TRANE	UD	1	50000	50.000,00 €
Electrical Heater	UD	1	2000	2.000,00 €
Adsorption chiller, Fahrenheit eCoo x40	UD	1	95000	95.000,00 €
Solar Panels				
Abora Solar, BASIC kit	UD	40	7894,79	315.791,60 €
Tank and other stuff included in the price				
roVa, aerogel coating shield	UD	38	450	17.100,00 €
Total investment				**1.089.259,60 €**

At first glance, the difference is staggering: the cost of Phase Change Materials significantly increases the total investment. Furthermore, it is important to note that installation costs are not directly accounted for in the initial Capital Expenditure but are instead reflected by an increase in Operational Expenditure.

This increase must be carefully evaluated within the overall investment context to determine the feasibility and sustainability of integrating PCM into the energy supply system.

6.15 PCMs Economic Analysis.

This economic analysis is conducted in the same manner as the previous configurations. For the WACC analysis, the input data are as follows, in table 54:

Table 54: Input for the WACC theory analysis, configuration 3.

PCMs CAPEX	480.000 €
Installation cost	96.000 €
EE savings	31 MWh
Gas savings	36 MWh
EE price	88 €/MWh
Gas price	119 €/MWh
Rate of increase of energy cost	4%
Discount rate	2%
CO2 emissions avoided	13,60 ton/year
Carbon tax	1.090 €

Notes:

- *Savings on thermal energy consumption are accounted for as gas savings, based on the assumption that heat is produced using conventional boilers with a 90% efficiency.*
- *Installation costs are incorporated directly, as defining an Operational Expenditure (OPEX) is deemed unnecessary. The projected installation costs amount to 20% of the total Capital Expenditure (CAPEX) allocated solely for materials.*

Table 55: output of the WACC theory for PCMs investment.

Year	Capex [€]	Opex[€]	Savings[€]	Cash flow[€]	Discounted cash flow[€]	Cum cash flow[€]	NPV[€]
0	-576.000,00 €	0,00 €	8.168,32 €	-567.831,68 €	-567.831,68 €	-567.831,68 €	-567.831,68 €
1		0,00 €	8.495,06 €	8.495,06 €	8.328,49 €	-559.336,62 €	-559.503,19 €
2		0,00 €	8.834,86 €	8.834,86 €	8.491,79 €	-550.501,77 €	-551.011,40 €
3		0,00 €	9.188,25 €	9.188,25 €	8.658,29 €	-541.313,51 €	-542.353,11 €
4		0,00 €	9.555,78 €	9.555,78 €	8.828,07 €	-531.757,73 €	-533.525,04 €
5		0,00 €	9.938,01 €	9.938,01 €	9.001,16 €	-521.819,72 €	-524.523,88 €
6		0,00 €	10.335,53 €	10.335,53 €	9.177,66 €	-511.484,19 €	-515.346,22 €
7		0,00 €	10.748,95 €	10.748,95 €	9.357,61 €	-500.735,23 €	-505.988,61 €
8		0,00 €	11.178,91 €	11.178,91 €	9.541,09 €	-489.556,32 €	-496.447,51 €
9		0,00 €	11.626,07 €	11.626,07 €	9.728,17 €	-477.930,25 €	-486.719,34 €
10		0,00 €	12.091,11 €	12.091,11 €	9.918,92 €	-465.839,14 €	-476.800,42 €
11		0,00 €	12.574,76 €	12.574,76 €	10.113,41 €	-453.264,38 €	-466.687,00 €
12		0,00 €	13.077,75 €	13.077,75 €	10.311,71 €	-440.186,63 €	-456.375,29 €
13		0,00 €	13.600,86 €	13.600,86 €	10.513,90 €	-426.585,78 €	-445.861,38 €
14		0,00 €	14.144,89 €	14.144,89 €	10.720,06 €	-412.440,88 €	-435.141,33 €
15		0,00 €	14.710,69 €	14.710,69 €	10.930,26 €	-397.730,20 €	-424.211,07 €
16		0,00 €	15.299,11 €	15.299,11 €	11.144,58 €	-382.431,08 €	-413.066,49 €
17		0,00 €	15.911,08 €	15.911,08 €	11.363,10 €	-366.520,00 €	-401.703,40 €
18		0,00 €	16.547,52 €	16.547,52 €	11.585,90 €	-349.972,48 €	-390.117,49 €
19		0,00 €	17.209,42 €	17.209,42 €	11.813,08 €	-332.763,06 €	-378.304,42 €
20		0,00 €	17.897,80 €	17.897,80 €	12.044,71 €	-314.865,26 €	-366.259,71 €

From Table 55, it is evident that this investment is economically unfeasible. This conclusion arises not only from the exceptionally high Capital Expenditure required but also from the Net Present Value of the investment, which is projected to be over 350.000€ negative at the 20-year mark.

However, the significant economic drawbacks do not necessarily reflect the technical viability of the investment. As previously demonstrated, the technical outcomes are more than satisfactory, indicating that while the financial aspects are unfavorable, the system performs effectively from an operational and technical standpoint.

6.16 Economic Analysis, global investment.

Based solely on the results of the WACC analysis for PCM alone, further analysis appears unnecessary. However, by conducting an economic analysis of the overall system, rather noteworthy results are obtained. The following tables present these findings.

Table 56 presents all the input data for the WACC theory.

Table 56: input data for the global system's WACC analysis.

Thermal Energy cost (Natural Gas)	119 €/MWh
Electricity cost	88€/MWh
N° of basic kits	40
CAPEX for the basic kit	7.894,80 €
EE produced	153 MWh
Thermal Energy produced	57 MWh
CAPEX for the adsorption chiller	95.000 €
EE saved	18,75 MWh
CAPEX for the heat pump	50.000 €
CAPEX for the electrical boiler	2.000 €
Gas saved	109 MWh
EE used	35 MWh
CAPEX for the PCMs	480.000 €
Gas saved	36,5 MWh
EE saved	6,25 MWh
CO2 emissions avoided	109 ton/year
Carbon tax fee	8.740 €

The output data for the analysis are shown in table 57 and figure 48.

Table 57: output results for the global system's WACC theory analysis.

Year	Capex [€]	Opex[€]	Savings[€]	Cash flow[€]	Discounted cash flow[€]	Cum cash flow[€]	NPV[€]
0	-942.792,00 €	-8.208,87 €	49.173,56 €	-901.827,31 €	-901.827,31 €	-901.827,31 €	-901.827,31 €
1		-8.208,87 €	51.140,50 €	42.931,63 €	42.089,83 €	-858.895,68 €	-859.737,48 €
2		-8.208,87 €	53.186,12 €	44.977,25 €	43.230,73 €	-813.918,44 €	-816.506,75 €
3		-8.208,87 €	55.313,56 €	47.104,69 €	44.387,80 €	-766.813,74 €	-772.118,95 €
4		-8.208,87 €	57.526,10 €	49.317,24 €	45.561,50 €	-717.496,51 €	-726.557,45 €
5		-8.208,87 €	59.827,15 €	51.618,28 €	46.752,27 €	-665.878,23 €	-679.805,18 €
6		-8.208,87 €	62.220,24 €	54.011,37 €	47.960,55 €	-611.866,86 €	-631.844,63 €
7		-8.208,87 €	64.709,04 €	56.500,18 €	49.186,80 €	-555.366,68 €	-582.657,83 €
8		-8.208,87 €	67.297,41 €	59.088,54 €	50.431,50 €	-496.278,15 €	-532.226,33 €
9		-8.208,87 €	69.989,30 €	61.780,43 €	51.695,10 €	-434.497,71 €	-480.531,23 €
10		-8.208,87 €	72.788,87 €	64.580,01 €	52.978,10 €	-369.917,71 €	-427.553,13 €
11		-8.208,87 €	75.700,43 €	67.491,56 €	54.280,97 €	-302.426,15 €	-373.272,16 €
12		-8.208,87 €	78.728,45 €	70.519,58 €	55.604,21 €	-231.906,57 €	-317.667,96 €
13		-8.208,87 €	81.877,58 €	73.668,72 €	56.948,31 €	-158.237,85 €	-260.719,64 €
14		-8.208,87 €	85.152,69 €	76.943,82 €	58.313,80 €	-81.294,03 €	-202.405,84 €
15		-8.208,87 €	88.558,80 €	80.349,93 €	59.701,18 €	-944,11 €	-142.704,66 €
16		-8.208,87 €	92.101,15 €	83.892,28 €	61.110,98 €	82.948,17 €	-81.593,69 €
17		-8.208,87 €	95.785,19 €	87.576,32 €	62.543,73 €	170.524,50 €	-19.049,95 €
18		**-8.208,87 €**	**99.616,60 €**	**91.407,73 €**	**63.999,98 €**	**261.932,23 €**	**44.950,03 €**
19		-8.208,87 €	103.601,27 €	95.392,40 €	65.480,28 €	357.324,63 €	110.430,30 €
20		-8.208,87 €	107.745,32 €	99.536,45 €	66.985,18 €	456.861,07 €	177.415,48 €

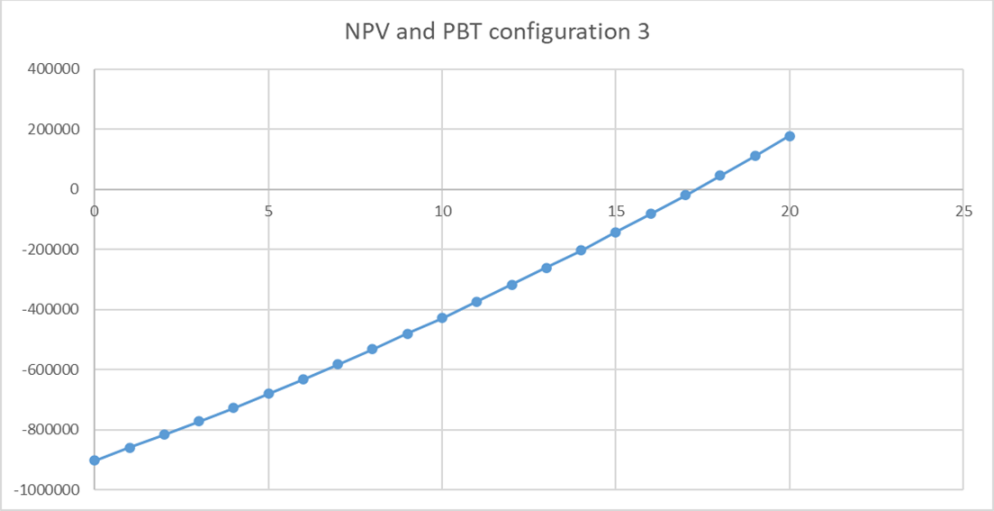

Figure 48: NPV and PBT for the global system's WACC analysis.

The results highlight that the investment potentially achieves a payback time of 18 years. This outcome is promising not only from an economic perspective but also, and particularly, from technical and environmental standpoints.

Specifically, when compared to Configuration 1, there are greater savings in terms of CO_2 emissions into the atmosphere, as well as substantial reductions in the sizing of the equipment selected.

Currently, Phase Change Materials are in the earliest stages of their commercial development.

Their minimal market demand has resulted in exceedingly high and uncompetitive prices. However, should market demand for PCMs increase significantly, coupled with substantial

governmental incentives for building energy efficiency improvements, it is plausible to anticipate a reduction in PCM costs from €200 per square meter to €100 per square meter, effectively halving their current price.

This projected price decrease assumes the successful implementation of these incentives, contrasting with the recently introduced “very Italian” "bonus facciata" and "bonus 110," which have not yielded reasonable and pleasant outcomes.

Based on these potentially optimistic assumptions, an economic analysis incorporating the updated PCM pricing was conducted.

The results of this analysis are astonishing, demonstrating that reduced PCM costs could substantially enhance the economic feasibility of integrating PCMs into energy systems.

Table 58: outcomes of configuration "3.1"

Year	Capex [€]	Opex[€]	Savings[€]	Cash flow[€]	Discounted cash flow[€]	Cum cash flow[€]	NPV[€]
0	-702.792,00 €	-6.672,87 €	49.173,56 €	-660.291,31 €	-660.291,31 €	-660.291,31 €	-660.291,31 €
1		-6.672,87 €	51.140,50 €	44.467,63 €	43.595,71 €	-615.823,68 €	-616.695,60 €
2		-6.672,87 €	53.186,12 €	46.513,25 €	44.707,08 €	-569.310,44 €	-571.988,52 €
3		-6.672,87 €	55.313,56 €	48.640,69 €	45.835,21 €	-520.669,74 €	-526.153,30 €
4		-6.672,87 €	57.526,10 €	50.853,24 €	46.980,53 €	-469.816,51 €	-479.172,77 €
5		-6.672,87 €	59.827,15 €	53.154,28 €	48.143,47 €	-416.662,23 €	-431.029,30 €
6		-6.672,87 €	62.220,24 €	55.547,37 €	49.324,47 €	-361.114,86 €	-381.704,83 €
7		-6.672,87 €	64.709,04 €	58.036,18 €	50.523,98 €	-303.078,68 €	-331.180,85 €
8		-6.672,87 €	67.297,41 €	60.624,54 €	51.742,46 €	-242.454,15 €	-279.438,39 €
9		-6.672,87 €	69.989,30 €	63.316,43 €	52.980,36 €	-179.137,71 €	-226.458,03 €
10		-6.672,87 €	72.788,87 €	66.116,01 €	54.238,15 €	-113.021,71 €	-172.219,88 €
11		-6.672,87 €	75.700,43 €	69.027,56 €	55.516,32 €	-43.994,15 €	-116.703,56 €
12		-6.672,87 €	78.728,45 €	72.055,58 €	56.815,33 €	28.061,43 €	-59.888,23 €
13		**-6.672,87 €**	**81.877,58 €**	**75.204,72 €**	**58.135,69 €**	**103.266,15 €**	**-1.752,54 €**
14		**-6.672,87 €**	**85.152,69 €**	**78.479,82 €**	**59.477,89 €**	**181.745,97 €**	**57.725,35 €**
15		-6.672,87 €	88.558,80 €	81.885,93 €	60.842,45 €	263.631,89 €	118.567,80 €
16		-6.672,87 €	92.101,15 €	85.428,28 €	62.229,87 €	349.060,17 €	180.797,68 €
17		-6.672,87 €	95.785,19 €	89.112,32 €	63.640,69 €	438.172,50 €	244.438,36 €
18		-6.672,87 €	99.616,60 €	92.943,73 €	65.075,43 €	531.116,23 €	309.513,79 €
19		-6.672,87 €	103.601,27 €	96.928,40 €	66.534,63 €	628.044,63 €	376.048,42 €
20		-6.672,87 €	107.745,32 €	101.072,45 €	68.018,86 €	729.117,07 €	444.067,28 €

Table 59: NPV and PBT of configuration 3.1

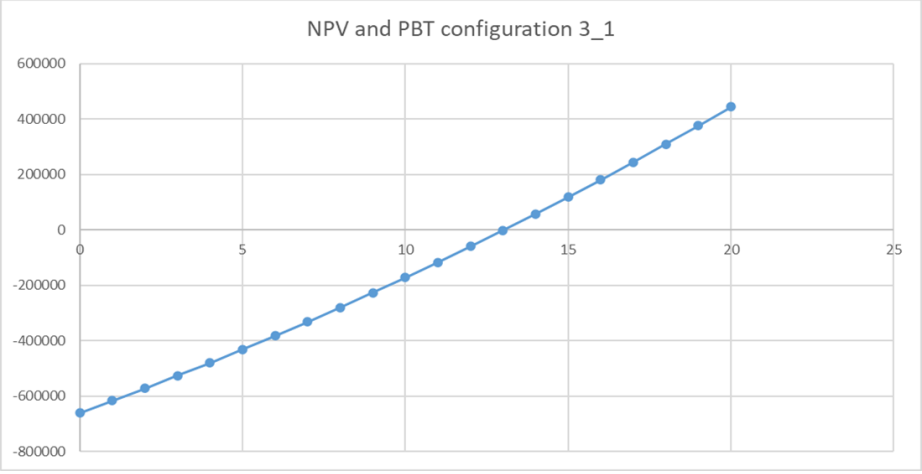

The Payback Time decreases by four years, reaching a value of thirteen years. This reduction in PCM prices results in achieving a Net Present Value of €450.000 by year twenty, which is approximately €300.000 higher compared to the previous scenario.

Additionally, when compared to Configuration 1, the PBT increases by only four years, thereby making both systems significantly more competitive than what was observed with the standard Configuration 3.

Figure 49 illustrates a visual comparison between Configuration 3 and Configuration 3.1. It is evident that the two configurations maintain identical technical parameters, as expected. However, they exhibit substantial differences in their economic parameters. This significant variation in economic factors could considerably influence the investment decision, potentially tipping the balance in favor of one configuration over the other.

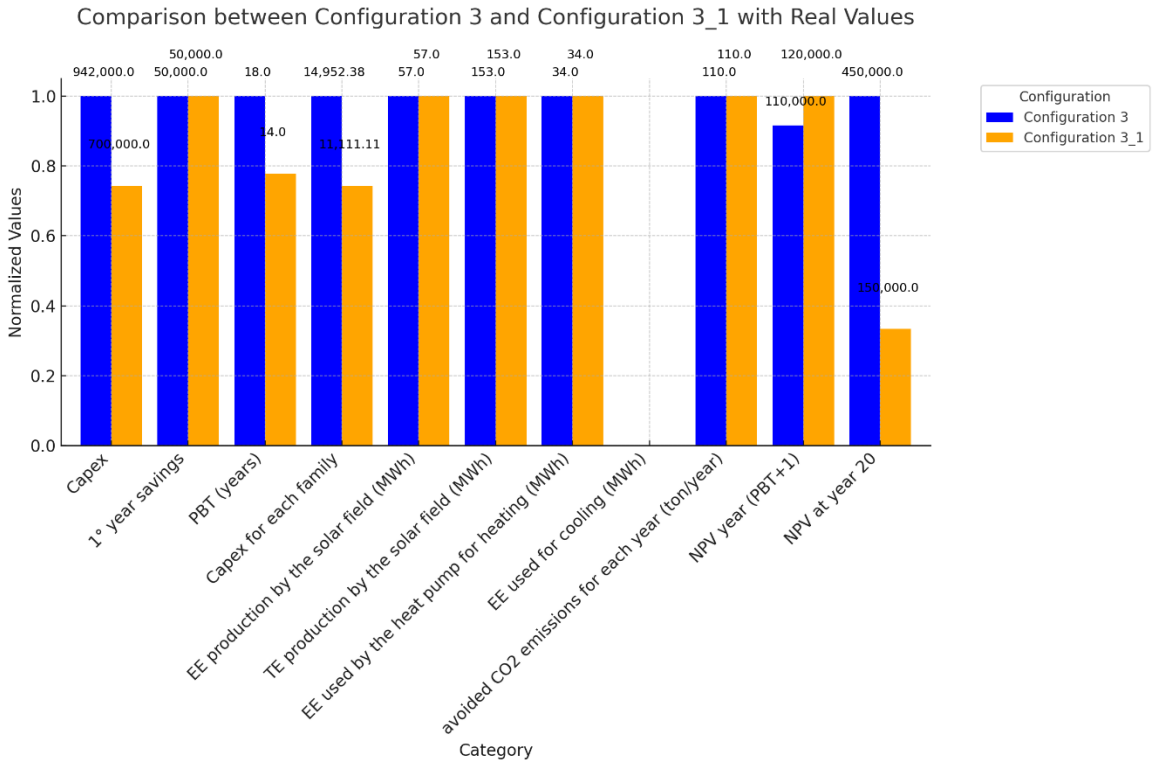

Figure 49: comparison between configuration 3 and 3.1

6.17 Comparison between the two best configurations.

This paragraph presents a comparison between the two most favorable configurations: Configuration 1 and Configuration 3.1.

Configuration 3.1 incorporates Phase Change Materials while assuming the most optimistic price forecast, specifically a 50% reduction in PCM costs within a short timeframe.

This assumption enables a meaningful and equitable comparison between the two configurations. Directly comparing Configuration 1 with Configuration 3 would not provide a balanced assessment, as the configuration without PCM would significantly outperform the alternative.

Therefore, the analysis focuses on Configuration 1 and Configuration 3.1 to ensure a fair and relevant evaluation.

Below, in figure 50 an initial graphical comparison between these two configurations is presented, highlighting the economic and technical distinctions that inform the investment decision.

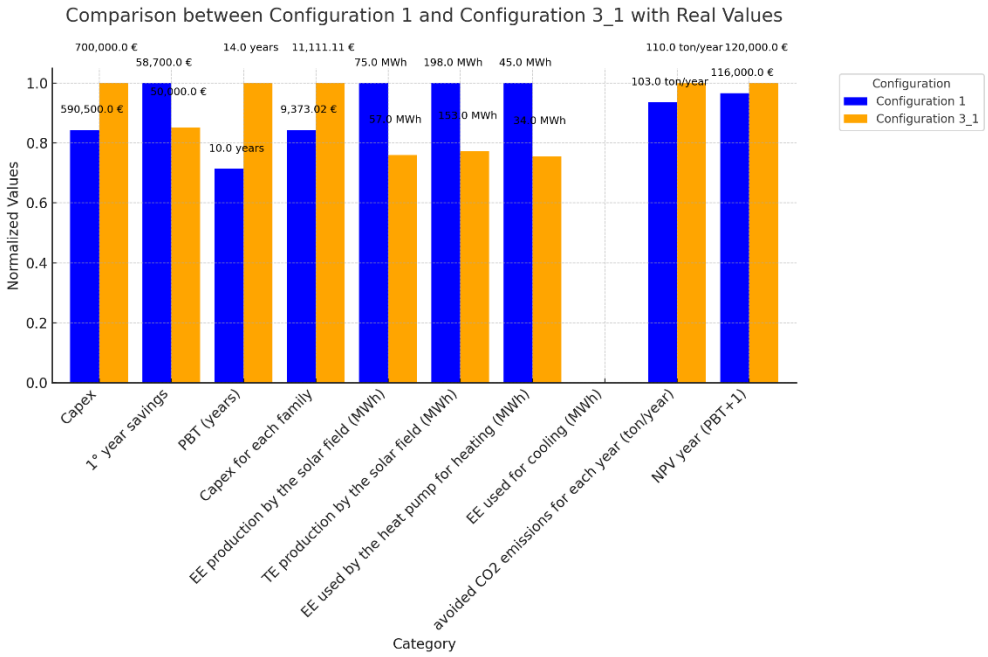

Figure 50: comparison between configuration 1 and configuration 3.1

Configuration 1 stands out in terms of initial investment, offering significant cost savings compared to Configuration 3.1, with an immediate reduction of approximately €110,000.

This difference is substantial and can make a decisive impact, especially when it comes to incentivizing the building occupants to take part in the investment.

Additionally, Configuration 1 performs better in terms of payback time (PBT), with a 4-year shorter period than Configuration 3.1. This discrepancy in PBT is particularly relevant, as a faster return on investment makes Configuration 1 more attractive for stakeholders who prioritize quicker financial recovery.

The first-year savings further reinforce Configuration 1's advantage, providing greater immediate financial relief compared to Configuration 3.1. These higher initial savings contribute to a faster investment recovery, enhancing the appeal of Configuration 1 for those seeking immediate cost reductions.

However, when examining other performance parameters related to energy efficiency and sustainability, Configuration 3.1 emerges as a more robust choice. This is especially evident in its ability to lower CO_2 emissions more effectively than Configuration 1, thus achieving a significantly reduced environmental footprint.

The improved energy efficiency and reduced dependency on external power sources in Configuration 3.1 counterbalance its higher initial investment by offering notable sustainability benefits over time.

Another key point lies in the reduced demand for grid-sourced electricity in Configuration 3.1, highlighting its capacity for greater energy independence.

Given that both configurations share the goal of self-sustainability, this reduced reliance on external electricity emphasizes Configuration 3.1’s ability to fulfill this objective more effectively. While Configuration 3.1 does require a more substantial initial outlay, it becomes evident that this investment pays off in the long run by delivering a system that not only meets but exceeds sustainability targets.

This advantage is further illustrated by the Net Present Value assessed one year after reaching PBT. In this comparison, Configuration 3.1 achieves a higher NPV, indicating that the future cash flow generated by this setup will more effectively compensate for the upfront cost than those from Configuration 1.

An additional consideration lies in the solar panel energy production and the energy consumption of the heat pump for heating. In both configurations, these metrics show systems designed to optimize energy production, though with a notable difference.

Configuration 1's systems appear slightly oversized compared to those of Configuration 3.1, leading to increased costs not only in capital expenditure but also in operational expenses.

In contrast, Configuration 3.1, with more appropriately sized systems for energy production and usage, achieves the same level of energy self-sufficiency but with a leaner footprint. This results in an optimized system that minimizes operational costs linked to maintenance and system management.

Thus, although Configuration 3.1 demands a higher initial investment, it delivers superior long-term advantages, both in energy efficiency and in reduced operational costs, making it the preferable option for a sustainable, cost-effective solution.

7. Conclusions

The technical conclusions have been extensively addressed in the previous chapters and sections for each configuration analyzed and sized in detail.

In this paragraph, general observations and overarching conclusions regarding the project are presented.

- **Project Insights**: The project has been highly stimulating, unveiling a world that initially seemed devoid of complexities, but the situation proved to be quite different.

  The challenges and intricacies encountered have provided valuable learning experiences, highlighting the multifaceted nature of energy system design and the importance of thorough analysis.

  This emphasized that theoretical expectations may not always align with practical outcomes, underscoring the necessity for comprehensive evaluation in engineering projects.

- **Necessity of Advanced Simulation Tools for PCMs**: To accurately size and effectively implement Phase Change Materials in the field of construction, advanced simulation tools are essential - tools that realistically depict in-field behaviors.

  Without such assets, predicting the true performance of PCMs becomes exceedingly challenging, and consequently, the significant cost of these materials heavily impacts the feasibility of investing in them.

  It is therefore evident that investing resources and capital in the creation and development of such software is crucial. This investment could have an enormous impact on the successful outcome of such projects, enabling more precise modeling and optimization of PCM applications, thereby enhancing their economic viability and encouraging broader adoption in the industry.

- **Economic Barriers to Sustainable Energy Systems**: Unfortunately, we must confront a disheartening reality today. The most efficient, renewable, and less polluting energy production systems are among the most expensive on the market. Until their prices decrease - unfortunately, given that the "driving force of the world" and human motivations is often money - nothing will change.

  Unless a definitive decision is made to alter market trends, more polluting systems will continue to prevail over environmentally friendly alternatives. This situation highlights the critical need for economic strategies and policies that can incentivize the adoption of sustainable technologies, making them more accessible and competitive in the market.

- **Importance of Governmental Support**: Significant assistance from governments and nations is imperative for large-scale investments that could facilitate the transition toward an eco-sustainable world.

The problem is that this support has been slow to materialize. It is necessary that economic assistance is provided, especially for PCMs - remarkable materials in terms of energy efficiency - and insulating materials in general.

Such support would help to reduce dependency on the volatile energy market, which unfortunately undergoes continuous fluctuations and speculations due to geopolitical situations that are beyond our control and stem from reasons far removed from humanitarian considerations.

Governmental intervention could thus play a pivotal role in stabilizing the market and promoting sustainable practices.

- **Attention to Climate Change**: Enormous attention must be paid to climate change. It is often underestimated, but when we least expect it, nature responds in kind, sometimes with compounded effects, as evidenced by events such as those that occurred in Valencia at the beginning of November 2024.

  This underscores the urgency of proactively addressing environmental issues, reinforcing the importance of implementing sustainable practices and technologies to mitigate adverse climatic impacts.

  Ignoring these warning signs could lead to irreversible damage, making it imperative to act decisively.

- **Personal Reflection**: On a personal note, it is not expected that these investments be made for free, in terms of money.

  What is expected, however, is the commitment and collective effort from all stakeholders. Humanity does not own nature; therefore, we must treat it with greater respect and care than we have historically demonstrated.

  It is essential that everyone contributes to this endeavor, recognizing that the preservation of the environment is a shared responsibility. By fostering a culture of sustainability and environmental stewardship, meaningful progress can be achieved toward safeguarding our planet for future generations.

Bibliography

1. ***Sonia Longo, Valeria Palomba, Marco Beccali, Maurizio Cellura, Salvatore Vasta; Energy balance and life cycle assessment of small size residential solar heating and cooling systems equipped with adsorption chillers, Solar Energy, Volume 158, 2017. .***

2. *Tomas Nunez, Walter Mittelbach, Hans-Martin Henning; Development of an adsorption chiller and heat pump for domestic heating and air-conditioning applications, 2005. .*

3. *B.B. Saha, A. Akisawa, T. Kashiwagi; Solar/waste heat driven two-stage adsorption chiller: the prototype, 2000. .*

4. *Shuai Du, Zhaopeng Cui, R.Z. Wang, Hongbin Wang, Quanwen Pan; Development and experimental study of a compact silica gel-water adsorption chiller for waste heat driven cooling in data centers, 2023. .*

5. *B. Hoffschmidt; Solar Thermal Systems: Components and Applications, in Comprehensive renewable Energy (second edition), 2022. .*

6. *Mahbubul Muttakin, Kazuhide Ito, Bidyut Baran Saha; Solar Thermal-Powered Adsorption Chiller, 2019. .*

7. *Mejdi Jeguirim, Patrick Dutournié; Renewable Energy Production and Distribution, Solution and Opportunities, Volume 2. .*

8. *John Wiley and Sons; Ruthven DM. Principles of adsorption and adsorption processes, 1984. .*

9. *Ahmad A. Alsarayreh, , Ayman Al-Maaitah, Menwer Attarakih, Hans-Jörg Bart, Energy and Exergy Analyses of Adsorption Chiller at Various Recooling-Water and Dead-State Temperatures, 2021. .*

10. https://aborasolar.com/?utm_source=google&utm_medium=busqueda&utm_campaign=SEPT23&gad_source=1&gclid=CjwKCAiAt5euBhB9EiwAdkXWO6VviLcHvpLJFQ0U6T3juDVAjRbkgrRTsesvb5tmgWiaajLWTSjCEhoCTDgQAvD_BwE. [Online]

11. https://fahrenheit.cool/en/. [Online]

12. https://trane.eu/it/equipment/2-heat-pumps/22-water-to-water-heat-pumps.html. [Online]

13. https://www.pvsyst.com/. [Online]

14. https://data.nasa.gov/. [Online]

15. https://www.omie.es/. [Online]

16. https://eniplenitude.es/blog/energia/precio-del-gas-natural-evolucion-en-espana-y-coste-en-2024/. [Online]

17. Guía Técnica "Condiciones climáticas exteriores de proyecto". IDAE 2010. [Online]

18. https://worldpopulationreview.com/country-rankings/carbon-tax-countries. [Online]

19. ***Dynamic simulation model and empirical validation for estimating thermal energy demand in indoor swimming pools. José Pablo Delgado Marín & José Ramón Garcia-Cascales .***

20. ***Energy analysis of swimming pools for sports activities: cost effective solutions for efficiency improvement; Zuccari F., Santiangeli A., Orecchini F. .***

21. ***Tesis Doctoral ANÁLISIS ENERGÉTICO DE UNA PISCINA CLIMATIZADA ASISTIDA CON ENERGÍAS RENOVABLES, MEDIANTE SU MODELADO DINÁMICO, PARA UNA MEJOR INTEGRACIÓN DE LA ENERGÍA SOLAR TÉRMICA Y LA BIOMASA, Autor: José Pablo Delgado Marín. .***

22. ***European Standard EN 12975: "Thermal solar systems and components - Solar collectors - Part 2: Test methods.".***

23. https://rovashield.com/rova-shield-insulation/. [Online]

24. www.woespana.es. [Online]

25. https://www.teknoring.com/guide/guide-architettura/guida-ai-pcm-i-materiali-a-cambiamento-di-fase/. [Online]

26. https://freddotiles.com/how-it-works/. [Online]

27. Solar Thermal Systems: Components and Applications. [book auth.] B. Hoffschmidt.

Appendix A

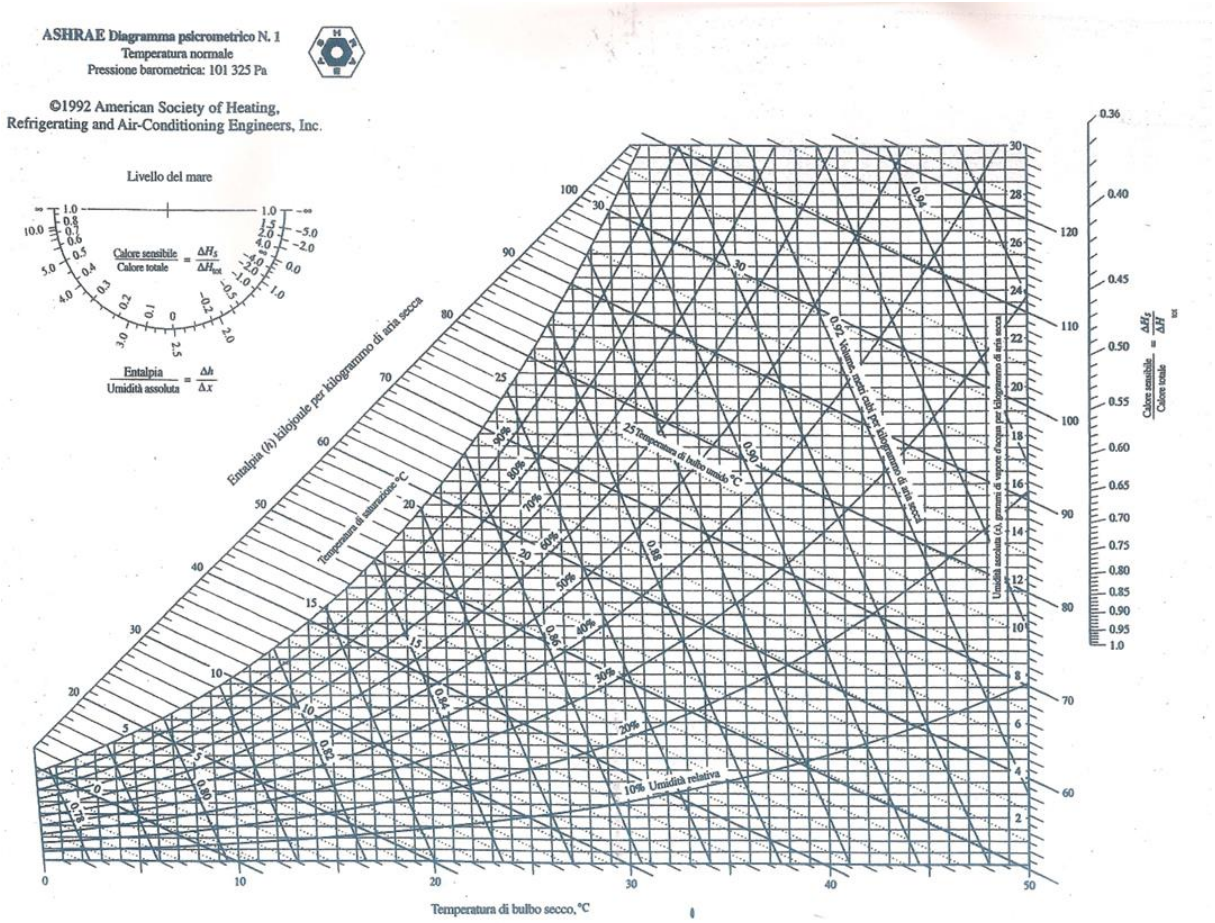

Figure 51: Psychrometric chart.